JUN N-TERMINAL KINASE 1 (JNK1) AS A MOLECULAR TARGET TO LIMIT CELLULAR MORTALITY UNDER HYPOXIA

by

SEEMA S. BETIGERI

A Dissertation submitted to the

Graduate School-New Brunswick

Rutgers, The State University of New Jersey

in partial fulfillment of the requirements

for the degree of

Doctor of Philosophy

Graduate Program in Pharmaceutical Science

written under the direction of

Professor Tamara Minko, Ph.D.

and approved by

_____

_____

_____

_____

New Brunswick, New Jersey

January, 2009

ABSTRACT OF THE DISSERTATION

JUN N-TERMINAL KINASE 1 (JNK1) AS A MOLECULAR TARGET TO LIMIT CELLULAR MORTALITY UNDER HYPOXIA

By SEEMA S. BETIGERI

Dissertation Director:

Tamara Minko, Ph.D.

Many pathological conditions and environmental impacts lead to a decrease in tissue oxygen supply and severe cellular hypoxia. This secondary hypoxia can disturb cellular homeostasis, limiting the efficacy of the prescribed treatment for the primary disease, eventually leading to cellular and organismal death. Jun N-terminal kinase 1 (JNK1) plays a central role in the development of cellular damage under hypoxia, hypoxia/reoxygenation and ischemia/reperfusion conditions. Therefore, we selected JNK1 protein as a molecular target to limit cellular damage and death during hypoxia. The primary objective of this research was to study the influence of the suppression of JNK1 on the development of cellular hypoxic damage. It was hypothesized that suppression of JNK1 will decrease cellular mortality under hypoxia and may increase the efficacy of traditional treatment of many pathological conditions. The hypothesis was verified under both *in vitro* and *in vivo* conditions. Another objective was to develop a non-viral system for intracellular delivery of antisense oligonucleotides (ASO) and small interfering RNA (siRNA). ASO and siRNA targeted to JNK1 mRNA delivered by neutral

and cationic liposomes, respectively, showed high efficiency in suppressing JNK1 protein. Such suppression limited the caspase dependent apoptosis signaling pathway and decreased cellular mortality induced by severe hypoxia. The results suggest that JNK1 protein might be an attractive target for antihypoxic therapy to increase resistance to many pathological conditions and diseases accompanied by cellular hypoxia.

DEDICATION

To Venkat, my husband and my best friend

To my daughter Maya, whose bright-eyed smiles made it easier to finish writing up

ACKNOWLEDGEMENTS

My days as a Ph.D student have been challenging, but wonderful and gratifying. One person, above all, who is directly responsible for that is my advisor, Dr. Tamara Minko. She has been an excellent mentor and provided strong motivation to me for completing each and every experiment in the present research. I would like to thank her not only for her sound advice, patience and encouragement, but also for her sheer energy and enthusiasm, which kept me going.

I would like to thank my committee members, Drs. Michniak, You and Mirochnitchenko for their suggestions and ideas and most importantly, their time, which allowed me to advance my research proposal and project.

My colleagues in the 'Minko' lab have been very helpful and supportive. They make our lab the cheerful work environment that it is. I am grateful to Drs. Isil Pakunlu, Yang Wang, Sonia Dharap and Jayant Khandare for their help during the early part of my research. I would also like to thank Dr. Mahesh Patil, Min Zhang and Pooja Chandna for their support and friendship. The *in vivo* experiments would not have been possible without the able support from Drs. Olga Garbuzenko and Elizabeth Ber.

I am also grateful to Marianne Shen, Amy Grabowski, Sharana Taylor and Hui Pung in the Department of Pharmaceutics and Barbara Sirman in the Graduate School for their assistance and patience in solving my problems.

One of the hardest things that I have ever done is doing my graduate work mostly part-time while holding a full-time job. I am indebted to my manager at Bristol-Myers Squibb Company, Dr. Ajit Thakur for his unflinching encouragement and support for the past seven years. I am also thankful to Dr. K. Raghavan for providing me the opportunity to pursue graduate studies outside of work.

I am eternally grateful to my parents for their love, patience and encouragement through every step along the way. Thanks to my brother, Sudarshan for lending an ear whenever I needed it. His patience and good sense is something that I have come to rely on. I would also like to thank my parents-in-law for their support.

My little daughter Maya has been incredible through the past two years. I am sure that she is the happiest of all to have got all this free time that Mommy now has!

To my husband, Venkat, I owe more than I can ever put into words. He is the one who I take my thoughts to at the end of each day. Thank you for supporting me through my graduate work, putting my needs ahead of yours, making me laugh when I was stressed and most of all, for your love.

TABLE OF CONTENTS

LIST OF TABLES

LIST OF FIGURES

LIST OF ABBREVIATIONS

AFM	Atomic Force Microscopy
a. u.	Arbitrary units
ASO	Antisense oligonucleotide
ATP	Adenosine triphosphate
BCA	Bincinchoninic acid
bp	base pairs
DLS	Dynamic light scattering
DNA	Deoxyribonucleic acid
dsRNA	Double stranded RNA
DOTAP	1,2 Dioleoyl-2-trimethylammonium propane
˚C	Degree Celcius
FITC	fluorescence isothiocyanate
KDa	Kilodaltons
kg	Kilogram
µL	Microliter
mL	Milliliter
mM	Millimolar
µM	Micromolar
mRNA	Messenger ribonucleic acid
MTT	(3-(4,5-dimethylthiazol-2-yl)-2,5-diphenyltetrazolium bromide)
nM	Nanomolar
nm	Nanometer
PBS	Phosphate buffered saline
pDNA	Plasmid DNA
RISC	RNA induced silencing complex
RT-PCR	Reverse transcriptase-polymerase chain reaction
siRNA	small interfering RNA

1 INTRODUCTION

Hypoxia is a state of oxygen deficiency. Many known pathological conditions lead to a decrease in oxygen supply of various cells causing oxygen deficit or secondary cellular hypoxia. When this secondary hypoxia becomes severe, it causes additional cellular damage, aggravating the primary disorder and leading to cell death. Therefore, remediation of secondary hypoxic damage should significantly increase the efficacy of treatment of primary disease and prevent extensive cellular damage. There are several environmental conditions that cause reduction in the oxygen supply of the body, such as high altitude, deep mining, diving, etc. Hypoxia influences the pathophysiology of anemia, polycythemia, tissue ischemia and cancer. The prevention of cellular death under these conditions may increase the working capacity of the whole organism and prevent severe adverse effects of tissue hypoxia.

Hypoxia inducible factor alpha (HIF1A) protein is a key initiator of cell death signal leading to the activation of caspases and causing cell death under hypoxia [1]. Recently, this protein was tested as a candidate for the remediation of hypoxic cellular damage. However, it was found that HIF1A plays a bimodal role during hypoxia [2]. While the activation of HIF1A initiates cell death signal inducing apoptosis, over expression of HIF1A simultaneously increases cellular resistance to hypoxia. Another protein family which is implicated in cellular hypoxic damage is mitogen-activated protein kinases (MAPKs), a family of serine-threonine protein kinases that participates in a major signaling system by which cells transduce extracellular stimuli into intracellular

responses [3]. The best-characterized vertebrate MAPKs fall into three sub-groups. The first sub-group includes the extracellular signal regulated kinases, ERK1 and ERK2. The second subgroup is the Jun N-terminal kinases (JNKs) so named, because they can activate the Jun transcription factor by phosphorylating two residues near its N-terminus. The third sub-group is the p38 MAPKs. The MAPK ERK pathway regulates growth proliferation and differentiation. Members of the MAPK JNK and MAPK p38 pathways are classified as stress activated protein kinases (SAPKs) because they are activated in response to stress such as osmotic shock, UV irradiation, inflammatory cytokines and hypoxia [4].

The major role in the activation of apoptosis signaling pathways and hypoxic damage is played by JNK – a stress-activated protein kinase that can be induced by inflammatory cytokines, bacterial endotoxin, osmotic shock, UV radiation, and hypoxia [5-7]. Activation of JNK by hypoxia mediates phosphorylation of activating transcriptional factor-2 (ATF2) and c-Jun bound to the *c-jun* promoter and stimulates their transcriptional activities leading to *c-jun* induction. The newly synthesized c-Jun protein combines with c-Fos protein to form stable transcriptional factor activator protein-1 (AP1) heterodimers. The formation of AP1 is a key step in the following induction of central cell death signal leading to the activation of caspase-dependent apoptosis signal and finally causing cell death. c-Jun N-terminal kinase 1 (JNK1, SAPK1, MAPK8) has been found to play a central role in the development of cellular damage under hypoxia, hypoxia/reoxygenation and ischemia/reperfusion.

The first set of studies in this research employ antisense oligonucleotides (ASO) and small interfering RNA (siRNA) against JNK1 mRNA in an *in vitro* hypoxia model for remediation of hypoxia. RNA interference mediated by small interfering RNAs is a powerful approach for dissecting gene function, drug target validation and disease therapy. The major obstacle to the use of siRNAs as therapeutics is the difficulty involved in effective delivery. An approach for the delivery of siRNAs into the cell has been investigated. The field of gene delivery, particularly siRNA, is still in its infancy and considerable advances are necessary to exploit its utility in mainstream therapeutics. Cationic lipids have been used in gene delivery because they can easily complex with anionic DNA/RNA molecules [8-11]. A positively charged complex is formed owing to electrostatic interaction of cationic polymers with anionic nucleic acids. The cationic polyplex can then interact with the negatively charged cell surface to improve uptake. When complexed with lipids, the nucleic acid is protected from nuclease degradation to various extents. N-[1-(2,3-Dioleoyloxy)]-N,N,N-trimethylammonium propane (DOTAP) is a widely used cationic lipid, is relatively cheap, and is efficient in both *in vitro* and *in vivo* applications. Cationic liposomes prepared using DOTAP have been used for delivery of siRNA. For the delivery of ASO, neutral liposomes have been used successfully in our laboratory [12,13]. We have proposed to increase the uptake and efficacy of ASO against JNK1 mRNA by delivering them using neutral liposomes.

Remediation of hypoxic damage has also been explored in an *in vivo* model of hypoxia. The efficiency of the liposomal drug delivery system for ASO and siRNA has been investigated in an *in vivo* mouse model. The final goal of the project is to effectively limit

apoptosis induction and cellular death under severe hypoxic conditions by suppressing JNK1 protein expression. The studies are expected to fill gaps in our understanding of the role of JNK1 in the development of hypoxic cellular damage. They address some of the issues related to the delivery of ASO and siRNA to suppress JNK1 mRNA and protein expression. The research findings provide promising evidence for the utility of JNK1-targeted ASO and siRNA delivered using liposomes for antihypoxic therapy to increase resistance to many pathological conditions and diseases due to oxygen deficit.

2 BACKGROUND AND SIGNIFICANCE

2.1 Hypoxia

Hypoxia is a state of oxygen deficiency in the body that is sufficient to cause an impairment of bodily functions. Hypoxia is caused by the reduction in partial pressure of oxygen, inadequate oxygen transport, or the inability of tissues to use oxygen.

Hypoxic Hypoxia is a reduction in the amount of oxygen passing into the blood. It is caused by a reduction in oxygen pressure in the lungs, by a reduced area of gas exchange, exposure to high altitude, or by lung disease.

Hypemic Hypoxia is defined as a reduction in the oxygen carrying capacity of the blood. It is caused by a reduction in the amount of hemoglobin in the blood or a reduced number of red blood cells. A reduction in the oxygen transport capacity of the blood occurs through blood donation, hemorrhage, or anemia.

Stagnant Hypoxia is an oxygen deficiency due to poor circulation of the blood or poor blood flow. Examples of this condition are high "G" forces, prolonged sitting in one position or hanging in a harness, cold temperatures and positive pressure breathing.

Histotoxic Hypoxia is defined as the inability of the tissues to use oxygen. Examples are carbon monoxide and cyanide poisoning.

2.1.1 Pathological conditions accompanied by hypoxia

Hypoxia influences the pathophysiology of anemia, polycythemia, tissue ischemia, stroke, myocardial infarction, lung edema and cancer. Several physiologically relevant genes are up regulated in response to changes in intracellular oxygen tension. These include erythropoietin, which regulates red blood cell production; vascular endothelial growth factor (VEGF), which is up-regulated in tumors and in ischemia tissue; tyrosine hydroxylase, an enzyme critical for dopamine synthesis in the carotid body; and glycolytic enzymes which maintain ATP production [14].

Ischemia is insufficient blood flow to provide adequate oxygenation. This, in turn, leads to tissue hypoxia (reduced oxygen) or anoxia (absence of oxygen). Ischemia always results in hypoxia; however, hypoxia can occur without ischemia if, for example, arterial hypoxia occurs. The most common causes of ischemia are acute arterial thrombus formation, chronic narrowing (stenosis) of a supply artery that is often caused by atherosclerotic disease, and arterial vasospasm. As blood flow is reduced to an organ, oxygen extraction increases. When the tissue is unable to extract adequate oxygen, the partial pressure of oxygen within the tissue falls (hypoxia) leading to a reduction in mitochondrial respiration and oxidative metabolism. High altitude residency, deep sea diving, air pollution, flying at high altitudes, endurance exercise, physical and emotional stress can also lead to tissue insufficiency.

Hypoxia affects many organ systems including the lungs, brain, heart, kidney and liver. There are several pathological conditions accompanied by hypoxia. For e.g. Acute Respiratory Distress Syndrome (ARDS) is acute lung injury accompanied by severe

hypoxia, increased microvascular permeability and diffuse pulmonary infiltrates. The mortality rates with ARDS are 40-50% [15]. Respiratory passageway obstruction, pulmonary insufficiency or right-to-left shunt in the heart can lead to attenuation in oxygen partial pressure in alveoli or arterial blood oxygen tension [16]. Hypoxia accompanies renal ischemia, which can result from kidney transplant, trauma, obstructive uropathy, surgery and cardiopulmonary bypass. Hypoxia has significant implications in the kidney, where large quantities of oxygen are required to sustain metabolic activity. During renal ischemia, oxygen partial pressures of $\leq$ 35 mm Hg are generally considered hypoxic. Chronic hypoxia is a final common pathway leading to end-stage renal failure [17]. Ischemia of the kidney is induced by the loss of peritubular capillaries in the tubulointerstitium in the late stage of renal disease. At the cellular level, ischemia can induce apoptosis and/or necrosis depending upon the severity and duration of the insult and the cell type. Upon reperfusion and reoxygenation, cellular injury may continue to occur [17,18]. The brain is known to be the most vulnerable tissue to stimuli such as hypoxia and ischemia.

2.1.2 Mechanisms of hypoxic damage and physiological response to hypoxia

Mammalian cells require a constant supply of oxygen to maintain adequate energy production, which is essential for maintaining normal function and for ensuring cell survival [19]. Even brief episodes of hypoxia can result in cessation of oxidative phosphorylation and depletion of cellular adenosine triphosphate (ATP), which results in profound deficiency in cellular function. Mitochondrial respiration is arrested by low

oxygen tension and ATP content decreases when cells are exposed to hypoxia. Sustained hypoxia can result in cell death. Brain cells are extremely sensitive to oxygen deprivation. Some brain cells actually start dying just under five minutes after their oxygen supply is cut. As a result, brain hypoxia can kill or cause severe brain damage rapidly. If the lack of oxygen to the brain is limited to a very brief period of time, coma may be reversible with varying levels of return to function, depending on the extent of injury.

HIF-1 (hypoxia-inducible factor-1) is the major transcription factor specifically activated by hypoxia. HIF-1 is a heterodimer consisting of an α- and a β-subunit. The α-subunit is specific for hypoxia. The HIF-1 heterodimer binds to response elements of a number of genes that are up-regulated by hypoxia. It induces the expression of different genes whose products play an adaptative role for hypoxic cells and tissues. Besides these protective responses, HIF-1 and/or hypoxia have also been shown to be either anti-apoptotic or pro-apoptotic, according to the cell type and experimental conditions. More severe or prolonged hypoxia induces apoptosis, at least in part, initiated by the direct association of HIF-1α and p53 and p53-induced gene expression. On the other hand, HIF-1α dimerized with ARNT, as an active transcription factor, can protect cells from apoptosis induced by several conditions.

2.1.3 Response to hypoxia

Sensing of increased or decreased oxygen levels occurs through specialized chemoreceptor cells that regulate cardiovascular and ventilatory rates. Cells sense oxygen concentration and respond to reduced oxygen availability acutely (within minutes) through the activation of pre-existing proteins and chronically (within hours) through the regulation of gene transcription. During episodes of compromised oxygen availability, several chemosensory systems, acting in concert, rapidly modulate pulmonary ventilation and perfusion as well as blood circulation to optimize the supply of oxygen to metabolizing tissues. These responses rely both on specialized cells such as the carotid bodies present in the airway and on the direct response of vascular smooth muscle cells to hypoxia. Airway neuroepithelial bodies sense changes in inspired oxygen, whereas arterial oxygen levels are monitored by the carotid bodies. Both respond to decreased O_2 supply by initiating activity in efferent chemosensory fibers to produce cardiorespiratory adjustments on exposure to low environmental O_2. At the cellular level, adaptation to hypoxia is brought about on one hand by increasing the efficiency of energy-producing pathways, mainly through increased anaerobic glycolysis activity, and on the other hand by decreasing energy-consuming processes. Several responses are developed by cells and tissues faced with a hypoxic challenge: 1) increased ventilation and cardiac output 2) a switch from aerobic to anaerobic metabolism 3) promotion of improved vascularization, and 4) enhancement of the oxygen carrying capacity of the blood. Most of these processes take place very early at the onset of hypoxia and occur through the activation of already present proteins, but in the long term all of them are also mediated by the upregulation of genes encoding key actors of these responses. The transcriptional response is mediated in a large part by HIF-1 [19].

2.2 Experimental models of hypoxia

There are a number of reports of experimental models of hypoxia in literature. These models have been used to study many pathological conditions accompanied or upregulated by hypoxia such as cardiac ischemia, angina, myocardial infarction, acute respiratory lung syndrome (ARS) and liver hypoxia. Some of these experimental models reported recently are noted below.

In a study by Agoretta et al., both *in vivo* and *in vitro* models of hypoxia were used for investigation of ARS/acute lung injury [15]. Their study evaluated the expression of adrenomedullin in acute lung injury using experimental models: an *in vivo* model of rats treated with acute normobaric hypoxia (9% O_2) and an *in vitro* model of rat lung cell lines exposed to hypoxia (1% O_2 calculated based on alveolar gas equations).
A novel and simple method for creating regional hypoxic and ischemic conditions in neonatal rat cardiac myocyte monolayers was described by Pitts et al. *In vitro* experimental models designed to study the effects of hypoxia and ischemia typically employ oxygen-depleted media and/or hypoxic chambers. The authors claimed that these approaches allow for metabolites to diffuse away into a large volume and may not replicate the high local concentrations that occur in ischemic myocardium *in vivo*. Their method consisted of creating a localized diffusion barrier by placing a glass coverslip over a portion of the cardiac myocytes monolayer. The coverslip restricts covered myocytes to a thin film of media while leaving uncovered myocytes free to access the surrounding bulk media volume. In contrast with existing models of hypoxia/ischemia,

this technique provides a simple and effective way to create hypoxic/ischemic conditions *in vitro*. Moreover, authors conclude that myocyte death is hastened by the combination of hypoxia, metabolites, and acidosis and is facilitated by a reduction in media volume, which may better represent ischemic conditions *in vivo* [20].

An *in vivo* temporal hepatic arterial hypoxic model was used in a study for investigating the mechanism of hypoxic injury and the critical point of liver hypoxia on hepatic and/or systemic hemodynamics and liver viability. The study introduced a novel experimental canine model of hepatic arterial deoxygenation using a membrane oxygenator to investigate the influence of hepatic arterial hypoxia on hepatic hemodynamics and energy metabolism. Deoxygenation was achieved by perfusion of a gas mixture of O_2 and N_2 through a membrane oxygenator, which was interposed between the femoral artery and the proper hepatic artery of the dog [21]. In another study, a model of nonischemic hypoxia of the jejunum was designed in dogs, by shunting of blood from the inferior vena cava directly into the regional mesenteric arterial supply, thereby lowering the partial oxygen pressure of the blood that reached the jejunal wall [22]. Poizat et al. developed an experimental model of hypoxia on isolated rat heart to study the effects of hypoxia on cardiac performance and metabolism. Isolated hearts, after 30 min preperfusion in an open system, were transferred to a recirculating system for 40 min and perfused in an environment of either normoxia (pO_2 = 660 mmHg) or hypoxia (pO_2 = 220 mmHg) [23].

To study the effect of hypoxic stress on rat myocardium, a model system consisting of a hypoxia chamber combined with a commercial narcosis apparatus adapted to small

animals was used to perform a controlled acute isobaric hypoxia on rats with N_2O/O_2. The authors note that the model can be recommended for studies concerning protective interventions in hypoxia experiments [24].

2.3 Remediation of hypoxia

At a certain stage of the primary disorder, oxygen delivery to tissues significantly decreases and disrupts the balance between cellular oxygen supply and demand. As a result, tissue hypoxia develops. This secondary tissue hypoxia and accompanied cellular metabolic disorders significantly complicate the primary disease or adaptation to the damaging environmental impacts. Therefore, in parallel with the measures directed for the correction of the main cause of secondary tissue hypoxia, it would be beneficial to simultaneously use antihypoxic drugs that increase cellular resistance to oxygen deficiency. This pharmacological remediation of secondary hypoxic damage will increase the efficacy of the treatment of the primary disease and prevent extensive cellular damage [16].

2.3.1 Pharmacological agents that remediate hypoxia

Antihypoxic agents should increase the resistance of the organism against hypoxia by breaking down the vicious cycle of hypoxic damage and inhibiting cellular apoptotic signal. Pharmacological antihypoxic agents (PAA) with antihypoxic action can be

divided into three groups 1) PAAs that regulate oxygen transport 2) PAAs that influence cellular metabolism 3) PAAs that limit hypoxic cellular damage [16].

2.3.1.1 PAAs that regulate oxygen transport

PAAs that increase oxygen delivery to tissues function by increasing the volume of ventilation and its efficacy, enhancing the blood oxygen transport and facilitating the oxygen release from blood to tissues.

PAAs that increase lung ventilation

The use of such PAAs is intended to increase oxygen tension in the arterial blood. Agents that can be classified in this group include substances of central action such as dopamine antagonists and other pharmacological agents that increase lung ventilation, inhibitors of carbo anhydrase which lead to the accumulation of carbon dioxide in the blood and chemoreceptor stimulation of ventilation. However, under excessive ventilation, carbon dioxide tension in the arterial blood significantly decreases leading to spasm of vessels that provide oxygen to brain and heart. Therefore, PAAs that increase lung ventilation can be prescribed only under marked hypoventilation accompanied by hypercapnia (decrease in CO_2).

PAAs that enhance efficiency of lung ventilation and gas exchange

This group of PAAs includes bronchospasmolytics [25-27] trypsin inhibitors [28,29], vasodilating agents [30-32] and surfactant substitutes [33-35]. It is known that rapid ascent to high altitude causes hypoxic pulmonary vasoconstriction and leads to high altitude pulmonary edema in susceptible humans. Therefore, vasodilating agents may potentially decrease the severity of hypoxic edema or eliminate it by preventing hypoxic pulmonary vasoconstriction. Examples of vasodilating agents include acetazolamide and nickel chloride.

The disturbances of metabolism in the lungs, activation of lipid peroxidation, shifts of the optimal ratio between synthesis and destruction of phospholipids in the lungs under severe hypoxia leads to significant changes in phospholipid composition of lung surfactant and parenchyma. The disturbance in lung phospholipid pattern decreases lung compliance. This in turn requires shift in respiratory pattern leading to increase of energy expense of breathing. The change in the lipid composition of parenchyma combined with its edema increases oxygen diffusion path from the air to the blood and leads to a decrease in the lung diffusion capacity. This disturbs lung gas exchange. Pharmacological stimulation of phospholipid production in the lungs has a low efficacy under oxygen and energy deficit and might be dangerous because it requires significant energy expenditure and might worsen tissue hypoxia. Therefore, a substitution therapy with artificial surfactant like Infasurf may be helpful and provide a temporary solution.

PAAs that enhance blood oxygen transport

Different oxygen transporters, agents that increase myocardial contractility and the volume of circulating blood, stimulators of erythropoeisis and respiratory function of blood, stimulators of angiogenesis and other agents can be classified among this group. Perfluorocarbon emulsions have been studied as oxygen transporters under experimental traumatic brain injury, hyperoxia, hypercapnia and hypoxia [36,37]. However, the emulsions did not prevent another determinant of hypoxic tissue injury, the increased free radical formation. Therefore the use of antioxidants combined with oxygen transporters may be helpful. The disadvantage of known artificial oxygen transporters is toxicity and degradation with generation of toxic products.

2.3.1.2 PAAs that influence cellular metabolism

These include agents that i) decrease cellular metabolism, ii) switch the pathways of cellular oxidation and iii) enhance biological oxidation

PAAs that decrease cellular metabolism

The agents in this group include beta-adrenomimetics [38-40], gutimine, GABA and taurine based agents [41-45] and L-carnitine [46]. This group of pharmaceutical agents that decrease tissue oxygen demand is under investigation and clinical evaluation. The methods based on the decrease in the actual oxygen consumption may be effective in extreme situations, but have limited usefulness for prolonged therapy of hypoxia.

PAAs that switch the pathways of cellular energy metabolism

There are three main pathways of cellular energy production. The first pathway, glycolysis, while resulting in relatively less energy provides energy fast. The second pathway, oxidative phosphorylation is the main pathway in aerobic conditions on the background of unlimited oxygen supply and availability. This pathway is limited under hypoxia when cellular oxygen supply is substantially reduced. The third pathway, pentose phosphate pathway represents direct oxidation in cytosol and provides more energy but is slower compared to glycolysis. The switch from the first to the third energy production pathway may be done using sodium oxybutyrate and gamma hydroxybutyrate, serotonin, barbiturates, venotropic drugs and phenotiasin [41,47-51]. However, activation of cellular aerobic processes is unlikely justified under hypoxic conditions accompanied by oxygen deficit. The switch of cellular energy metabolism from the third to the first pathway may be forced by insulin, application of which in combination with glucose and potassium may be beneficial under the situation when immediate energy production is required. Gamma hydroxybutyrate has been shown to produce a protective effect in animal models of cerebral ischemia/hypoxia as well as in human conditions of head injury-induced coma.

PAAs that enhance biological oxidation

This group includes vitamins, amino acids, methylene blue, unitol and dicaptol, pentoxyl, methyl uracil and cystamine [52-58]. The disadvantage of such agents is related to the necessity of their prolonged use.

2.3.1.3 PAAs that limit hypoxic cellular damage

These agents provide a decrease in the degree of hypoxic cellular damage and prevent cell death. Some of the main consequences of tissue hypoxia and the decreased efficiency of its compensation are metabolic acidosis, lipid peroxidation and apoptosis induction [34].

Metabolic acidosis

Therapy of metabolic acidosis includes measures that provide decrease in the production of lactic and other metabolic acid, pH correction and elimination of acids from the organism. Alkali therapy is the only method that is being currently used to increase blood pH [59-61]. During correction of acidosis, there is a characteristic resistance to injection of alkali. Acidosis persists despite the injection of high doses of alkali such as bicarbonates and tris-amine, while the concentration of lactic acid does not increase. Lactate acidosis in blood is generally accompanied by deep intracellular acidosis, which persists despite alkali therapy.

Antioxidants

Since lipid peroxidation plays an important role in hypoxic cellular damage, antioxidants can be successfully used to promote resistance to severe hypoxic damage. There are reports of use of natural (alpha tocopherol) and synthetic antioxidants [35,62-65] antioxidant enzymes (super-oxide dismutase, catalase) and their mimetics for this purpose. Alpha tocopherol was found to normalize phospholipid composition of lungs; it significantly inhibited lipid peroxidation and apoptosis induction thus limiting lung damage under severe hypoxia in rats. The main disadvantage of these PAAs includes the required prolonged use mainly for prophylaxis and the limited possibility to inject such substances directly into the blood or in the damaged organ.

Antiapoptotic therapy

Activation of cellular apoptotic signaling by hypoxia leads to cell death by apoptosis. Therefore, preventing apoptotic cell death should increase the resistance to severe hypoxia and hypoxic cellular damage. The limitation of cellular proapoptotic signal can be achieved by the decrease in initial hypoxic cellular damage that triggers cellular apoptotic cascade. Another way of preventing cellular apoptotic death is the increase in the activity of cellular antiapoptotic defense. Such increase may be achieved both by inhibition of the proapoptotic and/or activation of antiapoptotic members of the Bcl-2 protein family. PR39, a praline and arginine rich peptide was found to protect against hypoxia induced apoptosis [66]. Homocarnosine, a neuroprotective histidine dipeptide was found to prevent neuronal death induced by oxygen-glucose deprivation followed by

reoxygenation, possibly by inhibiting the apoptotic process and/or in relation to the differential attenuation of activity of MAPKs [67].

2.4 Apoptosis

Programmed cell death (apoptosis) plays a critical role in many biological processes in multicellular organisms, such as embryonic development, immune responses, tissue homeostasis and normal cell turnover [68-71]. The development and maintenance of healthy tissues involves apoptosis, a program of physiologically regulated cell death. Dysregulated apoptosis contributes to many pathologies, including tumor promotion, autoimmune and immunodeficiency diseases, and neurodegenerative disorders. Therefore, signaling pathways that trigger apoptosis are of intense interest. The initiation and execution of apoptosis depend on activation of extrinsic and/or intrinsic death pathways [72-75]. There are several different mechanisms by which a cell commits suicide by apoptosis (Fig. 2.1). One generated by signals arising within the cell; another triggered by death activators binding to receptors at the cell surface and a third that may be triggered by dangerous reactive oxygen species. A family of proteins known as caspases is typically activated in the early stages of apoptosis and these proteins in turn activate other degradative enzymes such as DNAses. Apoptosis involves cleavage of chromosomal DNA into nucleosomes in a systematic manner. This fragmentation of DNA is brought about by caspase activated DNAse enzyme, which is released from inactive state due to cleavage of its inhibitor by a caspase. Mitochondria play an important role in the regulation of cell death. Various proteins located on the outer

mitochondrial membrane regulate cell survival and death. Mitochondria release cytochrome C in response to the apoptotic signals, which together with Apaf-1 and ATP forms a complex with pro-caspase 9, leading to the activation of caspase 9 and the caspase cascade. The caspase cascade of proteolytic activity leads to digestion of structural proteins in the cytoplasm, degradation of chromosomal DNA, and phagocytosis of the cell.

Death receptors are another means by which cells can undergo programmed cell death (Fig. 2.1). They bind to specific ligands and initiate the apoptotic process and the caspase cascade. They include Tumor necrosis factor-alpha (TNF-α) that binds to the TNF receptor, Lymphotoxin (also known as TNF-β) that also binds to the TNF receptor and Fas ligand (FasL) that binds to Fas. The apoptotic process is regulated by many intracellular signaling pathways, including the JNK pathway [76-79]. Understanding the molecular mechanisms by which JNK regulates apoptosis should provide insights into treatment and prevention of many diseases. The c-Jun NH_2-terminal kinase (JNK) signaling pathway is essential for neuronal apoptosis in response to excitotoxic stress [19].

2.5 MAPK/JNK and hypoxia

The best-characterized vertebrate MAPKs fall into three sub-groups. The first sub-group includes the extracellular signal regulated kinases, ERK1 and ERK2. The second subgroup is the Jun N-terminal kinases (JNKs) so named, because they can activate the

Jun transcription factor by phosphorylating two residues near its N-terminus. The third sub-group is the p38 MAPKs. The MAPK ERK pathway regulates growth proliferation and differentiation. Members of the MAPK JNK and MAPK p38 pathways are classified as stress activated protein kinases because they are activated in response to osmotic shock, UV irradiation, inflammatory cytokines and hypoxia [4].

C-Jun N-terminal protein kinase (JNK) is a subfamily of the mitogen activated protein kinase (MAPK) superfamily [80,81]. JNK has three isoforms (JNK1, 2 and 3), with slicing variant [77]. Among them, JNK1 and JNK2 are ubiquitously expressed while JNK3 is mainly expressed in neuronal and heart tissues [37,76,78,79]. JNK was originally identified by its ability to specifically phosphorylate the transcription factor c-Jun on its N-terminal transactivation domain at two serine residues, Ser63 and Ser73 [80]. The transcription factor c-jun mediates cell stress response. It is a component of the AP-1 transcription complex, which is an important regulator of gene expression. AP-1 contributes to the control of many cytokine genes and is activated in response to environmental stress and growth factors [82]. AP-1 plays a central role in induction of cell death signal leading to the activation of caspase dependent apoptotic signal and finally causing cell death. Subsequent studies have shown that JNK also phosphorylates and regulates the activity of transcription factors other than c-Jun, including ATF2, Elk-1, p53 and c-Myc [36,37,39,83] and non-transcription factors, such as members of the BCL2 family (BCL2, BCLXL, BIM and BAD), in response to a variety of extracellular stimuli (Fig. 2.2). Activation of JNK is mediated by a MAP kinase module, i.e., MAP3K, MAP2K and MAPK, through sequential protein phosphorylation. Hypoxia plays a role in

regulating mitogen activated protein kinase (MAPK) pathways via upstream and downstream mechanisms (Fig. 2.3).

2.5.1 JNK as a proapoptotic protein kinase

There is evidence showing that JNK can function as a proapoptotic kinase [9, 12]. Biochemical studies revealed that apoptosis induced by nerve growth factor (NGF) withdrawal in rat PC-12 pheochromocytoma cells was suppressed by inhibiting the JNK pathway, whereas activation of the JNK pathway by expressing a constitutively active MEKK1 induced apoptosis in PC-12 cells. Yet, the exact molecular mechanism by which c-Jun mediates the proapoptotic function of JNK remains to be elucidated. JNK is also involved in apoptosis induced by other death stimuli in non-neuronal cells. Mouse embryonic fibroblasts (MEFs) deficient in both jnk1 and jnk2 were resistant to ultraviolet (UV) irradiation induced apoptosis. Recent studies showed that genetic disruption of JNK1 alleles alone was sufficient to render immortalized mouse fibroblasts resistant to UV induced apoptosis.

2.5.1.1 How JNK contributes to apoptosis

It is clear that activation of the JNK pathway is involved in apoptosis induced by certain death stimuli. Two hypotheses have recently been proposed to explain how JNK activation may contribute to apoptosis. The major difference between these two hypotheses is whether JNK activation is sufficient to induce or only promote apoptosis,

as discussed below. The key evidence that suggests JNK could induce apoptosis came from the observation that *jnk*1$^{-/-}$*jnk*2$^{-/-}$mice were resistant to apoptosis induced by UV irradiation, anisomycin and MMS [81]. Since UV was unable to induce cytochrome C release or depolarization of mitochondrial membrane potential in *jnk*1$^{-/-}$*jnk*2$^{-/-}$mice, it was proposed that JNK is an intrinsic component of the mitochondrial-dependent death pathway during stress-induced apoptosis. In support of this conclusion, it was reported that in CHO cells the constitutively active JNKK2-JNK1 fusion protein was sufficient to induce apoptosis by activating the intrinsic death pathway. However, overexpression of a JNKK2-JNK1 fusion protein, which has constitutive JNK activity, did not induce apoptosis in *Rel*A$^{-/-}$ fibroblasts or in other cells including wild type or *Ikk*$^{-/-}$ fibroblasts and HeLa cells. In addition, no increased caspase activation or DNA fragmentation occurred in cells that express the constitutively active JNK when compared to cells that express control vector or a kinase-deficient JNKK2 (K149M)-JNK1 mutant. Identification of JNK target(s) in apoptosis is critical to test these two hypotheses. Further studies are needed to determine whether JNK activation is sufficient to induce or only promote apoptosis.

2.5.1.2 The JNK-dependent apoptotic signaling pathway

It has been established that the JNK pathway is activated by the exposure of cells to stress. However, the exact role of JNK in the stress-response pathway has not been elucidated. It is possible that JNK may mediate some of the effects of stress on cells. Alternatively, JNK may also represent a protective response that is initiated by the

exposure to stress. The specific role of JNK in apoptosis may therefore depend upon the cell type, the nature of the death stimulus, the duration of its activation and probably, the activity of other signaling pathways [77,78]. Indeed, the JNK pathway has been implicated in both apoptosis and survival signaling.

The indication that the JNK pathway might be involved in apoptosis came from studies in neuronal cells. Injection of neutralizing antibodies against c-Jun or overexpression of a c-Jun truncated mutant lacking its N-terminal transactivation domain blocked apoptosis induced by nerve growth factor (NGF) withdrawal [84]. Conversely, overexpression of wild-type c-Jun induced apoptosis of cultured sympathetic neurons. Subsequently, it was reported that apoptosis of rat PC-12 pheochromocytoma cells following NGF withdrawal was inhibited by expressing dominant negative mutants of the JNK pathway, while overexpression of a constitutively active MEKK1, which is a MAP3K for JNK was able to induce apoptosis in PC-12 cells [85,86].

It has been reported that c-Jun NH2-terminal kinase (JNK) is activated when cells are exposed to ultraviolet (UV) radiation. It was shown that primary murine embryonic fibroblasts with simultaneous targeted disruptions of all the functional JNK genes were protected against UV-stimulated apoptosis. The absence of JNK caused a defect in the mitochondrial death signaling pathway, including the failure to release cytochrome c. The data indicate that mitochondria are influenced by proapoptotic signal transduction through the JNK pathway [87].

2.6 siRNA

RNA interference (RNAi) is an evolutionarily conserved mechanism for silencing gene expression. In primitive organisms, RNAi protects the genome from viruses and other insertable genetic elements and regulates gene expression during development. RNAi was first described in animal cells by Fire and colleagues in the nematode Caenorhabitis elegans [88]. They found that introducing long double-stranded RNA (dsRNA) into C. elegans led to the targeted degradation of homologous mRNA. Tuschl and colleagues showed that RNAi also occurs in mammalian cells [89]. The discovery that RNAi works in mammalian cells has sparked intense investigation into its role in normal mammalian cell function, its use as a tool to understand or screen for genes functioning in cellular pathways in healthy and diseased cells and animals, and its potential for therapeutic gene silencing. In the past few years there has been an RNAi revolution as researchers have sought to understand how RNAi works to regulate gene expression, have used it to perform reverse genetics in mammalian cells and have begun to explore its potential therapeutic use. RNAi may provide an important new therapeutic modality for treating infection, cancer, neurodegenerative disease, and other illnesses, although *in vivo* delivery of small interfering RNAs into cells remains a significant obstacle [90].

2.6.1 The silencing mechanism

The effector molecules that guide mRNA degradation are small (21 to 25 oligonucleotide dsRNA), termed small interfering RNAs, produced by cleavage of long dsRNAs.

Silencing triggers in the form of double-stranded RNA may be presented in the cell as synthetic RNAs, replicating viruses or may be transcribed from nuclear genes. These are recognized and processed by cytoplasmic highly conserved Dicer family of RNAse II-like enzymes into small interfering duplex RNAs with symmetric 2- to 3-nt 3' overhangs. The duplex siRNAs are passed to RISC (RNA-induced silencing complex), and the complex becomes activated by unwinding of the duplex. The antisense (guide) strand of the siRNA directs the endonuclease activity of RISC to the homologous (target) site on the mRNA resulting in mRNA cleavage (Fig. 2.4). Activated RISC complexes can regulate gene expression at many levels. Almost certainly, such complexes act by promoting RNA degradation and translational inhibition. However, similar complexes probably also target chromatin remodeling [88,91]. The antisense (guide) strand of short double-stranded RNAs is incorporated into an RNA-induced silencing complex that can either suppress protein expression or direct degradation of messenger RNAs that contain homologous sequence(s).

There is increasing enthusiasm for developing therapies based on RNA interference (RNAi). The advantage of RNAi lies in its high specificity and potent gene silencing, coupled with the fact that it can potentially target every gene and every cell has the necessary machinery. Although some questions remain about specificity and activation of off-target effects, none of these problems has yet been documented *in vivo*. Moreover, some potential untoward events can likely be avoided by judicious choice of sequences or chemical modification of siRNAs [92].

2.6.2 Delivery of siRNA

One of the major challenges in transforming small interfering RNA duplexes from laboratory reagents to therapeutics is developing an effective drug delivery mechanism. Although the delivery of siRNA to cultured cells is satisfactory for most *in vitro* applications, therapeutic delivery *in vivo* presents an altogether more daunting challenge. The main obstacle to the use of siRNA is delivery into the cytosol, where they need to be present for silencing. Naked siRNA are not efficiently taken up even by cells such as macrophages and dendritic cells, which are actively sampling their environment using pinocytosis. A further obstacle is the short *in vivo* half-life of siRNAs (minutes) due to rapid renal clearance. In addition, some serum RNases can degrade siRNAs leading to a short serum half-life. Ideally, a delivery mechanism would be capable of binding siRNAs in a reversible manner (to ensure subsequent efficient release of the siRNAs in target cells), allow protection (from nucleases) during transit through the circulation and on release into endosomes, be biocompatible (nontoxic and nonimmunogenic) and biodegradable, and avoid rapid capture and clearance by the liver and kidney.

Some early steps in addressing these challenges have been made. There are two main strategies that have been used to deliver siRNAs *in vivo*. One is to stably express siRNA precursors, such as shRNA from viral vectors using gene therapy. The other is to deliver synthetic siRNAs by complexing or covalently linking duplex RNA with lipids and/or delivery proteins. Coupling of siRNAs to basic fusogenic peptides has been reported to facilitate the transport of siRNAs across the cell membrane [93]. In a recent study, a

significant improvement in siRNA delivery *in vivo* was achieved by covalent attachment of cholesterol to one of the siRNA strands, which were then introduced intravenously, via low-pressure injection, into mice [94]. These studies resulted in effective reduction of the apolipoprotein B and consequently, cholesterol levels in the animals in both liver and jejunum.

One of the most common methods used for the delivery of charged nucleic acids involves their electrostatic interaction with cationic carriers. Several types of cationic carriers such as liposome/lipids, dendrimers, and polymeric amines have been successfully used for the delivery of plasmid DNA and oligonucleotides *in vitro* [95]. Even though siRNA is structurally similar to plasmid DNA with negatively charged anionic phosphodiester backbones, electrostatic interaction of siRNA largely differs from that of plasmid DNA [96]. The molecular weight and molecular topography of siRNA and plasmid DNA plays an important role in their electrostatic interaction with cationic agents. All pDNA condenses into small nanoparticles of 60-100 nm after neutralization of 70-90% of its phosphodiester backbone charge with a cationic agent. Cationic agent-condensed pDNA can then exist in a variety of different morphologies depending upon the cationic condensing agent, such as spheres, toroids, and rods. Such behavior ensures that pDNA is almost entirely encapsulated or encased by the cationic agent and protected from enzymatic or physical degradation within nanometric particles. In contrast to pDNA, siRNA cannot condense into particles of nanometric dimensions, being already a small subnanometric nucleic acid. Nonviral vectors, and especially polymers, form looser complexes with siRNA than with plasmid DNA and incomplete encapsulation of the

nucleic acid sometimes leads to the exposure of siRNA to enzymatic or physical degradation prior to delivery to the targeted cells. Consequently, carriers that are successfully used for the delivery of plasmid DNA cannot necessarily be efficiently employed for the delivery of siRNA, and a different approach may be required.

Efforts to deliver naked siRNAs involved high pressure tail-vein injections, resulting in target-specific degradation of a reporter gene transcript in the liver [97]. However, this harsh treatment requires the rapid injection of solutions two-and-a-half times the blood volume of the animal. Song *et al*. developed heavy-chain antibody fragment (Fab)-protamine fusion protein that deliver noncovalently bound siRNAs via surface receptors to cells [92]. Some lipid-mediated transfection methods that work *in vitro* can also be used for *in vivo* delivery. Cationic polymer and lipid based siRNA complexes have been used for systemic delivery in mice [98,99]. In one study, pretreatment by intraperitoneal injection of cationic liposomes containing siRNAs that targeted TNF-alpha were found to be successful for the intended purpose of providing protection from sepsis induced by lipopolysaccharides [98]. Intravenous immunoliposomes have shown efficacy in delivering siRNAs across the blood brain barrier into glioma cells in the central nervous system [100]. Optimization of the *in vivo* stability of siRNAs has been accomplished by chemically modifying the RNA backbone, and several strategies have been used with some success for improved *in vivo* stability that may eventually reduce the requirement for high dosage. These include 2′F, 2′O–Me and 2′H substitutions in the RNA backbone, all of which increase serum stability without significant compromise in activity [101].

Other *in vivo* delivery approaches for siRNAs include conjugation of cholesterol to the siRNA sense strand [94], antibody-protamine fusions that bind siRNAs [92], cyclodextrin nanoparticles [102] and aptamer-siRNA conjugates [103]. Development of RNAi based therapeutics is still in its infancy. Some early clinical studies have shown potential for the use of this new class of therapeutics to tackle challenging diseases in medicine [101].

2.7 Antisense oligonucleotides

Oligonucleotides that control gene expression at the translational level are known as antisense oligonucleotides (ASO). They are small, chemically modified strands of DNA, engineered in a sequence that is exactly opposite (hence, "anti") to the coding ("sense") sequence of mRNA. ASOs work at post-transcriptional levels. Normally, transcription of any given gene is carried out by the RNA polymerase II from a transcription start site to give rise to heteronuclear RNA, which is processed by splicing and polyadenylates to mature mRNA that is transported to the cytoplasm where it gets translated into protein. ASOs are designed to bind to their target sense RNA sequence through the formation of reverse complementary strands with the mRNA (Fig. 2.5). The two mechanisms that likely play a part in inhibition of gene expression by ASO are: 1) direct blocking in pre-mRNA and/or mRNA of sequences important for processing or translation, and 2) degradation of the RNA transcript by RNase H at the site of oligonucleotide binding. The ASO is undamaged by enzymatic attack and is free to hybridize with multiple RNA molecules leading to their destruction in a catalytic manner (Fig. 2.5).

There has been a tremendous progress in the understanding and application of antisense oligonucleotides since first proposed in 1978 by Zamecnik and Stephensen [97]. Extensive medicinal chemistry has been done on antisense nucleic acids and hundreds of compounds have been tested in a search for modifications that improve nuclease stability, increase binding affinity (melting temperature, or Tm), and improve the *in vivo* pharmacodynamic properties of oligonucleotides as drugs [7,8]. Pharmaceutical companies have been working to develop antisense drugs for more than 15 years and extensive knowledge of the pharmacology and toxicology of synthetic nucleic acids in vivo has been compiled [9]. As of 2005, one antisense drug is on the market. Formivirsen (Vitravene), a product of Isis Pharmaceuticals and Novartis Ophthalmics, is a 21-mer phosphorothioate DNA oligonucleotide that is complementary to the immediate early region 2 of cytomegalovirus (CMV). This compound has been shown to be effective in the treatment of CMV retinitis and was approved by the FDA for use by direct intravitreal injection in 1998 [10,11]. A number of different ASOs have been in clinical trials against many diseases such as human immunodeficiency virus HIV infections and cytomeglovirus CMV ocular infections as well as in the control of hematological disorders [101].

2.7.1 Design of oligonucleotides

Design is critical for the clinical efficacy of oligonucleotides and should include consideration of length, chemistry, conformation, and ability to hybridize with the target mRNA [104]. The suggested optimal length for oligonucleotides with efficient antisense

activity ranges from 12 to 28 bases. There is a consensus that very short sequences are likely to be nonspecific and sequences longer than 25 bases would experience difficulty in cellular uptake. Oligonucleotides having the endogenous phosphodiester backbone are susceptible to degradation by serum and cellular nucleases and hence have limited use for antisense applications. Various chemical modifications to the backbone have been used to improve oligonucleotide stability. The most common modifications include the introduction of phosphorothioate and methyl phosphonate linkages in the backbone. Phosphorothioate analogs are chosen for their stability against nucleases and the methylphosphonate backbone for its relative hydrophobicity and ease of diffusion across membranes. Phosphorothioate backbone oligonucleotides can have significantly increased biological half-life compared to their corresponding unmodified phosphodiester oligonucleotides [104].

2.7.2 Delivery of oligonucleotides

Delivery systems play a critical role in the realization of the therapeutic potential of oligonucleotides and other DNA based therapeutics. The *in vitro* and *in vivo* stability of oligonucleotides is an important consideration for their delivery. Due to their polyanionic properties, cells take up the nucleic acids by a combination of pinocytosis, adsorptive and receptor-mediated endocytosis. After the binding of an oligonucleotide to a cell-surface protein, internalization into the endocytic compartment occurs. This is an active process and despite previous data, it now appears that in many cell types, adsorptive endocytosis is the major mechanism by which naked oligonucleotides are internalized. The process of

fluid phase endocytosis (pinocytosis) contributes a relatively small amount at a relatively low oligonucleotide concentration, but a cell-type-dependent increasing percentage as the concentration increases. Oligonucleotide classes that adsorb well (e.g. phosphorothioates) to the cell membrane are internalized well and tend to produce `antisense' effects. Conversely, oligonucleotide classes that do not adsorb well to the cell surface (e.g.morpholino oligonucleotides, peptide nucleic acids (PNAs), methylphosphonates, and virtually all other uncharged species) are not internalized well when delivered naked and do not produce `antisense' effects [105]. However, the uptake of free oligonucleotides into various organs in the body is still not very efficient. Many strategies have been proposed to improve their cellular uptake including the use of liposomes, polymeric carriers or by direct conjugation with carrier molecules. For their action at a target site within the body, there are many biological barriers that need to be overcome: moving from the bloodstream into tissues, from the extracellular space across the plasma membrane into the cytoplasm, and from the cytoplasm into the nucleus [106].

Cellular uptake of oligonucleotides appears to be an active process dependent on cell type, time, concentration, energy, temperature and type of oligonucleotides. Several strategies have been developed to enhance the cellular uptake of oligonucleotides to target cells. Oligonucleotides form complexes with cationic liposomes, which can condense and impart an overall positive charge that facilitates attachment to the cell membrane while the lipid tails enhance subsequent passage through the lipid bilayer of the cell membrane. Cationic liposome- oligonucleotides are taken up by endocytosis and oligonucleotides are released from the liposomes into the cytoplasm due to the

protonation of the lipids. Some of the ideal properties in an oligonucleotide delivery vector for therapeutic purposes include high transfection efficiency with a high degree of target cell specificity, low occurrence of toxicity and immunogenicity, biodegradability, and stability of the pharmaceutical formulation. In addition, the ideal delivery system would be simple to formulate and would lend itself to easy modification for customized oligonucleotide release, delivery, and expression. Currently available oligonucleotide delivery systems can be classified into 2 types based on their origin (Fig. 2.6):
1) Biological viral delivery systems and 2) Chemical nonviral delivery systems. The description of non-viral delivery systems is applicable to both ASO and siRNA therapeutics.

1) Viral Delivery systems

Nonpathogenic attenuated viruses can be used as delivery systems for DNA based therapeutics. Through millions of years of evolution as infective agents, viruses can transfer oligonucleotides into cells. For therapeutic purposes, the transgene of interest is assembled in the viral genome and the virus uses its innate mechanism of infection to enter the cell and release the expression cassette. The gene then enters the nucleus, is integrated into the host gene pool, and is eventually expressed. One significant advantage of viral DNA vectors is their extremely high transfection efficiency in a variety of human tissues. Retroviral vectors are capable of transfecting high populations (45%-95%) of primary human endothelial and smooth muscle cells, a class of cells that are generally extremely difficult to transfect [104]. Despite such impressive statistics for gene transfer,

there are several concerns over the use of viruses to deliver DNA therapeutics in humans. The chief concern is the toxicity of the viruses and the potential for generating a strong immune response owing to their proteinaceous capsid.

2) Nonviral delivery system

Nonviral delivery systems can circumvent some of the problems associated with viral vectors and are emerging as favorable alternatives to viral vectors. Among the greatest advantages of nonviral gene vectors are lack of immune response and ease of formulation and assembly. Commonly used nonviral vectors for delivery of DNA-based therapeutics can be classified into 2 major types based on the nature of the synthetic material: i) Polymeric delivery systems (nucleic acid-polymer complexes) and ii) Liposomal delivery systems.

Cationic polymers are used in gene delivery because they can easily complex with anionic nucleic acid molecules. Polymer- nucleic acid complexes, also known as polyplexes, can be used to deliver nucleic acid into cells. The general mechanism of action of polyplexes is based on the generation of a positively charged complex owing to electrostatic interaction of these cationic polymers with anionic nucleic acid. The cationic polyplex can then interact with the negatively charged cell surface to improve nucleic acid uptake. Versatility of physicochemical properties and easy manipulation are some of the most important advantages of polymeric gene carriers. Some of the disadvantages of

polymeric delivery systems are low transfection, problems in the control of molecular weight distributions and dispersities of the polyplexes.

2.8 Liposomes

Liposomes are layer lattices of closed bimolecular lipid vesicles intercalated by aqueous spaces. When formed from typical membrane amphiphiles they persist as equilibrium structures even in the presence of excess water. Their usefulness as a delivery system derives from the fact that as dry amphiphiles undergo their sequence of molecular rearrangement upon addition of aqueous solutions, there is an opportunity for unrestricted entry of solutes such as enzymes, small molecules or macromolecules and oligonucleotides before the unfavorable entropy situation of an extended oil-water interface intervenes. Subsequently, and because of this unfavorable entropy associated with further addition of water, a further arrangement of the amphiphilic molecules takes place to yield a series of closed membranes [107].

Each membrane represents an unbroken bimolecular sheet of molecules such that the hydrocarbon tail of the amphiphiles are back to back and shielded from the aqueous phase by their hydrophilic head groups. Certain attributes make liposomes potentially useful vehicles for the purpose of gene delivery. Firstly, they use and recycle natural membrane molecules that are themselves biodegradable. Secondly, their composition can be modified to suit a variety of situations, and they can be used to depot or attenuate the release of either lipophilic or hydrophilic drugs.

Three common types of cationic lipids are currently employed in lipid-based gene delivery. The first group is represented by two quaternary ammonium salts with long mono-unsaturated aliphatic chains, those being N-(1-(2,3-dioleyloxy)propyl)-N,N,N-trimethyl ammonium chloride (DOTMA, one component of the commercially available transfection agent Lipofectin®), and N,N-dioleyl-N,N-dimethylammonium chloride (DODAC). 3b-(N-(N-(dimethylaminoethane)carbamoyl) cholesterol (DC-Chol), a cationic derivative of cholesterol, belongs to the second group. Lipids of a third category are distinguished by the presence of multivalent head groups, such as dioctadecyldi-methylammonium chloride (DOGS), commercially available as Transfectam®.

For systemic *in vivo* gene therapy, it is critical that the integrity of a plasmid or oligonucleotide is maintained in the blood for a sufficient length of time for the nucleic acid to reach tissue sites. When complexed with lipids, the nucleic acid is protected from nuclease degradation to various extents. Similar to what has been observed with naked oligonucleotides, the delivery of the complexes of oligonucleotide by lipids into the cell cytoplasm occurs by the endocytotic / lysosomal pathway, and not by direct delivery through the fusion of lipid ± oligonucleotide particles with the plasma membrane. Delivery of ASOs using the combination of a viral vector and liposome (virosome) has also been reported using Hemagglutinating virus of Japan (HJV) [108] and adenovirus [109]. Influenza virus A envelopes were used in cationic virosomes for the delivery antisense L-myc oligonucleotides to small cell lung cancer cells. HJV has been used for virosome construction and antisense oligonucleotide delivery into the myocardium of

adult rats [105]. Cationic virosomes delivered oligonucleotide into the cytoplasm more efficiently than cationic liposomes.

Liposomes may also be used *in vivo* for the delivery of oligonucleotides in the therapy of intracellular infections (e.g. HIV infections, especially when targeting the pool of virus harbored in macrophages). The major disadvantages of liposomes (e.g. toxicity, serum instability) may affect their use in *in vivo* delivery. Nevertheless, novel liposomal compositions possess tolerable toxicity and are sufficiently stable in the presence of plasma and serum. For example, the phosphorothioate oligonucleotides targeted against the influenza A virus and encapsulated into serum-resistant Tfx-10 liposomes inhibited viral growth in lung tissues, and increased the overall survival rates of mice infected with influenza A. Another limitation on the use of liposome technology for systemic drug delivery is their preferable accumulation in the liver and spleen. This problem can be partially ameliorated by the use of long-circulating liposomes and/or antibody targeted liposomes.

2.9 DOTAP

A typical cationic amphiphile generally comprises of three important elements: cationic head group, hydrophobic anchor, and linker (Fig. 2.7). The positively charged head group is necessary for binding and complexation to nucleic acid phosphate groups. While the function of the hydrophobic part is less clear, it probably assists in assembling the lipids

into a polycationic scaffold as well as in facilitating absorptive endocytosis and/or fusion with cell membranes.

Cationic lipid-mediated nucleic acid and protein delivery is becoming increasingly popular for *in vitro* and *in vivo* applications because of its simplicity (chemical synthesis), reproducibility, and relatively low toxicity. N-[1-(2,3-Dioleoyloxy)]-N,N,N-trimethylammonium propane methylsulfate) (DOTAP) is the most widely used cationic lipid, is relatively cheap, and is efficient in both *in vitro* and *in vivo* applications. The use of DOTAP, an ester analogue of DOTMA, as transfection reagent was reported in 1988. The idea behind DOTAP was that using an ester bond instead of the DOTMA ether bond should reduce toxicity through degradation of the otherwise toxic amphiphile, despite a trade-off of the ester bond's sensitivity to alkaline hydrolysis thus making it biodegradable.

DOTAP belongs to and represents the group of monocationic quaternary surfactants, in which the amine-based cationic headgroup is connected through a linker to two hydrocarbon tails. The geometry of lipids could be described by the ratio between cross-section of the hydrophobic part and the polar headgroup area, referred to as packing parameter P. DOTAP, having P ~0.9, prefers bilayer organization. DOTAP is soluble in alcohols (e.g., t/-butanol) and other common organic solvents (e.g., chloroform). DOTAP-containing liposomes are generally prepared either from DOTAP alone or by mixing DOTAP and helper lipids in common organic solvents, with subsequent evaporation under vacuum or freeze-drying. The dried lipid layer or "cake" is hydrated

and dispersed with suitable aqueous solution, usually pure water or buffer, or isotonic 5% dextrose or 150 mM NaCl, and vortexed. The final lipid concentration in such dispersions ranges from 1 mM to 20 mM. Lipoplexes are prepared by diluting the desired amounts of nucleic acid and lipid in aqueous vehicle, with subsequent careful addition of the nucleic to the lipid, or vice versa [110].

Physical and chemical stability of DOTAP

The degradable components of DOTAP liposomes are DOTAP itself (by virtue of being an ester lipid) and neutral lipids coformulated with DOTAP, generally a phospholipid or cholesterol. Because of a high surface pH imposed by DOTAP (pH > 11.0 at surface, bulk is pH 7.4) DOTAP is prone to base-catalyzed hydrolysis. The rate of DOTAP hydrolysis at room temperature is quite high, 2×10^{-7} s^{-1}. When DOTAP liposomes are stored as powder at 4 °C, the stability is preserved for more than 3 years. After storage for 1 month in HEPES buffer at pH 7.4 at 4ºC over 20% of DOTAP molecules undergo hydrolysis and release one fatty acid. In neutral liposomes, the hydrolysis of ester lipids is relatively slow because of poor accessibility of ester bonds to water. On the other hand, the accelerated hydrolysis of DOTAP acyl esters in the liposomes stems from the high positive charge at the bilayer surface, leading to attraction of hydroxyls to the lipid-water interface [110].

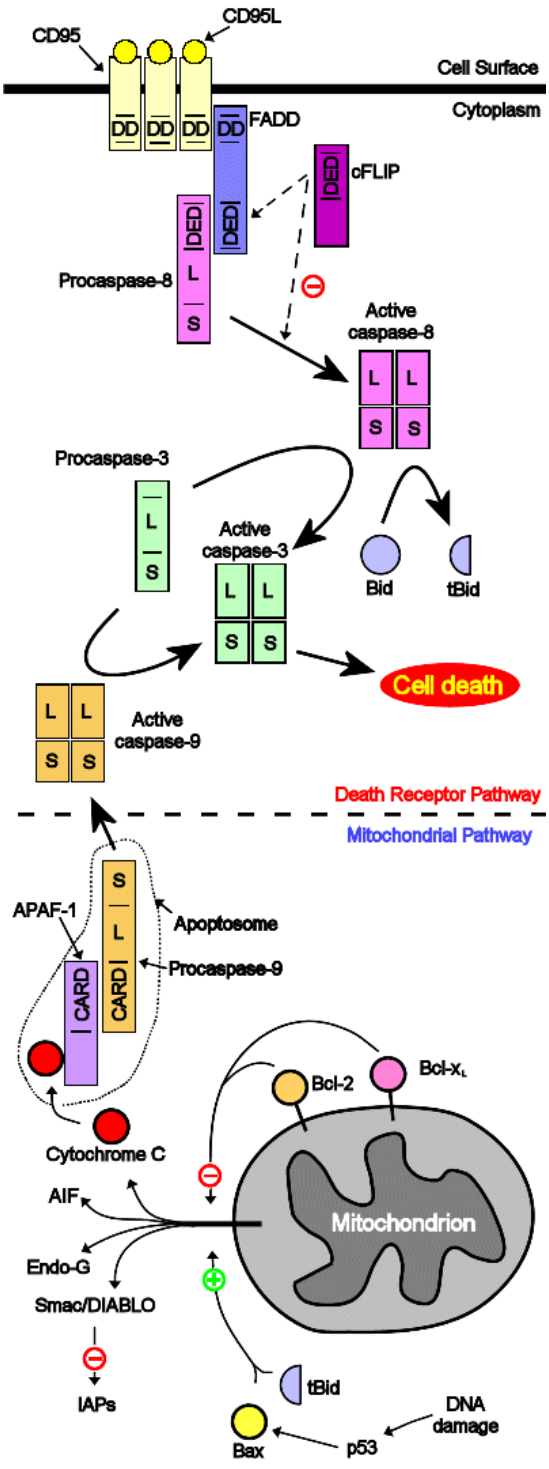

Figure 2.1. Summary diagram of the two main apoptotic pathways; the mitochondrial pathway and the death receptor pathway. (http://fbspcu01.leeds.ac.uk/users/bmbatrl/atrl_topic.htm)

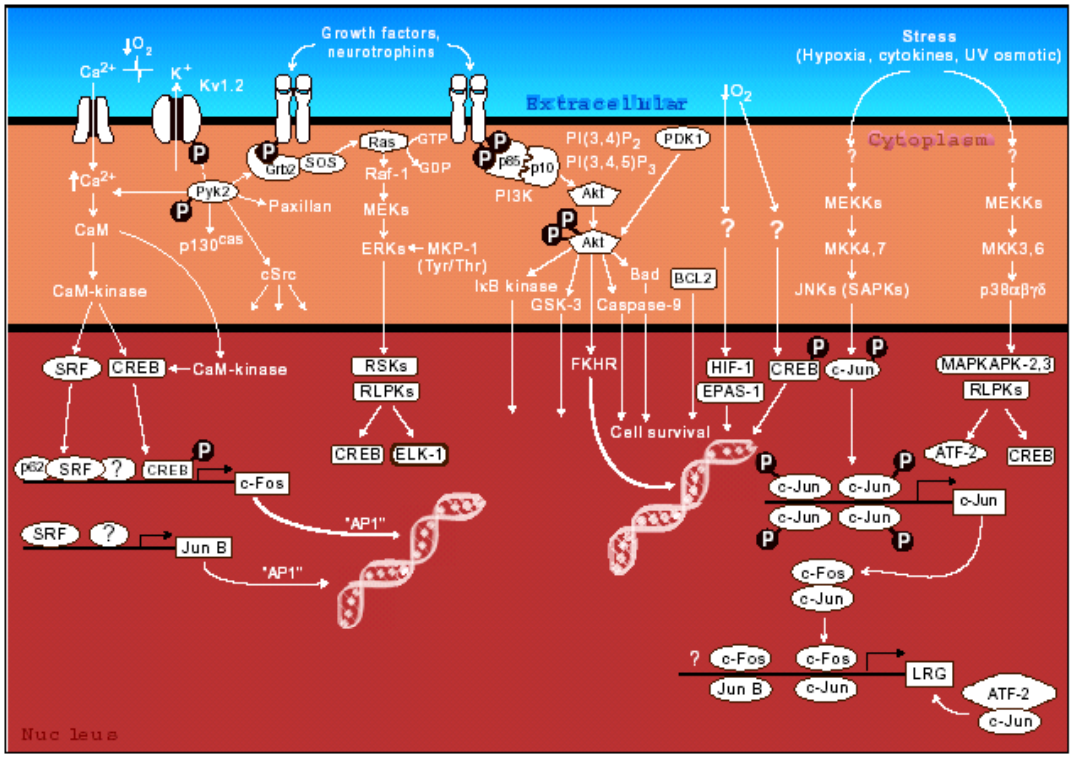

Figure 2.2. Overview of the signal transduction pathways activated by hypoxia [19]. The left part of the figure highlights the signaling pathways activated in response to decreased oxygen. The middle shows how decreased oxygen signals impact cell survival and growth factor signaling pathways. The right side highlights the stress-activated pathways that are involved in cellular responses to decreased oxygen.

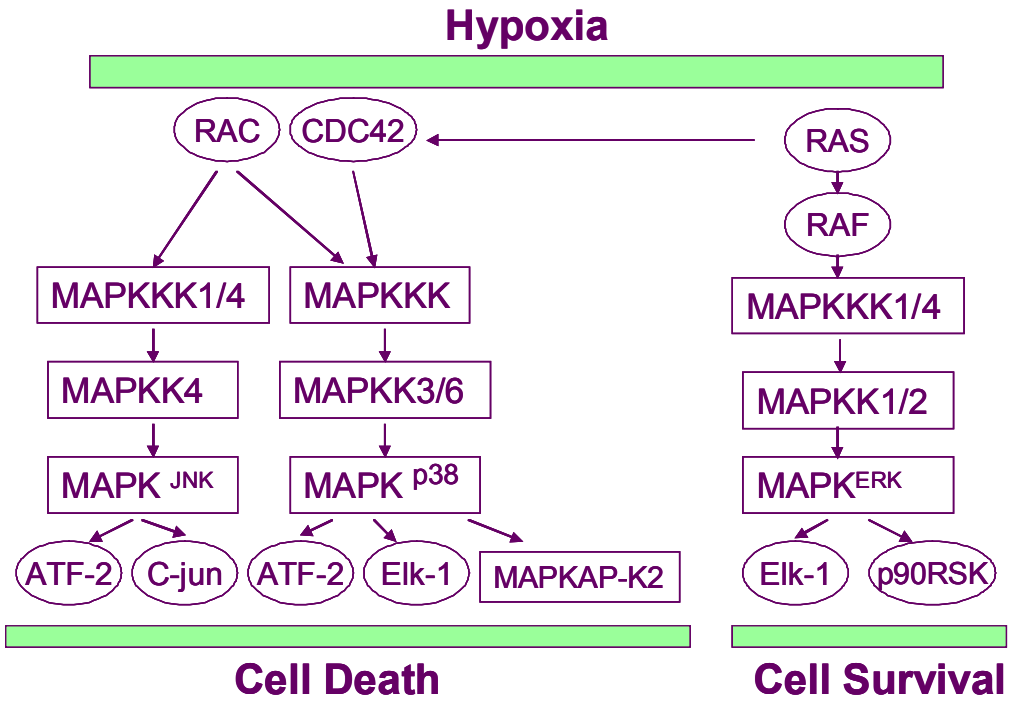

Figure 2.3. Hypoxia-mediated regulation of MAPK signaling pathways: The role of the different MAPK signaling pathways in regulating cellular responses, including cell survival and death, in response to incoming signals such as hypoxia [4].

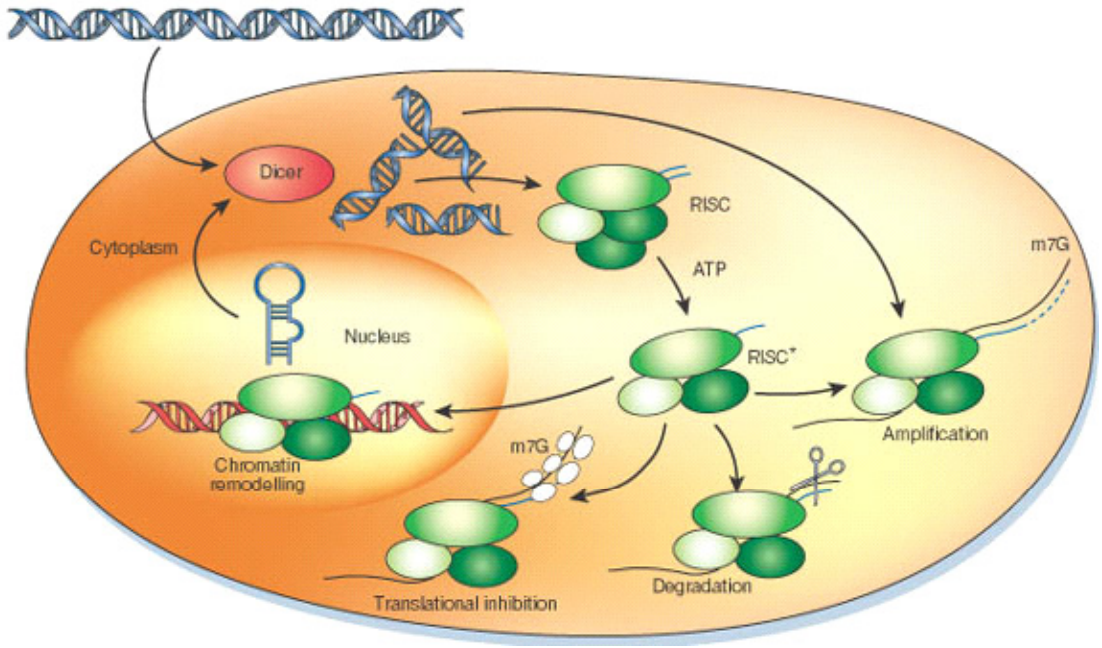

Figure 2.4. A model for the mechanism of RNAi [87]

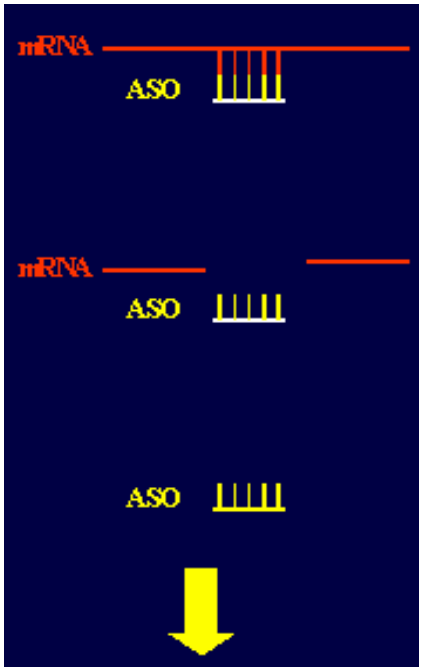

Figure 2.5. Mechanism of action of ASO. Binding of ASO to the target mRNA leads to enzymatic degradation of the mRNA portion of the duplex and prevents the synthesis of specific protein. The ASO is released for further binding to another mRNA.

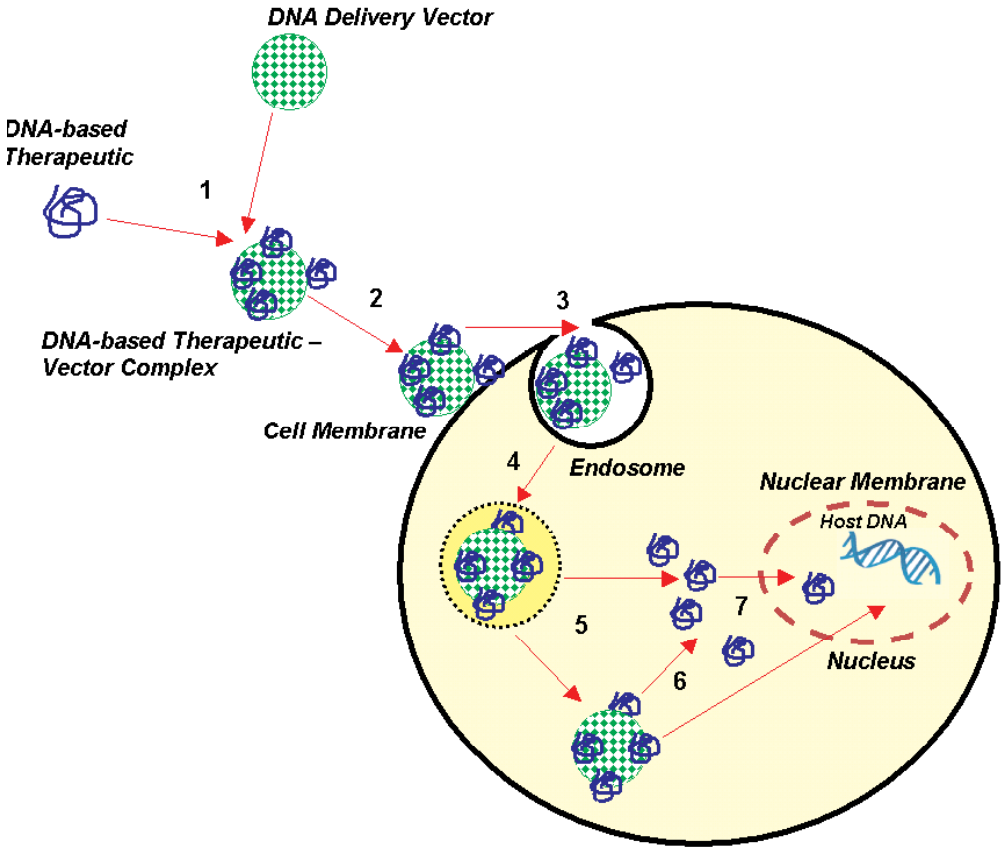

Figure 2.6. Schematic generalized representation of delivery of a DNA-based therapeutic using a viral or nonviral DNA delivery vector: (1) complexation and/or entrapment of DNA-based therapeutic with DNA delivery vector; (2) interaction of DNA-based therapeutic-vector complex with cell membrane; (3) cellular internalization via receptor- or non-receptor-mediated endocytotic pathways; (4) endosomal breakdown; (5) cytoplasmic release of DNA-based therapeutic-vector complex or DNA-based therapeutic alone (Cytoplasm is the site of action for antisense oligonucleotides, aptamer, ribozymes, DNAzymes, and cytoplasmic plasmid DNA expression systems); (6) dissociation of DNA-based therapeutic from vector; (7) nuclear translocation of viral vectors or DNA-based therapeutics. (Nucleus is the site of action for transgenes in plasmids for gene therapy, siRNA generating plasmids, and antigene oligonucleotides) [104].

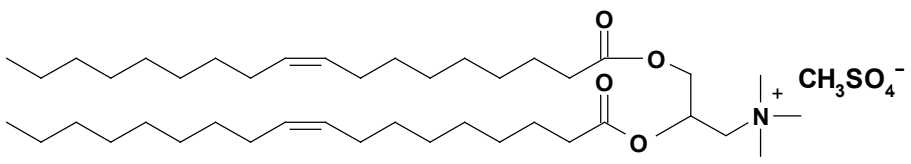

Figure 2.7. Chemical structure of DOTAP.

3 SPECIFIC AIMS

1. **To develop a non-viral liposomal delivery system for intracellular delivery of siRNA and antisense oligonucleotides.**

RNA interference mediated by small interfering RNAs is a powerful approach for dissecting gene function, drug target validation and disease therapy. The major obstacle to the use of siRNAs as therapeutics is the difficulty involved in effective delivery. While considerable efforts have recently been made to develop new siRNA carriers, the research on delivery of siRNA is still in a preliminary stage [111]. Non-viral vectors as siRNA delivery agents have attracted more and more attention in comparison to viral vectors, as they have the advantages over non-viral vectors such as ease of synthesis, low immune response against the vector and potential benefits in terms of safety.

The field of ASO is relatively long-standing compared to siRNA. Early clinical trials were conducted using naked chemically modified phosphorothioate ASO. Since these have several toxicological drawbacks, the use of second generation chemically modified ASO coupled with a delivery agent is desirable. The aims for optimal delivery of ASO are similar to that of siRNA i.e. enhanced cellular uptake, improved exit from subcellular compartments and accurate targeting to a particular site of action.

Liposomes are layer lattices of closed bimolecular lipid vesicles intercalated by aqueous spaces. The dry amphiphiles undergo molecular rearrangement upon addition of aqueous

solutions and there is an opportunity for unrestricted entry of solutes such as oligonucleotides in the lipid bilayers. Neutral liposomes have been used successfully in our laboratory for delivery of drugs, antioxidants and ASO [2,12,13,112,113]. We propose to increase the uptake and efficacy of ASO by delivering them using neutral liposomes.

Cationic polymers are used in gene delivery because they can easily complex with the anionic DNA/RNA molecules. The general mechanism of action of cationic liposomes and cationic lipid complexes with nucleic acids (lipoplex) is based on the generation of a positively charged complex owing to electrostatic interaction of these cationic lipids with anionic nucleic acids. By virtue of their positive charge, these delivery systems have a high affinity for most cell membranes, which are negatively charged under physiological conditions and usually gain entry to cells by adsorptive endocytosis. When complexed with these lipids, the nucleic acid is protected from nuclease degradation to various extents [114]. N-[1-(2,3-Dioleoyloxy)]-N,N,N-trimethylammonium propane methylsulfate (DOTAP) is a widely used cationic lipid, is relatively cheap, and is efficient in both *in vitro* and *in vivo* applications. DOTAP belongs to the group of monocationic quaternary surfactants, in which the amine-based cationic head group is connected through a linker to two hydrocarbon tails. Cationic liposomes with DOTAP will be used for delivery of siRNA.

2. To decrease cellular mortality under hypoxia via suppression of JNK1 by ASO and siRNA targeted to JNK1 mRNA.

There is a decrease in systemic oxygen supply in many pathological conditions that leads to secondary cellular hypoxia. When this hypoxia becomes severe, it causes additional cellular damage, aggravating the primary disorder and leading to cell death. Therefore, remediation of secondary hypoxic damage may significantly increase the efficacy of the treatment of the primary disease condition and prevent extensive cellular damage. Mitogen-activated protein kinases (MAPKs), a family of serine-threonine protein kinases, play an important role in cell proliferation and cell death. It was found that c-Jun N-terminal kinase 1 plays a central role in the development of cellular damage under hypoxia, hypoxia/reoxygenation and ischemia/reperfusion conditions [115-117]. Therefore, JNK1 protein was selected as a molecular target to limit cellular damage and death during hypoxia.

The second goal of this research study is to inhibit JNK1 by ASO and siRNA *in vitro*.

3. To study the *in vivo* body and organ distribution of liposomal ASO and siRNA

Following optimization of the liposomal delivery system for ASO and siRNA *in vitro*, our goal is to test it in an *in vivo* mouse model of hypoxia. In order to assess the feasibility of this approach, the body and organ distribution of the liposomal ASO and siRNA will be evaluated in mouse.

The efficiency of siRNA *in vivo* is limited by its low resistance against enzymatic degradation, limited permeability across cell membrane, and substantial liver and renal

clearance [118]. A wide variety of methods have been used to facilitate delivery of siRNA. Cationic polymers are usually employed to bind the siRNA, neutralize charge, and assist with transport across the cell membrane. Previous studies to investigate organ distribution of cationic liposomes usually showed a high accumulation in the lung after intravenous administration [119]. The pattern of organ distribution showed initial deposition in the lung and subsequent rapid uptake predominantly into Kupffer cells of the liver. Some studies have discovered a rapid crossing of the endothelial barrier by lipoplexes, although the mechanism of this transport has yet to be elucidated. It has been suggested that at sites where the vasculature is fragile, as in the alveoli, small complexes may be able to pass the endothelial barrier, due to vascular leakage [119].

The *in vivo* properties of various chemically modified ASOs administered naked (without a delivery system) have been reported previously [120]. Tissue distribution studies of both free and liposome encapsulated ASO have indicated that ASO distribution was dictated primarily by the liposomal carrier when administered in liposomal form [121]. The body and tissue distribution studies that are proposed will aid in the design of appropriate strategy for delivery of ASO and siRNA in sufficient quantities to the target sites of action and for the desired time frame to achieve the desired level of gene inhibition or functional down-regulation.

4. **To develop an experimental *in vivo* model of hypoxia and explore remediation of hypoxic damage by ASO and siRNA targeted to JNK1 mRNA.**

Hypoxia has elicited a great deal of interest among the scientific community due to its role in life-threatening pathologies such as stroke, acute renal failure, myocardial infarction and cancer. Hypoxia that accompanies ischemia has been investigated both *in vivo* and *in vitro* within the last decade [20,122]. An experimental model for lung tissue hypoxia and acute lung injury induced by hypoxia has been reported previously [15]. There are a few reports in literature wherein inhibition of JNK using either small molecules or siRNA/ASO was achieved *in vitro* for elucidation of biochemical and signal transduction pathways that regulate JNK expression [123-125]. However, inhibition of JNK in animal models *in vivo* has not been reported till date. We propose to study the effect of ASO and siRNA targeted to JNK1 in an experimental mouse model exposed to acute normobaric hypoxia. Treatment of rat *in vivo* will be reproduced from the treatment used in the *in vitro* experiments.

4 TO DEVELOP A NON-VIRAL LIPOSOMAL SYSTEM FOR INTRACELLULAR DELIVERY OF siRNA AND ANTISENSE OLIGONUCLEOTIDES

4.1 Introduction

Antisense oligonucleotides and siRNAs are both very effective tools to understand gene function, as drug validation target tools and potential therapeutics agents. The antisense and RNA interference strategies, in principle, allow for the rational design of highly sequence-specific nucleic acid drugs that can target a given mRNA inhibiting or suppressing the expression of the corresponding gene. However, both ASO and siRNA share similar pharmaceutical problems. They are generally polyanionic macromolecules that do not readily cross biological barriers. The pharmaceutical challenge is the effective delivery of these molecules in cell culture and ultimately, in vivo.

Biological instability is the first barrier to consider when delivering ASO and siRNA to cells. Unmodified phosphodiester (PO) backbone oligonucleotides are rapidly degraded in biological fluids by a combination of both endo- and exo-nucleases [114,126-128]. To overcome this problem, a variety of chemically modified antisense oligonucleotides have been developed [129,130]. The most widely studied of these are the phosphorothioate (PS) oligonucleotides where one of the non-bridging oxygens in the phophodiester backbone is replaced with sulphur. More recently other modifications such as peptide nucleic acids, 2′-methoxyethyl- and morpholino-based oligonucleotides have also been

investigated [114]. In the present research studies, the DNA backbone of all bases in the antisense oligonucleotides is P-ethoxy modified to enhance nuclease resistance and increase incorporation efficacy into liposomes [131]

SiRNAs, due to their double stranded nature are more resistant to nuclease degradation than antisense oligonucleotides [132]. However, both naked ASO and siRNA cannot efficiently penetrate cellular lipid membranes and a very small number can gain entry into the cell. It is widely thought that cellular uptake of siRNA and ASO occurs via nonreceptor-mediated endocytosis. Thus, delivery systems are typically used to increase cellular accumulation of these molecules and to facilitate release from endosomes to the cytosol [133]. Therefore, there is a need for development of efficient delivery systems for siRNA and ASO. Among the vectors that have been studied, non-viral vectors have attracted considerable attention in comparison to viral vectors, due to the advantages of non-viral vectors such as ease of synthesis, low toxicity and low immune response. The most researched non-viral vectors include liposomes and other nanoparticles. The aims for optimal delivery of oligonucleotides are enhanced cellular uptake, improved exit from sub-cellular compartments and cytoplasm of cells, and correct targeting (spatial and temporal) to a particular site of action.

Liposomes are composed of an aqueous compartment enclosed within a phospholipid bilayer. They are the most widely used system for nucleic acid delivery and afford protection to the nucleic acid whilst enhancing cellular delivery. Liposomes usually gain entry into the cells by absorptive endocytosis. In case of cationic liposomes, the

efficiency of the lipoplex is partially attributed to a rapid and efficient escape from the endosomal/lysosomal compartments. It is reported that lipoplexes are able to destabilize endosomal/lysosomal membranes possibly by perforation. This process is explained by electrostatic interactions between the oppositely charged cationic lipids of the lipoplex and anionic phospholipids composing intracellular compartments, leading to disturbances in the curvature of the vesicles and finally leakage or bursting and release of endosomal contents to the cytoplasm [119].

In the present research, neutral liposomes were used to deliver antisense oligonucleotides to cells. These liposomes have been successfully used in our laboratory to deliver genetic material [12,13]. Cationic liposomes and cationic lipid complexes with siRNA have been the most successful delivery system in cell culture [132,134]. We used liposomes formulated with the monocationic lipid DOTAP for delivery of siRNA into cells.

4.2 Materials and Methods

4.2.1 Cell Line

The human embryonic kidney 293 cells were obtained form American Type of Tissue Culture (Manassas, VA). Cells were cultured in Dulbecco's modified Eagle's medium (GIBCO Inc., Cincinnati, OH) supplemented with 10% fetal bovine serum (Fisher Chemicals, Fairlawn, NJ). All experiments were performed on cells in the exponential growth phase.

4.2.2 Liposomal composition for the delivery of ASO and intracellular localization of liposomal ASO

Antisense oligonucleotides (ASO) were synthesized by Oligos Etc. (Wilsonville, OR). The DNA backbone of all bases in oligonucleotides was P-ethoxy modified to enhance nuclease resistance and increase incorporation efficacy into liposomes [131]. To analyze intracellular localization of ASO released from liposomes, a portion of oligonucleotides were labeled using fluorescein isothiocyanate (FITC) prior to incorporation into liposomes. The labeling was performed by Oligos Etc. Neutral liposomes were prepared using previously described lipid film rehydration method [2,13,112]. Briefly, lipids (Avanti Polar Lipids, Alabaster, AL) were dissolved in chloroform, evaporated to a thin film in a rotary evaporator, and rehydrated with citrate buffer. The lipid ratio was 7:3:10 (egg phosphatidylcholine: 1,2-dipalmitoyl-sn-glycero-3-phosphatidylcholine: cholesterol). Oligonucleotides were loaded into the liposomes by dissolving them in the rehydration buffer at concentrations of ~1.4 mM. After preparation, free ASO was separated from the liposomes by passing the liposome suspension through a Sephadex G-50 column. The encapsulation efficacy ranged from 50 to 60% in different series of experiments. The mean liposome diameter was about 100-200 nm.

Intracellular localization of ASO was studied by fluorescent and confocal microscopy. In these experiments cell nuclei were additionally stained by Hoechst 33258 nuclear dye (Sigma, St. Louis, MO). To study intracellular localization of liposomes, part of the liposomes were labeled with Cy5.5 and osmium tetroxide and visualized by confocal and electron transmission microscopy, respectively.

Labeling of liposomes for electron transmission microscopy was done by adding osmium tetroxide (0.5%) to rehydration buffer. Cells and tissue sections were fixed prior to electron microscopy using standard techniques [135,136]. Briefly, cells were primary fixed for 2 hours in Trump's EM Fixative (combination of low concentration of both formaldehyde and glutaraldehyde in 0.1 M Milloning's phosphate buffer, pH 7.3). Postfixation was carried out in 1% osmium tetroxide in buffer for 1 hour followed by dehydration in graded Ethanol series and embedded in Spurr's low viscosity resin. Sections were prepared using a diamond knife by LKB-2088 Ultramicrotome (LKB-Produkter, Bromma, Sweden). Observation and micrographs were made with a JEM-100CXII Electron Microscope (JEOL LTD., Tokyo, Japan).

An aliquot of neutral liposomes was labeled with fluorescent dye Cy5.5 Mono NHS Ester (GE Healthcare, Amersham, UK). To this end, lipids and Cy5.5 were dissolved in chloroform, evaporated to a thin film layer in rotary evaporator and rehydrated with citrate buffer. Antisense oligonucleotides were loaded into liposomes by dissolving in rehydration buffer at a concentration of 0.5 mM. Liposomes were extruded gradually using polycarbonate membranes 200 nm and 100 nm at room temperature using extruder device from Northern Lipids Inc. (Vancouver, BC, Canada).

4.2.3 Liposomal composition for the delivery of siRNA and intracellular localization of cationic liposome-siRNA complex (lipoplex)

To analyze intracellular localization of siRNA, siGLO (siRNA) labeled with Pierce NuLight DY-547 fluorophore (Dharmacon Inc. Chicago, IL) was used. Cationic liposomes were labeled with 7-nitrobenz-2-oxa-1,3-diazol-4-yl (NBD) [137]. The liposomes were prepared using 1,2 Dioleoyl-2-trimethylammonium-propane - DOTAP (Avanti Polar Lipids, Alabaster, AL) at a concentration of 1 mg/mL. DOTAP and NBD were dissolved in chloroform, evaporated to a thin film layer in rotary evaporator and rehydrated with water followed by extrusion through 100 nm polycarbonate membranes. siRNA was dissolved in phosphate buffered saline at a concentration of 100 μM. To this solution, DOTAP (1 mg/mL) was added, mixed by pipette and incubated for 15 minutes at room temperature. The charge ratio of siRNA: DOTAP was 1:2.5. Resulting siRNA-cationic liposome complex (lipoplex) was added to tissue culture flask containing 5-10 mL of medium and 1.5-2.5 x 10^6 cells. Mean particle size of the complex was >500 nm.

In another set of experiments, aliquots of cationic liposomes were labeled with fluorescent dye Cy5.5 Mono NHS Ester (GE Healthcare, Amersham, UK). To this end, lipid and Cy5.5 were dissolved in chloroform, evaporated to a thin film layer in rotary evaporator and rehydrated with 0.9% NaCl to final concentration of 5 mg/mL of DOTAP. Liposomes were extruded gradually using polycarbonate membranes 200 nm and 100 nm at room temperature using extruder device from Northern Lipids Inc. (Vancouver, BC, Canada).

4.2.4 Particle size and zeta potential measurements

Particles size measurements were carried out by dynamic light scattering using 90 Plus Particle Size Analyzer (Brookhaven Instruments Corp., New York, NY). Aliquot of 40 μL of each sample was diluted in 2 mL of water or buffer. Zeta potential was measured on PALS Zeta Potential Analyzer (Brookhaven Instruments Corp, New York, NY). A 1.5 mL sample aliquot was taken for each measurement. All measurements were carried out at room temperature. The analysis was performed thrice and average values were taken.

4.2.5 Atomic Force Microscopy

The shape of neutral and cationic liposomes was studied by atomic force microscopy (AFM) imaging using the previously described procedure [138]. Briefly, 50 μL of liposome suspension in water was deposited on pre-cut (25x25 mm^2) and pre-cleaned Plain Premium microscope slides (Fisher Scientific Co, Pittsburgh, PA) and kept for 10 min at 100% humidity to achieve particles precipitation. Water was removed by dry nitrogen flow and dried samples were subjected to imaging with an atomic force microscope (Nano-R AFM Pacific Nanotechnology Instrument, PNI, Santa Clara, CA) in close contact using tapping mode etched OMCLAC160TS silicon probes (Olympus Optical Co. Tokyo, Japan). The captioning was performed in the height mode. The images were processed, and the measurements were performed with Femtoscan software v. 2.2.85(5.1) (Advanced Technologies Center, Moscow, Russia). For statistics, no less than 50 objects of each sample were analyzed.

4.2.6 Confocal microscopy

Cellular internalization of liposomes, ASO and siRNA was monitored in cells by confocal microscopy. Two series of experiments were carried out: (1) Neutral liposomes labeled with Cy5.5 (red fluorescence) contained ASO labeled with FITC (green fluorescence); (2) NBD-labeled cationic liposomes (green fluorescence) contained siGLO Red (red fluorescence). Cells were separately incubated for 24 hours at 37 ^{o}C with each liposomal formulation. Red and green fluorescence images were photographed and digitally overlaid. Superposition of images allows for detecting co-localization of labeled liposomes and their payload (yellow color).

4.3 Results

4.3.1 Particle size and zeta potential measurements

Table I shows the size and zeta potential of liposomal compositions used in the study. As can be seen, neutral liposomes have no charge. Inclusion of ASO into neutral liposomes did not change their size and zeta potential. The size of positively charged DOTAP liposomes after extrusion was about 100-140 nm (same as for neutral liposomes). Mixing with siRNA to form a lipoplex led to formation of rather large DOTAP: siRNA complexes and decreased surface charge due to the electrostatic interactions between positively charged lipid and negatively charged siRNA.

4.3.2 Atomic force microscopy

Atomic force microscopy (AFM) has been widely used during the last decade to characterize morphology of nanoparticles. AFM topographical images of the liposome preparations revealed convex meniscus shaped particles that were uniformly distributed on the mica surface (Fig. 4.1 and 4.2). There was no substantial presence of liposome aggregates observed, as expected from physico-chemical properties of uniformly charged particles. Since liposomes flattening on the mica surface after deposition and drying results in distortion of their actual shape in suspension, we calculated the value of reconstructed diameter (d) from the liposome volume measured by AFM (V) under the assumption that liposomes adopt spherical shape in aqueous solutions, using the equation $d= (6V/\pi)1/3$ as previously described [139]. The complexation of liposomes with siRNA resulted in more than 2.5-fold increase of their d to over 500 nm. Liposomes modification with siRNA makes their appearance “fuzzy”, thus hiding object topology.

4.3.3 Intracellular localization of ASO and neutral liposomes

The use of ASO or siRNA to suppress the expression of a targeted mRNA is limited by their low ability to penetrate the cellular plasma membrane and interfere with genetic material. Therefore, a special delivery system is required to enhance their cell penetration. Liposomes were labeled with osmium tetroxide and ASO with fluorescein isothiocyanate (FITC) and incubated with human embryonic kidney 293 cells for 24-48 hours. Cell nuclei were stained by Hoeschst 33258 nuclear dye. The labels were

visualized by electron transmission microscopy (osmium tetroxide) or fluorescence microscopy (FITC and Hoeschst 33258). Typical images obtained in these experiments are presented in Figures 4.3 and 4.4. Fluorescent microscopy analysis showed that FITC-labeled antisense oligonucleotides delivered by liposomes penetrated cells and accumulated in the cytoplasm and nuclei (Fig. 4.3). The latter can be seen in Figure 4.3 B as blue-colored structures. Osmium-labeled liposomes were found in cellular perinuclear regions on electron microscopic evaluation as black spheres with average diameter of 100-200 nm (identified by arrows in Fig. 4.4). Thus, we showed that liposomes could penetrate human cells and deliver genetic material in the cytoplasm and cellular nuclei. The delivery of ASO by liposomes into cells was also studied *in vitro* using confocal microscopy. Both liposomes and ASO were labeled and studies were conducted by incubation of cells with these substances for 24 hours. Results are shown in Figure 4.5. As observed, fluorescence of neutral liposomes and ASO was detected both in the cellular cytoplasm and nucleus. It is known that liposomes quench the fluorescence of any loaded agent [140]. Therefore, the visualization of fluorescence suggests that after 24 hours of incubation ASOs were completely released from liposomes and localized in the cellular cytoplasm and nucleus.

4.3.4 Intracellular Localization of siRNA and cationic liposomes

To study cellular uptake of cationic liposomes, human embryonic kidney 293 cells were incubated with Cy5.5 labeled cationic liposomes and their intracellular distribution was examined by confocal fluorescent microscopy. After 24 hours incubation, cationic

liposomes were detected in the cellular cytoplasm and nucleus (Fig. 4.6) indicating their effective internalization within cells.

The cellular uptake of DY-547 labeled siRNA (red fluorescence) either free or complexed with NBD labeled cationic liposomes (green fluorescence) was also studied *in vitro* using confocal fluorescent microscopy. Human embryonic kidney 293 cells were incubated with labeled free siRNA or cationic liposome: siRNA complex for 120 minutes and then intracellular distribution was examined with time. Results are shown in Figure 4.7. The free siRNA failed to internalize into cells, which was evident by the absence of measurable red fluorescence in the cellular cytoplasm and nuclei (top panel, Fig. 4.7). In contrast, when siRNA was delivered using cationic liposomes, fluorescence was registered in the cellular cytoplasm and nucleus starting at 15 minutes. This can be observed in the bottom panel of Figure 4.7, where the visible light image digitally overlaid with both fluorescence images to obtain a composite image showed co-localization of liposomes and their payload (in yellow color). The results obtained also show that substantial amount of cationic liposome:siRNA complex penetrated into cellular cytoplasm area despite their relatively big size (>500 nm). In order to prove that liposomes were not adhered on the cell surface but actually penetrated the cells, we analyzed their distribution in different cellular layers from the upper to the lower layer of the fixed cells (*z*-sections). The data obtained show that the distribution of either small (100-140 nm) neutral and cationic liposomes or big (>500 nm) cationic liposome: siRNA complexes in cytoplasm and nucleus was very similar in different cell layers. The z-section of cationic liposome-siRNA complex is shown in Figure 4.8. Therefore, both

neutral and cationic liposome systems can be used for delivery of therapeutic agents with biological activity into the cellular cytoplasm and nuclei.

4.4 Discussion

It is well known that liposomal drug formulations are more efficient in terms of their cellular internalization, specific activity, and adverse side effects when compared with free drugs [2,12,13,139,141-145]. Liposomes of different sizes and surface electric charge are currently being used for the delivery of encapsulated drugs or complexed large molecules. While the high effectiveness of liposomal formulations is widely acknowledged, several aspects of liposomal drug delivery are not clearly understood. The optimum size and charge of liposomal drugs for their successful intracellular uptake has not yet been identified. We have made an attempt to better understand the problem in the present study by investigating *in vitro* cellular uptake and intracellular localization of neutral and positively charged liposomes as well as their relatively large complexes with siRNA.

We used small neutral and positively charged DOTAP liposomes. Uncharged P-ethoxy ASOs were used as a payload for neutral liposomes while siRNA was complexed to cationic liposomes. Atomic force microscopy and light scattering data showed that empty liposomes of both types represent homogenous spherical structures with size of 100-140 nm. Loading of neutral liposomes with neutral modified ASO did not change their average size and homogeneity. In contrast, complexation of cationic liposomes with

siRNA led to dramatic (up to 10-times) increase in their size. Investigation of cellular internalization and localization of liposomes showed that despite the differences in size, both small empty and loaded liposomes as well as relatively large complexes were able to deliver their payload to the cellular cytoplasm and even nuclei. Moreover, labeled neutral liposomes, as well as their payload, were found inside cellular nuclei. These data reconfirm our transmission electron and fluorescence microscopy findings for the nuclear penetration of conventional and neutral liposomes with average size of 100-200 nm both *in vitro* and *in vivo* [139,141,142]. Liposomes and liposomal complexes of different sizes (100-1000 nm) used in this study were able to provide an efficient delivery of biologically active substances, antisense oligonucleotides and small interfering RNA into the cellular cytoplasm.

Table 4.1. Size and zeta potential of liposomes at room temperature

Liposomes/Parameter	**Size (nm)[a]**	**Zeta potential (mV)[a]**
Neutral liposomes (EPC/Chol/DPPC)	120 ± 20	0
Neutral liposomes loaded with ASO	130 ± 10	0
Cationic liposomes (DOTAP)	120 ± 15	+25 ± 4
Cationic liposome: siRNA complexes	>500 nm	+4 ± 2

[a]Means ± SD are shown.

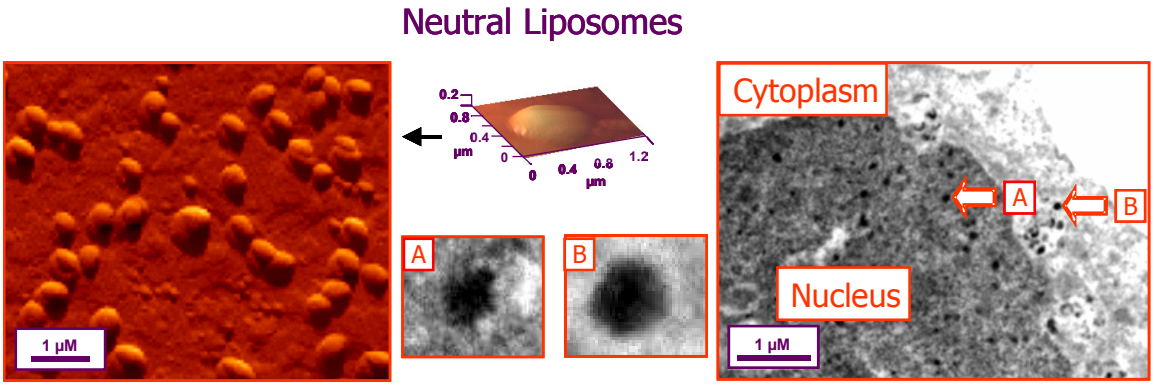

Figure 4.1. Assessment of neutral liposomes by Atomic force and Electron microscopy.

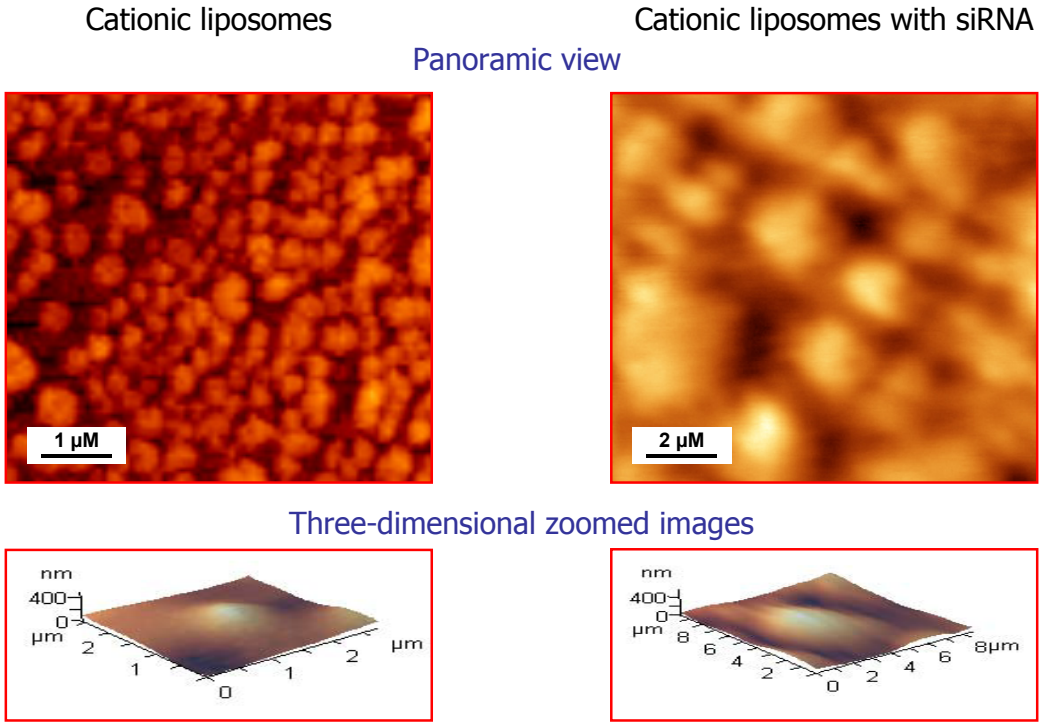

Figure 4.2. Assessment of cationic liposomes with and without siRNA using Atomic force microscopy.

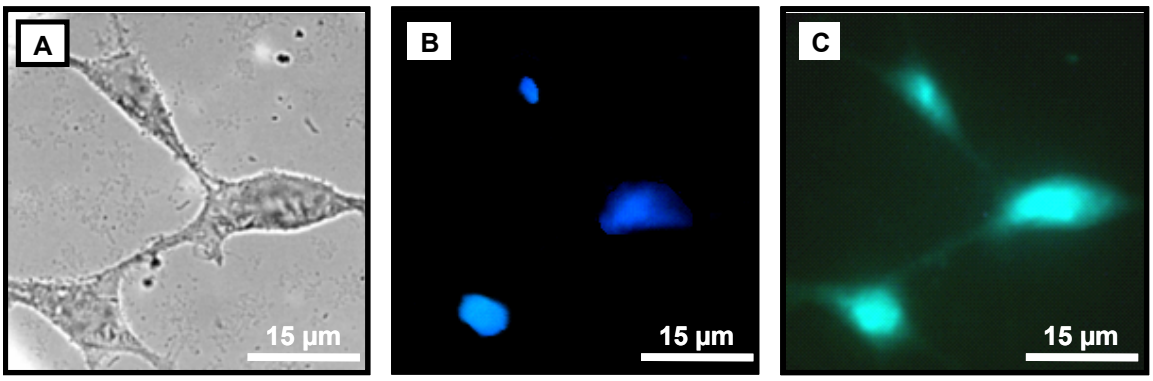

Figure 4.3. Internalization of liposomal antisense oligonucleotides in human embryonic kidney 293 cells studied by fluorescence (A-C) microscopy. A – visible light image. Cellular nuclei were stained by Hoechst 33258 nuclear dye (B, blue fluorescence); antisense oligonucleotides were labeled with fluorescein isothiocyanate (C, green fluorescence).

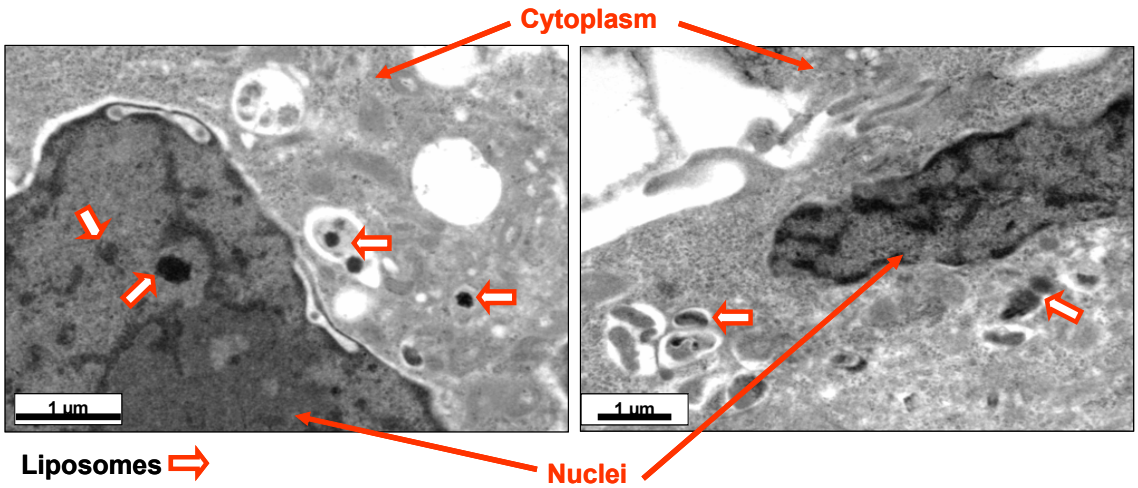

Figure 4.4. Internalization of liposomes in human embryonic kidney 293 cells studied by transmission electron microscopy. Liposomes were labeled with osmium tetroxide (arrows).

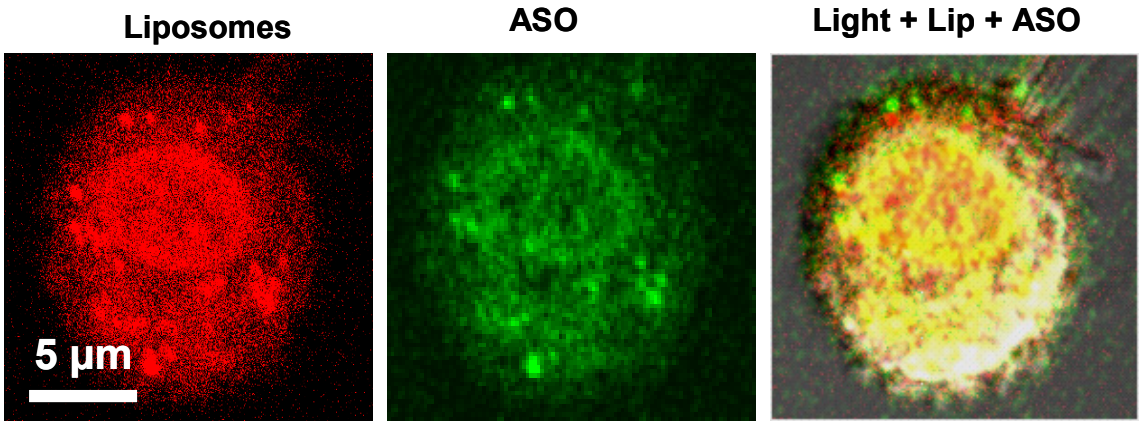

Figure 4.5. Cy5.5-Neutral liposomes-ASO-FITC. Intracellular localization of neutral liposomes and their payload. Cells were incubated with Cy5.5 labeled neutral liposomes with FITC labeled ASO for 24 hours and visible light and fluorescent images (red and green fluorescence) were taken by a confocal microscope. Visible light image was digitally overlaid with both fluorescence images to obtain a composite image showing co-localization of liposomes and their payload (in yellow color). The panel contains representative images of neutral liposomes labeled with near infrared dye Cy5.5 (red fluorescence) containing FITC labeled antisense oligonucleotides (green fluorescence).

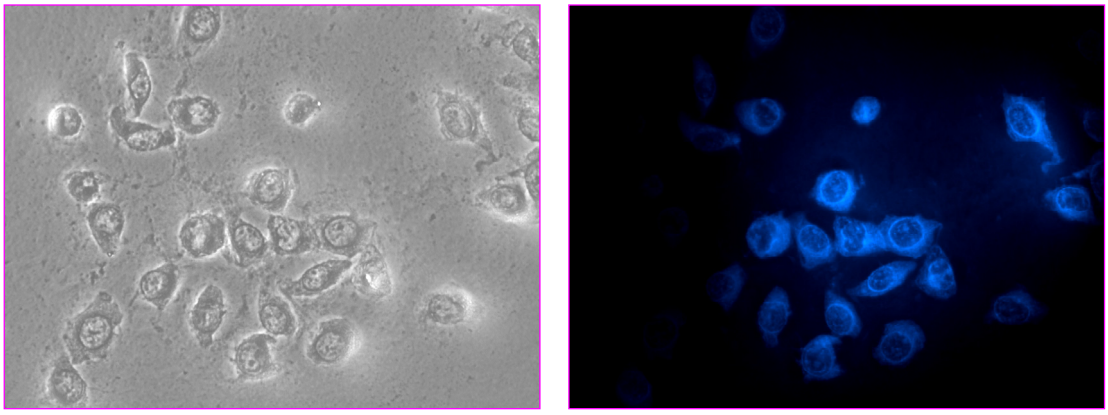

A B

Figure 4.6. Internalization of Cy5.5-labeled cationic liposomes incubated with human embryonic kidney 293 cells for 24 hours studied by fluorescence microscopy. A – Visible light image. B – Image showing fluorescence of Cy5.5 labeled cationic liposomes.

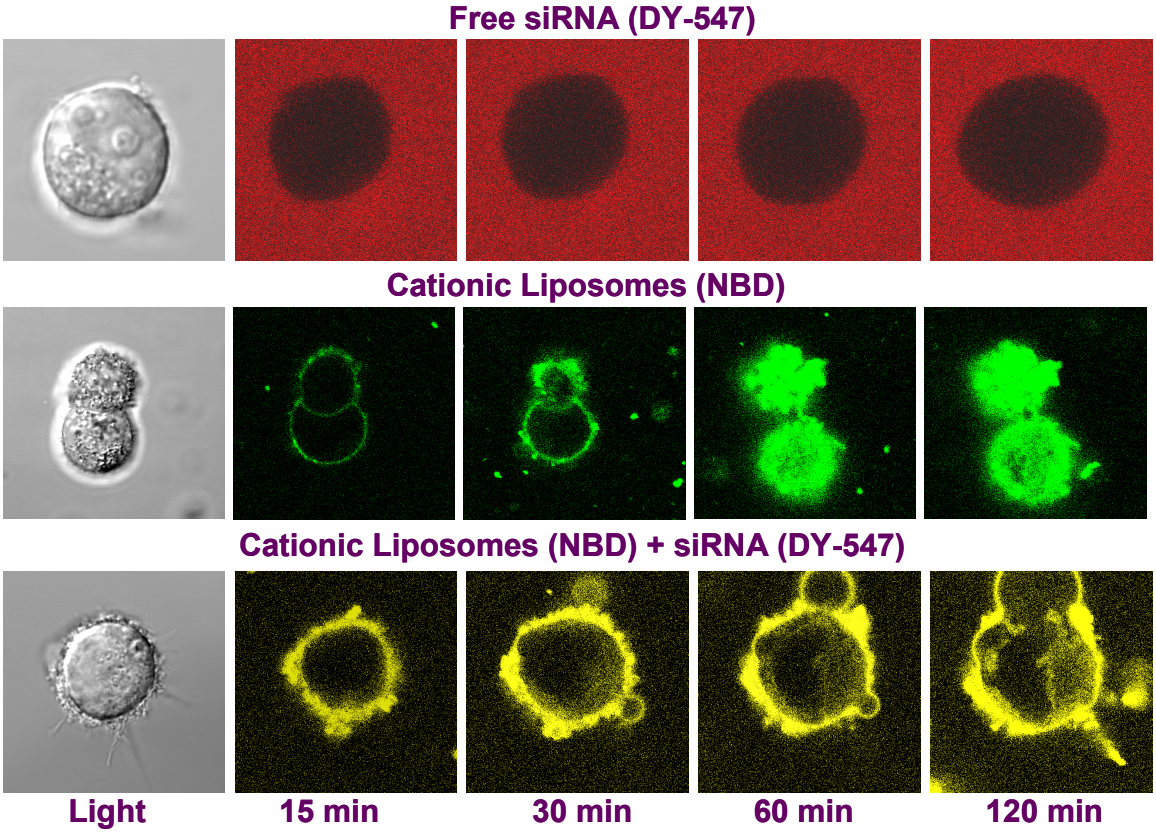

Figure 4.7. Confocal microscopy images of 293 cells incubated with free siRNA (top panel), cationic liposomes (middle panel) and cationic liposome-siRNA complex (bottom panel), labeled with fluorescent label as indicated: Time Series. Fluorescence of siRNA and cationic liposomes was observed using FITC and rhodamine filters, respectively.

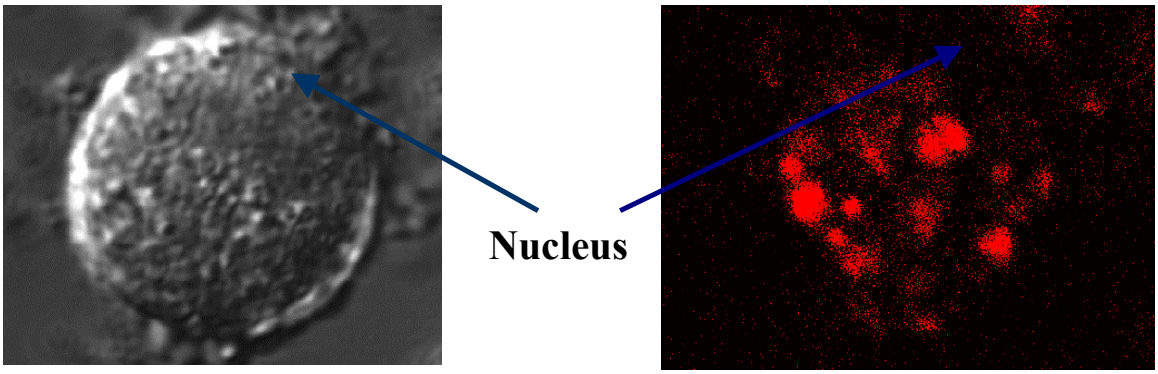

A B

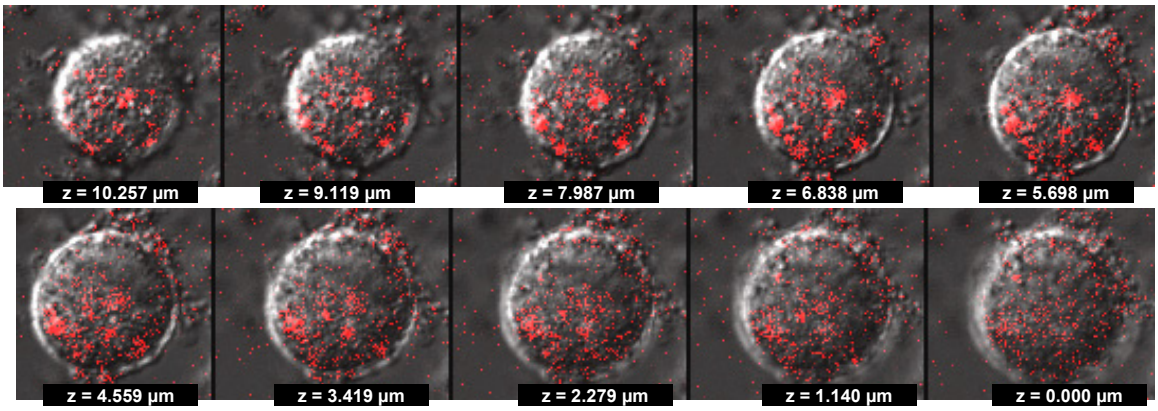

Figure 4.8. Confocal microscopy images (light + fluorescence) of cationic liposome-siRNA complexes. A- Visible light image, B- Image showing fluorescence of Dy-547 labeled siRNA visualized using rhodamine filter. C: Z-series of complex, from the top of the cell to the bottom.

5 INTRACELLULAR LIPOSOMAL DELIVERY OF siRNA AND ASO TARGETED TO JNK1 MRNA LIMITS CELLULAR MORTALITY UNDER SEVERE HYPOXIA

5.1 Introduction

Many known pathological conditions lead to a decrease in systemic oxygen supply leading to secondary cellular hypoxia. When this hypoxia becomes severe, it causes additional cellular damage, aggravating the primary disorder and leading to cell death. Therefore, remediation of secondary hypoxic damage should significantly increase the efficacy of treatment of the primary lesion and prevent extensive cellular damage. Moreover, the prevention of cellular death under environmental conditions which cause reduction in body oxygen supply (high altitude, deep mining, diving, etc.) might increase working capacity of tissues and prevent severe adverse side effects of hypoxia.

A cell death signal leading to the activation of caspases and finally causing cell death plays an important role in initiating and promoting cellular hypoxic damage [16,112]. Hypoxia inducible factor alpha (HIF1A) protein is a key initiator of such a signal under hypoxic conditions [1]. Therefore, recently we investigated the role of this protein as a possible target for the remediation of hypoxic cellular damage. However, we found that HIF1A plays a bimodal role during hypoxia [2]. On the one hand, the activation of HIF1A during hypoxia initiates cell death signal inducing apoptosis (programmed cell death, or cellular suicide) and necrosis (pathological cell death). On the other hand,

overexpression of HIF1A boosts the power of anti-hypoxic systems that increase cellular resistance to hypoxia. Moreover we found that suppression of HIF1A predominantly led to the activation of apoptosis and promoted cell death. Therefore we used this approach to enhance the efficacy of cancer chemotherapy [12].

The next protein family which attracts attention as a possible target for the remediation of cellular hypoxic damage is mitogen-activated protein kinases (MAPKs), a family of serine-threonine protein kinases that participate in a major signaling system by which cells transduce extracellular stimuli into intracellular responses [3]. Within this group, two subfamilies are usually distinguished: the extracellular regulated kinases (ERKs) and the stress-activated protein kinases (SAPK). The major player in the activation of apoptosis signaling pathways and hypoxic damage is Jun N-terminal kinase (JNK) – a stress-activated protein kinase that can be induced by inflammatory cytokines, bacterial endotoxin, osmotic shock, UV radiation, and hypoxia [5-7]. Analysis of literature data [7,146,147] showed that the activation of cell death under hypoxia includes the following major steps (Fig. 5.1). Activation of JNK by hypoxia mediates phosphorylation of activating transcriptional factor-2 (ATF2) and c-Jun bound to the *c-jun* promoter and stimulates their transcriptional activities leading to *c-jun* induction. The newly synthesized c-Jun protein combines with c-Fos protein to form stable transcriptional factor activator protein-1 (AP1) heterodimers. The formation of AP1 is a key step in the induction of central cell death signal leading to the activation of caspase-dependent apoptosis signal and finally causing cell death. It was found that c-Jun N-terminal kinase 1 plays a central role in the development of cellular damage under hypoxia,

hypoxia/reoxygenation and ischemia/reperfusion conditions [115-117]. Therefore, we selected JNK1 protein as a molecular target to limit cellular damage and death during hypoxia. Here, we report our recent experimental data that clearly support our hypothesis and demonstrate that inhibition of JNK1 by antisense oligonucleotides or small interfering RNA targeted to JNK1 mRNA substantially suppresses JNK1 protein expression and effectively limits apoptosis induction and cellular death under severe hypoxic conditions.

5.2 Material and Methods

5.2.1 Cell line

Human embryonic kidney 293 cells were obtained form American Type of Tissue Culture (Manassas, VA). Cells were cultured in Dulbecco's modified Eagle's medium (GIBCO Inc., Cincinnati, OH) supplemented with 10% fetal bovine serum (Fisher Chemicals, Fairlawn, NJ). All experiments were performed on cells in the exponential growth phase.

5.2.2 *In vitro* hypoxia model

Cells were maintained at 37°C in a humidified incubator containing 21% O_2, 5% CO_2 in air (referred to as normoxic conditions). Hypoxia was produced by placing cell culture plates in a modular incubator chamber (Billups-Rothenberg Inc., Del Mar, CA) and then

flushing with a mixture of 1% O_2, 5% CO_2 and 94% N_2 at a flow rate of 3 L/min for 15 min [148]. The chamber was sealed and placed at 37°C for 48 hours. The flushing procedure was repeated every 12 hours.

5.2.3 Liposomal delivery of ASO and siRNA

The sequence of JNK1 targeted antisense oligonucleotides was 5' – CTC TCT GTA GGC CCG CTT GG – 3' [116]. The DNA backbone of all bases in oligonucleotides was P-ethoxy modified to enhance nuclease resistance and increase incorporation efficacy into liposomes. Antisense oligonucleotides were synthesized by Oligos Etc. (Wilsonville, OR). P-ethoxy modification of oligonucleotides neutralizes negative charge of their DNA backbone making whole ASO neutral. Consequently, neutral liposomes were used to deliver neutral antisense oligonucleotides to cells. Liposomes were prepared using previously described lipid film rehydration method [2,13,112]. Briefly, lipids (Avanti Polar Lipids, Alabaster, AL) were dissolved in chloroform, evaporated to a thin film in a rotary evaporator, and rehydrated with citrate buffer. The lipid ratio was 7:3:10 (egg phosphatidylcholine: 1,2-dipalmitoyl-sn-glycero-3-phosphatidylcholine: cholesterol). Oligonucleotides were loaded into the liposomes by dissolving them in the rehydration buffer at a concentration of 1.4 mM. The encapsulation efficacy ranged from 50 to 60% in different series of experiments. The mean liposome diameter was about 100-200 nm. SiRNA possesses negative charge requiring positively charged (cationic) liposomes to form stable complexes. 1,2 Dioleoyl-2-trimethylammonium-propane (DOTAP, Biontex Laboratories, Munich Germany) was used to prepare cationic liposomes for the delivery

of siRNA (Ambion, Austin, TX). The siRNA (7.5 μg, 300 μL) was dissolved in phosphate buffered saline (pH 7.4) at room temperature. To this solution, 50 μL of DOTAP liposomes (1 mg/mL) were added, mixed by pipette and incubated for 15 min at room temperature. Resulting siRNA-cationic liposome complex was added to the tissue culture flask containing 5-10 mL of medium and 1.5-2.5 x 10^6 cells.

5.2.4 Intracellular localization of ASO and liposomes

To analyze intracellular localization of ASO released from liposomes, a portion of oligonucleotides were labeled by fluorescein isothiocyanate (FITC) prior to incorporation into the liposomes. The labeling was performed by Oligos Etc. (Wilsonville, OR). These labeled ASO were used only in ASO release and localization experiments. Intracellular localization of ASO was studied by fluorescent and confocal microscopy. In these experiments cell nuclei were additionally stained by Hoechst 33258 nuclear dye (Sigma, St. Louis, MO). Part of the liposomes were labeled with rhodamine and osmium tetroxide and visualized by confocal and electron transmission microscopy respectively. Some of the liposomes were labeled with rhodamine or osmium tetroxide and visualized by confocal or electron transmission microscopy, respectively. Rhodamine red succinimidyl ester (Invitrogen, Molecular Probes, Carlsbad, CA) was covalently conjugated with DSPE−PEG lipid. Rhodamine red succinimidyl ester (RRSE, 2 mg, 0.0026 mM) was dissolved in 1 mL of anhydrous dimethylformamide (DMF, Fisher Chemicals), and 4.0 mL of N,N-diisopropylethylamine (Fisher Chemicals) was added to adjust the pH to alkaline and maintain the amine group of the DSPE−PEG lipid in its

nonprotonated form. The DSPE−PEG lipid (14.5 mg, 0.0075 mM) was dissolved separately in 2.0 mL of dimethylformamide and mixed with the RRSE solution. The reaction mixture was stirred for 2 hours protected from light. The DSPE−PEG−RRSE conjugate was purified to remove free RRSE using a dialysis membrane (MW cutoff of 2000 Da) in DMF as a solvent. The conjugate was further purified by size exclusion G10 Sephadex column chromatography, and the solution was dried under vacuum. The DSPE−PEG lipid labeled with rhodamine red was used to prepare rhodamine-labeled liposomes as described earlier. Labeling of liposomes for electron transmission microscopy was done by adding osmium tetroxide (0.5%) to rehydration buffer. Cells were fixed prior to electron microscopy using standard techniques [135,136]. Briefly, cells were primary fixed for 2 hours in Trump's EM Fixative (combination of a low concentration of both formaldehyde and glutaraldehyde in 0.1 M Milloning's phosphate buffer, pH 7.3). Postfixation was carried out in 1% osmium tetroxide in buffer for 1 hour followed by dehydration in graded ethanol series and embedded in Spurr's low-viscosity resin. Sections were prepared using a diamond knife with an LKB-2088 Ultramicrotome (LKB-Produkter, Bromma, Sweden). Observations and micrographs were made with a JEM-100CXII electron microscope (JEOL Ltd., Tokyo, Japan).

5.2.5 Lactic acid and protein concentration

To confirm the existence of cellular hypoxia, the concentration of lactic acid in cell lysates was measured by enzymatic assay kit 755-10 (Sigma, St. Louis, MO) and was

expressed per g of protein determined using the BCA protein assay kit (Pierce, Rockford, IL).

5.2.6 Gene expression

Quantitative RT-PCR was used for the analysis of genes encoding JNK1, caspase 9 and β_2-microglobulin (β_2-m) as previously described [2,112,113,149]. RNA was isolated using an RNeasy kit (Qiagen, Valencia, CA). The following pair of primers were used: JNK1, 5' –TTGGAACACCATGTCCTGAA – 3' (sense) and 5' – ATG TAC GGG TGT TGG AGA GC – 3' (antisense); caspase 9, 5' – TGA CTG CCA AGA AAA TGG TG – 3' (sense) and 5' – CAG CTG GTC CCA TTG AAG AT – 3' (antisense); and β_2-m, 5' – ACC CCC ACT GAA AAA GAT GA – 3' (sense) and 5’ – ATC TTC AAA CCT CCA TGA TG – 3' (antisense). Gene expression was calculated as the ratio of analyzed RT-PCR product to the internal standard (β_2-m).

5.2.7 Protein expression

To confirm RT-PCR data the expression of JNK1 protein and caspase 9 were measured. The identification of the above proteins was determined by Western immunoblotting analysis and processed using scanning densitometry to quantify the expressed protein. To this end, harvested cells were lysed in Ripa buffer (Santa Cruz Biotechnologies, Inc., Santa Cruz, CA) using a needle and syringe. Following incubation on ice for 45 minutes, the cells were centrifuged at 10,000 g for 10 min. Protein content in the supernatant was

determined using the BCA Protein Assay Kit (Pierce, Rockford, IL) and 50 μg of protein was run on a 15% sodium dodecyl sulphate (SDS) polyacrylamide gel immersed in Tris/Glycine/SDS buffer (BioRad, Hercules, CA) for 90 minutes at 70 V. Proteins were transferred to an Immobilon-P nitrocellulose membrane (Millipore, Bedford, MA) in a Tris/Glycine buffer (BioRad, Hercules, CA) for 90 minutes at 100 V. The membrane was blocked in non-fat milk for 2 hours at room temperature on a rotating shaker to prevent non-specific binding, washed and incubated overnight with anti-JNK1 mouse primary antibody (1:2,000 dilution, Cell Signaling Technology, Inc., Beverly, MA), anti-caspase 9 rabbit primary antibody (1:2,000 dilution, Stress Gen Biotechnologies, Victoria State, BC Canada) and anti-β-actin mice primary antibody (1:2,000 dilution, Oncogene Research, San Diego, CA) at 4ºC. Following further washing, the membrane was immersed in goat anti-rabbit and goat anti-mouse IgG biotinylated antibody (1:3000 and 1:1000 dilution, respectively, BioRad, Hercules, CA) at room temperature for 1.5 hours on a rotating shaker. Bands were visualized using an alkaline phosphatase color development reagent (BioRad, Hercules, CA). The bands were digitally photographed and scanned using Gel Documentation System 920 (NucleoTech, San Mateo, CA). β-Actin was used as an internal standard to normalize protein expression. Protein expression was calculated as the ratio of mean band density of analyzed protein to that of the internal standard (β-actin).

5.2.8 Apoptosis

Apoptosis was analyzed by measuring the enrichment of histone-associated DNA fragments (mono- and oligo-nucleosomes) in the cell cytoplasm using anti-histone and anti-DNA antibodies by a cell death detection ELISA Plus kit (Roche, Nutley, NJ) as previously described [2,13,112,113].

5.2.9 Cellular Viability

Cellular viability after hypoxic exposure and/or JNK1 suppression was assessed using a modified MTT (3-(4,5-dimethylthiazol-2-yl)-2,5-diphenyltetrazolium bromide) assay as previously described [150].

5.2.10 Statistical analysis

Data obtained were analyzed using descriptive statistics, single factor analysis of variance (ANOVA) and presented as mean value ± SD from 4 to 8 independent measurements. The difference between variants was considered significant if $P < 0.05$.

5.3 Results

5.3.1 Intracellular localization of liposomes and antisense oligonucleotides

The use of ASO or siRNA to suppress the expression of a targeted mRNA is limited by their low ability to penetrate the cellular plasma membrane and interfere with cell genetic

material. Therefore, a special delivery system is required to enhance the cell penetration. We have successfully used liposomes to deliver genetic material [12,13]. To show that liposomes and incorporated ASO can penetrate into the cellular cytoplasm and nuclei, we labeled liposomes with rhodamine or osmium tetroxide and ASO with fluorescein isothiocyanate (FITC) and incubated with human embryonic kidney 293 cells for 48 hours. In addition, cell nuclei were stained by Hoechst 33258 nuclear dye. The labels were visualized by confocal microscopy (rhodamine), electron transmission microscopy (osmium tetroxide) or fluorescence microscopy (FITC and Hoechst 33258). Typical images obtained in these experiments are presented in Figure 4.3 (Chapter 4) and Figure 5.2 in the present chapter. Confocal microscope images show that rhodamine-labeled liposomes (red fluorescence) penetrated and accumulated inside cells (Fig. 5.2 A, B). Osmium-labeled liposomes were found in cellular perinuclear regions on electron microscopy images as black spheres with average diameter of 100-200 nm (identified by arrows in Fig. 5.2 C). These data show that liposomes were most probably internalized intact by endocytosis (not by the fusion with the plasma membrane) and after destruction release their payload in the perinuclear region. Further fluorescent microscopy analysis showed that FITC-labeled antisense oligonucleotides delivered by liposomes did penetrate cells and accumulated in the cytoplasm and nuclei (Chapter 4, Fig. 4.3 A, C). The latter can be seen in Chapter 4, Figure 4.3 B as blue-colored structures. Therefore, we showed that liposomes can penetrate human cells and deliver genetic material in the cytoplasm and nuclei.

5.3.2 Selection of antisense oligonucleotides and siRNA sequences

The sequence of ASO targeted to JNK1 mRNA was selected based on the data reported by Garay et al [116]. The DNA backbone of all bases in oligonucleotides was P-ethoxy modified to enhance nuclease resistance, eliminate electric charge and increase incorporation efficacy into liposomes. Neutral liposomes were used for intracellular delivery of antisense oligonucleotides. Three siRNA sequences targeted to exon 1, exons 1-2 and exon 8 of JNK1 protein (locus 5599) were selected as possible candidates for JNK1 suppression. Cationic liposomes were used for intracellular delivery of siRNA. Selected liposomal ASO and siRNA were tested on human embryonic kidney 293 cells. Untreated cells and cells treated with empty neutral and cationic liposomes, free (not incorporated into liposomes) ASO and siRNA were used as controls. The expression of gene encoding JNK1 protein was measured by RT-PCR in cells incubated for 48 hours with above-mentioned substances (Fig. 5.3). As expected, empty liposomes did not influence the level of targeted mRNA (please compare bands 1, 3 with the band 1 in Fig. 5.3). Free non-liposomal ASO and all non-liposomal siRNA samples showed a limited or no impact on the expression of JNK1 mRNA. In contrast, liposomal forms of ASO (band 5) and siRNA targeted to exon 1 (band 7) and exons 1, 2 (band 9) substantially decreased the expression of JNK1 mRNA. Based on the results of these experiments, we selected siRNA targeted to exon 1 of JNK1 mRNA (sense sequence GGA GCU CAA GGA AUA GUA Utt) for future experiments. Taken together, these data show that the delivery of ASO and siRNA by liposomes substantially enhanced their specific activity and in turn resulted in the decrease in expression of targeted mRNA.

5.3.3 Suppression of JNK1 decreases apoptosis and mortality under hypoxia

Hypoxia was induced in cell culture by incubation of human embryonic kidney 293 cells for 48 hours in humidified atmosphere of 1% O_2, 5% CO_2 and 94% N_2 at 37° C. The incubation led to statistically significant ($P < 0.05$) lactate accumulation in cell homogenates indicating that cellular hypoxia was severe and was accompanied by the substantial activation of anaerobic glycolysis (Fig. 5.4). As expected, suppression of JNK1 did not influence the severity of cellular hypoxia and did not change the concentration of lactic acid in normoxic and hypoxic conditions.

Analysis of JNK1 mRNA and protein (Fig. 5.5 and 5.6 A, B) showed that hypoxia significantly ($P < 0.05$) increased the expression of JNK1 mRNA and protein. The level of expression of JNK1 protein increased with the duration of hypoxic exposure and reached a plateau at 36-48 h of hypoxia (Fig. 5.5). Upregulation of this protein led to the overexpression of procaspase 9 and, more importantly, active form of caspase 9 (Fig. 5.7) initiating caspase-dependent signaling pathway of apoptosis.

The activation of caspases finally led to significant ($P < 0.05$) apoptosis induction (Fig. 5.8 A) and decrease in cellular viability (Fig. 5.8 B). About 50% of cells died under hypoxia. Empty liposomes and free (non-liposomal) ASO did not influence significantly the expression of JNK1 gene and protein, caspase 9 expression, apoptosis induction and cell death both in normoxia and hypoxia. Free siRNA slightly but significantly ($P < 0.05$) limited this overexpression under hypoxia. However, such limitation did not change the

expression of pro- and active caspase 9 (Fig. 5.7), apoptosis and cellular viability (Fig. 5.8). In contrast, liposomal ASO and siRNA significantly ($P < 0.05$) decreased the expression of JNK1 gene and protein both in normoxia and hypoxia and prevented the overexpression of this protein in hypoxic conditions. The expression of JNK1 mRNA and protein under hypoxia after treatment with liposomal ASO and siRNA was significantly ($P < 0.05$) lower when compared with untreated control in normoxic conditions. The suppression of JNK1 protein led to a statistically significant decrease in the expression of pro- and active caspase 9. Consequently, the level of apoptosis in hypoxic conditions after treatment with liposomal ASO and siRNA was decreased to control levels (Fig. 5.8 A) and cellular viability after hypoxia was significantly ($P < 0.05$) higher (Fig. 5.8 B).

5.4 Discussion

Tissue hypoxia is often a concomitant manifestation of the primary disorders caused by environmental impacts, stress and diseases of different etiology. This secondary tissue hypoxia and accompanying cellular metabolic disorders complicate the progress of the primary disease and/or the normal physiological adaptive responses to the damaging environmental impacts. Therefore, along with measures directed toward correcting the main cause of secondary tissue hypoxia, it would be beneficial to use preparations that increase the cellular resistance to oxygen deficiency. This pharmacological remediation of secondary hypoxic damage should significantly increase the efficacy of treatment of the primary disease, increase the effectiveness of the adaptive responses and prevent extensive cellular damage and death. However, despite many investigations aimed at the

study of antihypoxic action of different physiologically active substances, antihypoxants are not widely used in clinical practice and environmental physiology. Therefore, the search for an effective antihypoxic therapy is an important task of modern pharmacology.

Based on our previous research and literature search [16,112], we concluded that the most effective strategy which can lead to substantial limitation of tissue damage under the conditions of continuous severe secondary hypoxia is the increase in cellular resistance against hypoxia. Because apoptosis plays a significant role in the development of tissue damage under severe tissue hypoxia [2,12,16,112], our attention was focused on the apoptosis signaling cascade under severe hypoxia. The study of the main regulator of cellular response to oxygen deficit – Hypoxia Inducible Factor – showed that its activation in hypoxic conditions induces a bimodal effect: it triggers apoptosis and simultaneously increases the power of antiapoptotic defense [2]. Further investigations showed that the latter prevails in hypoxic conditions and the suppression of this protein finally leads to the increase in apoptotic cellular damage and death [12].

The second protein, Jun N-terminal kinase, attracted our attention as a key regulator of cellular damage under different stresses including hypoxia [5-7]. In the present research, we tested antisense oligonucleotides and siRNA targeted to JNK1 mRNA as a tool to break cell death signal induced by severe hypoxia and therefore prevent apoptosis activation and cell death in the conditions of severe oxygen deficit. We also developed and tested an effective liposomal delivery system that is capable of delivering active ingredients into intracellular perinuclear region. The selected ASO and siRNA delivered

by our liposomal system showed high efficiency in suppressing JNK1 protein. Such suppression prevented activation of caspase-dependent signaling pathway of apoptosis under both continuous hypoxia and accompanied cellular metabolic disturbances. Finally, it decreased hypoxic activation of apoptosis almost down to normal levels and consequently significantly limited cellular mortality induced by severe cellular hypoxia. Although the ASO and siRNA targeted to JNK1 decreased the expression of this protein down to its control levels and prevented caspase-dependent activation of apoptosis under hypoxia, cellular viability was not restored to control levels. This fact shows that in addition to apoptosis, hypoxia induced additional JNK1-independent pathways of cellular mortality. Previously, we found that severe hypoxia limits cellular respiration, induces acidosis, activates lipid peroxidation, stimulates production of prostaglandins and leukotrienes and substantially disturbs phospholipid composition of cellular membranes finally leading to the initiation of both apoptosis and necrosis [112]. It is logical to hypothesize that JNK1-independent necrosis was responsible for the additional cell death induction by hypoxia on the background of suppressed JNK1 protein.

5.5 Conclusion

The present investigation shows that suppression of JNK1 protein substantially limits apoptosis and cellular mortality induced by severe cellular hypoxia. It can be concluded that JNK1 protein may be an attractive target for antihypoxic therapy to increase resistance to many pathological conditions and diseases leading to oxygen deficit.

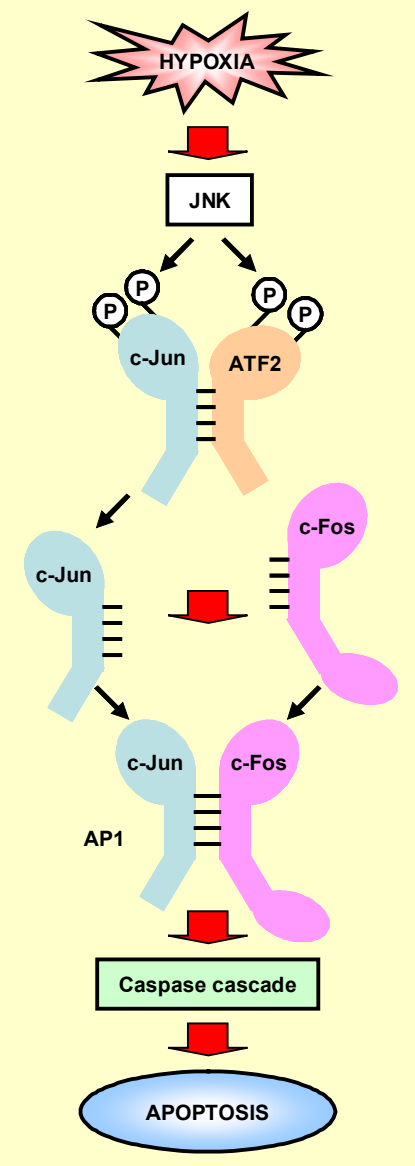

Figure 5.1. Schematic of apoptosis induction by hypoxia. Activation of Jun N-terminal kinase (JNK) by hypoxia mediates phosphorylation of activating transcriptional factor-2 (ATF2) and c-Jun and stimulates their transcriptional activities. The newly synthesized c-Jun protein combines with c-Fos protein to form stable transcriptional factor activator protein-1 (AP1) heterodimers. The formation of AP1 activates caspase-dependent apoptosis signal and finally induces cell death by apoptosis.

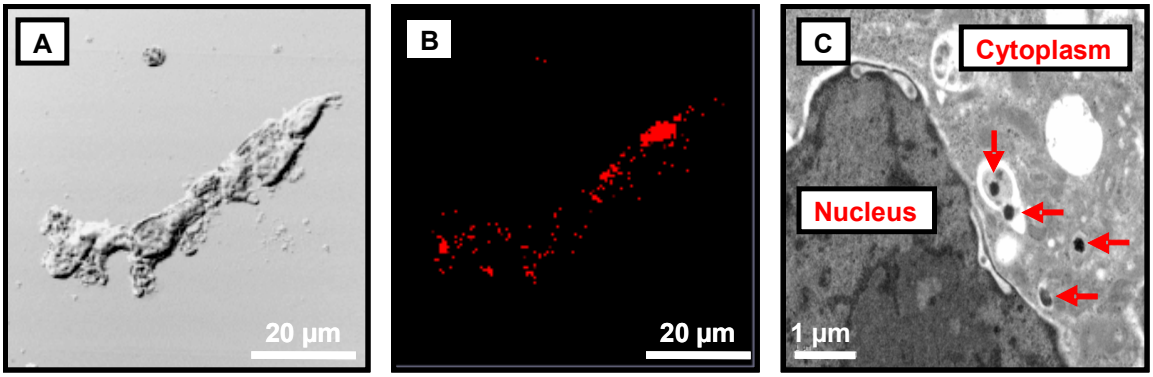

Figure 5.2. Internalization of liposomes in human embryonic kidney 293 cells studied by confocal (A, B) and transmission electron microscopy. A – visible light image. Liposomes were labeled with rhodamine (B, red fluorescence), osmium tetroxide (C, arrows).

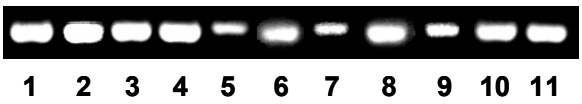

Figure 5.3. Typical image of RT-PCR products of RNA isolated from human embryonic kidney 293 cells incubated with: 1 – Fresh medium (control); 2 – Empty neutral liposomes; 3 – Empty cationic liposomes; 4 – Free (non-liposomal) ASO targeted to JNK1; 5 – Liposomal ASO targeted to JNK1; 6 – Free (non-liposomal) siRNA targeted to JNK1 (Exon 1); 7 – Liposomal siRNA targeted to JNK1 (Exon 1); 8 – Free (non-liposomal) siRNA targeted to JNK1 (Exons 1, 2); 9 – Liposomal siRNA targeted to JNK1 (Exons 1, 2); 10 – Free (non-liposomal) siRNA targeted to JNK1 (Exon 8); 11 – Liposomal siRNA targeted to JNK1 (Exon 8).

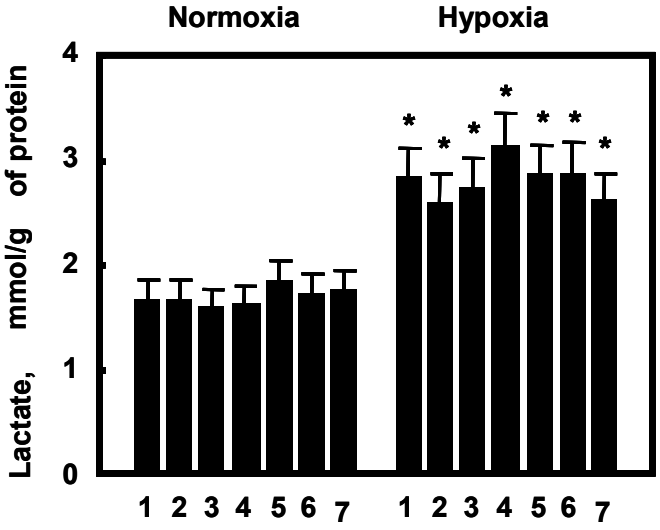

Figure 5.4. Lactate concentration in human embryonic kidney 293 cells in normoxia and hypoxia. Means ± SD are shown. 1 – Control (fresh medium); 2 – Empty neutral liposomes; 3 – Empty cationic liposomes; 4 – Free (non-liposomal) ASO targeted to JNK1; 5 – Free (non-liposomal) siRNA targeted to JNK1 (Exon 1); 6 – Liposomal ASO targeted to JNK1; 7 – Liposomal siRNA targeted to JNK1 (Exon 1).

* $P < 0.05$ when compared with control

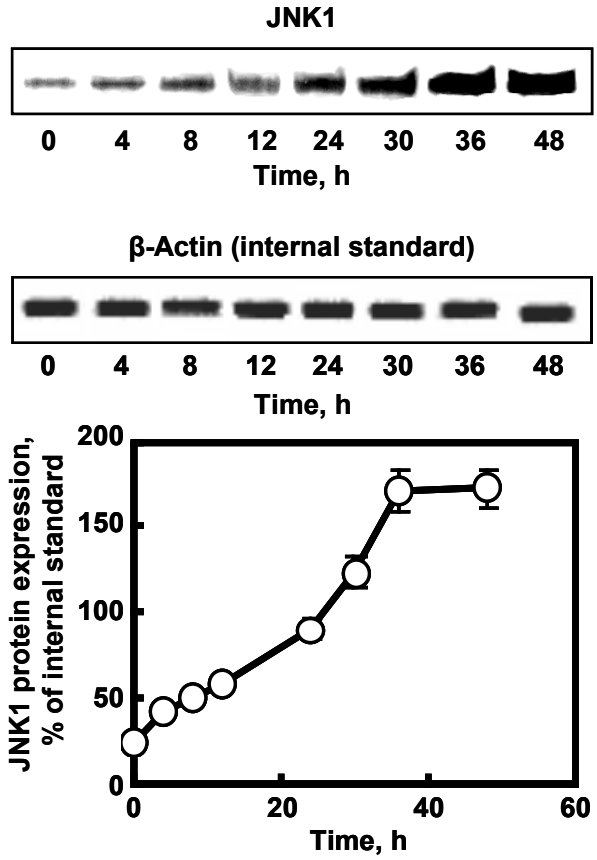

Figure 5.5. Influence of hypoxia on the expression of JNK1 protein (Western blotting) in human embryonic kidney 293 cells

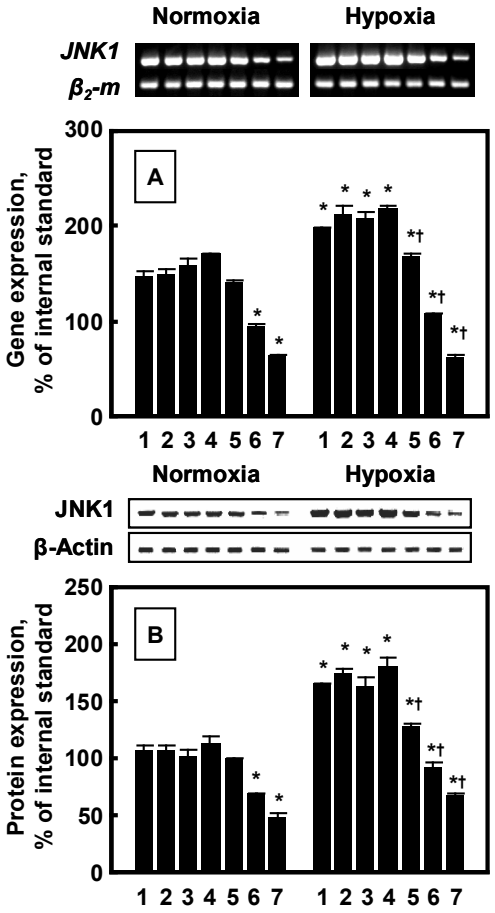

Figure 5.6. Expression of JNK1 mRNA (RT-PCR, A) and protein (Western blotting, B) in human embryonic kidney 293 cells in normoxia and hypoxia. Means ± SD are shown. 1 – Control (fresh medium); 2 – Empty neutral liposomes; 3 – Empty cationic liposomes; 4 – Free (non-liposomal) ASO targeted to JNK1; 5 – Free (non-liposomal) siRNA targeted to JNK1 (Exon 1); 6 – Liposomal ASO targeted to JNK1; 7 – Liposomal siRNA targeted to JNK1 (Exon 1).

* $P < 0.05$ when compared with control

† $P < 0.05$ when compared with hypoxia, no treatment

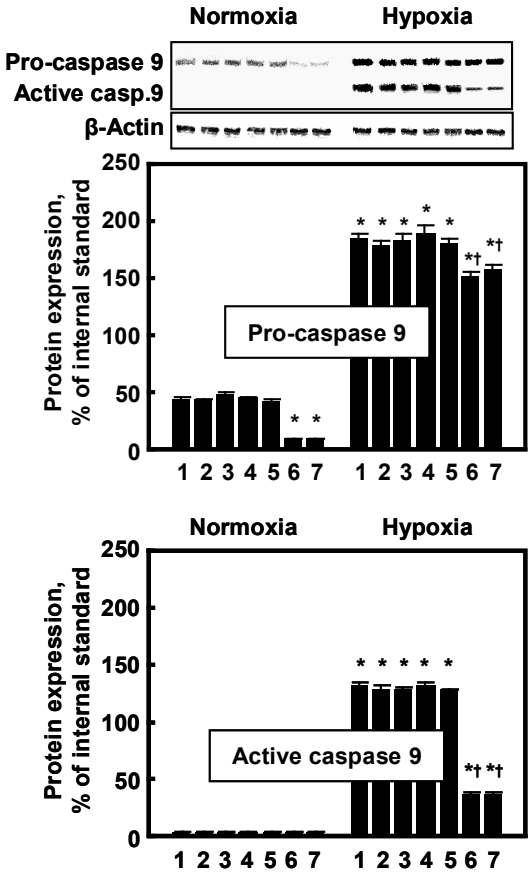

Figure 5.7. Influence of the suppression of JNK1 on the expression of pro- and active caspase 9 in human embryonic kidney 293 cells in normoxia and hypoxia. Means ± SD are shown. 1 – Control (fresh medium); 2 – Empty neutral liposomes; 3 – Empty cationic liposomes; 4 – Free (non-liposomal) ASO targeted to JNK1; 5 – Free (non-liposomal) siRNA targeted to JNK1 (Exon 1); 6 – Liposomal ASO targeted to JNK1; 7 – Liposomal siRNA targeted to JNK1 (Exon 1).

* $P < 0.05$ when compared with control

† $P < 0.05$ when compared with hypoxia, no treatment

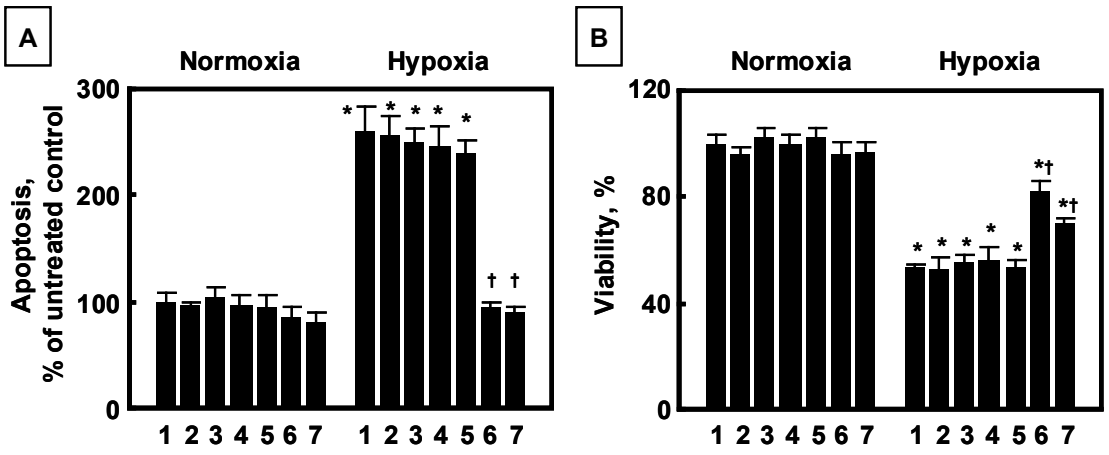

Figure 5.8. Influence of the suppression of JNK1 on apoptosis (A) and cellular viability (B) in human embryonic kidney 293 cells in normoxia and hypoxia. Means ± SD are shown. 1 – Control (fresh medium); 2 – Empty neutral liposomes; 3 – Empty cationic liposomes; 4 – Free (non-liposomal) ASO targeted to JNK1; 5 – Free (non-liposomal) siRNA targeted to JNK1 (Exon 1); 6 – Liposomal ASO targeted to JNK1; 7 – Liposomal siRNA targeted to JNK1 (Exon 1).

* $P < 0.05$ when compared with control

† $P < 0.05$ when compared with hypoxia, no treatment

6 TO STUDY THE *IN VIVO* BODY AND ORGAN DISTRIBUTION OF LIPOSOMAL ANTISENSE OLIGONUCLEOTIDES AND siRNA

6.1 Introduction

During the past 20 years, liposomes have been investigated for the delivery of a variety of small molecules as well as DNA based drugs. These include conventional small molecules and plasmid DNA-containing therapeutic genes, antisense oligonucleotides, and small interfering RNA [12,13,32,101,112,142,151,152]. Lipophilic and hydrophilic drugs can be incorporated into the lipid membrane or inner aqueous space of liposomes, respectively. The delivery of different types of payloads requires different properties of carriers, including their surface charge. While modified uncharged nucleotides can be delivered by neutral or slightly charged liposomes, native negatively charged ASO, siRNA, or DNA molecules require cationic liposomes.

For effective delivery of oligonucleotides *in vivo*, there are a number of important parameters that need to be considered. There are several biological barriers that stand between the oligonucleotide and its ultimate site of action in the cytosol or nucleus of tissue cells. For free oligonucleotides, an important limitation is rapid excretion via the kidney. For large carriers of oligonucleotides, the vascular endothelial wall comprises a major barrier. Degradation by serum and tissue nucleases is another barrier affecting efficient delivery of ASO and siRNA. For large molecules or carrier systems, uptake by phagocytes of the reticuloendothelial system leading to sequestration in liver and spleen,

failure to cross capillary endothelium and slow diffusion/binding in extracellular matrix are all issues to consider. Both small and large delivery agents can be affected by poor cellular uptake and inefficient release from endosomes. The aims for optimal delivery of oligonucleotides are therefore enhanced cellular uptake, improved exit from subcellular compartments and correct targeting (spatial and temporal) to a particular site of action [114,153].

Modified phosphodiester analogs, such as phosphorothioates, have been made to overcome the nuclease hydrolysis problem, but they have not provided a completely satisfactory solution to the problem. Another modified phosphodiester analog that has been prepared is p-ethoxy (pE) oligos. The modifications of pE oligos are made in the phosphate backbone so that the modification will not interfere with the binding of these oligos to the target mRNA. pE oligos are made by adding an ethyl group to the nonbridging oxygen atom of the phosphate backbone, thus rendering these oligos uncharged compounds. In spite of their resistance to nucleases, the cellular uptake and intracellular delivery of pE oligos are still not completely satisfactory because upon internalization, these oligos remain sequestered inside the endosomal/lysosomal vacuoles, impeding their access to the target mRNA.

Above and beyond the stability issue, functional delivery of siRNA molecules *in vivo* is still the major obstacle and a prerequisite for the development of siRNA therapeutics. Several recent reports have shown local delivery of siRNAs *in vivo*, including local administration to the eye for the treatment of age-related macular degeneration, intranasal

administration for pulmonary delivery and direct delivery into the central nervous system. Despite these promising results on local delivery, an effective, non-toxic systemic application of siRNA-based therapeutics has not yet been developed for clinical application due to the absence of appropriate non-viral delivery technologies [154].

A large number of previous studies report the *in vivo* pharmacokinetics and metabolism of various modified antisense oligonucleotides [120]. For e.g. PS ASOs have been well characterized in many species, including humans. PS ASOs are well absorbed from parenteral sites [155], and display rapid distribution and prolonged elimination from tissue distribution sites [156,157]. PS ASOs distribute broadly in peripheral tissues with liver and kidney accumulating the highest concentrations. Eventual elimination from tissue is believed to be primarily a function of metabolism with little to no intact drug recovered in urine or feces at doses below 10 mg/kg [120]. Compared to ASO, very little is known about the pharmacokinetics and pharmacodynamics of siRNA. Intravenous or intraperitoneal injection of siRNAs resulted in a broad tissue distribution with accumulation preferentially in the liver, jejunum and kidney [94,158]. Literature evidence suggests that systemically administered lipoplexed siRNAs have better pharmacokinetic properties than non-formulated siRNA molecules that are rapidly excreted through the kidney. Recent data demonstrate that cationic lipid-based formulations of siRNAs improve the biodistribution properties of siRNAs and allow for a predominant uptake of siRNAs into endothelial cells throughout the body. In contrast to naked or nonformulated siRNA molecules, the siRNA-lipoplexes were strongly taken up by the vascular endothelium in the liver, heart and lung [154].

In the present study, traditional neutral and 1,2-dioleoyl-3-trimethylammonium-propane (DOTAP) cationic liposomes were investigated. Neutral P-ethoxy-ASO was used as payload for neutral liposomes while DOTAP liposomes were used to deliver negatively charged siRNA.

6.2 Materials and Methods

6.2.1 Animals

Studies were conducted in 6-8 week old female SKH1 mice weighing 25-35 g (Charles River Laboratories, Wilmington, MA). All mice were maintained in micro-isolated cages under pathogen free conditions in the animal maintenance facilities of Rutgers, The State University of New Jersey.

6.2.2 Liposomal composition for the delivery of antisense oligonucleotides

Antisense oligonucleotides were synthesized by Oligos Etc. (Wilsonville, OR). The DNA backbone of all bases in oligonucleotides was P-ethoxy modified to enhance nuclease resistance and increase incorporation efficacy into liposomes [131]. To analyze biodistribution of ASO released from liposomes, a portion of oligonucleotides were labeled with fluorescein isothiocyanate (FITC) prior to incorporation into the liposomes. The labeling was performed by Oligos Etc. Neutral liposomes were prepared using

previously described lipid film rehydration method [2,13,112]. Briefly, lipids (Avanti Polar Lipids, Alabaster, AL) were dissolved in chloroform, evaporated to a thin film in a rotary evaporator, and rehydrated with citrate buffer. The lipid mole ratio for this formulation was 51:44:5 egg phosphatidylcholine/cholesterol/1,2,-distearoyl-sn-glycero-3-phosphoethanolamine-N-aminopolyethelenglycol-MW-2000 ammonium salt, respectively. ASOs were loaded into the liposomes by dissolving them in the rehydration buffer at a concentration of ~0.5 mM. After preparation, free ASO was separated from the liposomes by passing the liposome suspension through a Sephadex G-50 column. The encapsulation efficacy ranged from 50 to 60% in different series of experiments. The mean liposome diameter was about 100-200 nm.

An aliquot of neutral liposomes was labeled with near infrared fluorescent dye Cy5.5 Mono NHS Ester (GE Healthcare, Amersham, UK). To this end, lipids and Cy5.5 were dissolved in chloroform, evaporated to a thin film layer in a rotary evaporator and rehydrated with citrate buffer. Antisense oligonucleotides were loaded into liposomes by dissolving in rehydration buffer at a concentration of 0.5 mM. Liposomes were extruded gradually using polycarbonate membranes, 200 and 100 nm at room temperature using extruder device from Northern Lipids Inc. (Vancouver, BC, Canada).

6.2.3 Liposomal composition for the delivery of siRNA

Cationic liposomes were prepared using 1,2 Dioleoyl-2-trimethylammonium-propane - DOTAP (Avanti Polar Lipids, Alabaster, AL) at a concentration of 5 mg/mL. DOTAP

was dissolved in chloroform, evaporated to a thin film layer in a rotary evaporator and rehydrated with 0.9% NaCl followed by extrusion through 100 nm polycarbonate membrane. To analyze intracellular localization of siRNA, siGLO Red (siRNA labeled with Pierce NuLight DY-547 fluorophore) purchased from Dharmacon Inc. (Chicago, IL) was used. siGLO was dissolved in phosphate buffered saline at a concentration of 200uM. DOTAP liposomes were mixed with siGLO in ratio 6:1 v/v and incubated at room temperature for 15 minutes before use. Mean particle size of the complex was >500 nm.

An aliquot of cationic liposomes was labeled with fluorescent dye Cy5.5 Mono NHS Ester (GE Healthcare, Amersham, UK). To this end, lipid and Cy5.5 were dissolved in chloroform, evaporated to a thin film layer in rotary evaporator and rehydrated with 0.9% NaCl to a final concentration of 5 mg/mL of DOTAP. Liposomes were extruded gradually using polycarbonate membranes, 200 and 100 nm at room temperature using extruder device from Northern Lipids Inc. (Vancouver, BC, Canada).

6.2.4 Body distribution of liposomes

The distribution of different liposomes and their payload was examined in mice. Labeled, empty neutral and cationic liposomes as well as liposomes containing labeled ASO or siRNA were delivered by intravenous administration. Injected volume of liposomes was 100 μL for each formulation. Animals were anesthetized with isoflurane and entire body images were taken by IVIS imaging system (Xenogen Corporation, Alameda, CA) 30

minutes, 1 hour, 2 hours and 24 hours after treatment. The animals were euthanized and lungs, heart, liver, spleen, and kidneys were excised, rinsed in saline and fluorescence was registered by IVIS imaging system. Visible light and fluorescence images were taken and overlaid by an imaging system. The intensity of fluorescence was represented on composite light/fluorescent images by different colors with blue color reflecting the lowest fluorescence intensity and red color, the highest intensity. Images of each organ were then scanned and total fluorescence intensity was calculated by a special computer program developed for our laboratory by Dr. V. P. Pozharov. Preliminary experiments showed a strong linear correlation between the total amount of labeled substance accumulated in the organ and calculated total fluorescence intensity (data are not shown). The fluorescence was expressed in arbitrary units, where, 1 unit represented approximately 2×10^{10} photons/s/sr/cm^2. The method allowed a quantitative comparison of the accumulation of the same fluorescent dye between different series of experiments.

6.2.5 Statistical analysis

Data were analyzed using descriptive statistics, single-factor analysis of variance (ANOVA), and presented as mean values ± the standard deviation from four to eight independent measurements. The difference between variants is considered significant if $P < 0.05$.

6.3 Results

6.3.1 Body distribution of neutral and cationic liposomes

Body distribution of neutral and cationic liposomes possessed several common and distinct features (Figs. 6.1 and 6.3). First, after intravenous (i.v.) injection both types of liposomes accumulated predominately in liver, kidneys and lungs. However, the total amount of neutral liposomes accumulated in these organs was higher when compared with cationic liposomes. Substantial amounts of neutral liposomes accumulated in all organs starting 30 minutes after injection, highest level of fluorescence being observed in the liver and lungs. In the liver, the level of fluorescence increased gradually within the 24-hour period. In the lung, liposomes accumulated over time resulting in an increased amount of fluorescence at one hour post-injection, before tapering off at 24 hours. The total accumulation of cationic liposomes was less as compared to neutral liposomes in all organs. In this case also, fluorescence was visible starting 30 minutes post-injection. The liver and lung showed highest level of fluorescence one hour post-injection of cationic liposomes, after which it decreased. The kidneys showed accumulation of same levels of fluorescence throughout the experiment.

6.3.2 Body distribution of ASO and siRNA delivered by neutral and cationic liposomes

Body distribution of ASO and siRNA delivered by neutral and cationic liposomes was similar to the distribution of liposomes alone (Figs. 6.2 and 6.4). Intravenous delivery led to predominant accumulation of ASO and siRNA in the liver, kidneys and lungs. In most

cases, 24 hours after i.v. injection, liposomal payloads were accumulated mainly in the liver and kidney, while their amount retained in the lungs substantially decreased when compared with earlier periods after the treatment. It is interesting, that amount of relatively large DOTAP: siRNA complexes (>500 nm) accumulated in the lungs was higher in the later stages of the experiment (1-24 hours), while the quantity of smaller cationic liposomes without siRNA (10-140 nm) was higher in the earlier stages (0.5-1 hour). It is possible that larger liposome/siRNA complexes require longer time for the degradation of entire complex and siRNA release.

Both neutral and cationic liposomes did not appear to penetrate through the blood-brain barrier, as indicated by negligible fluorescence observed in the brain. Consequently, only trace amounts of ASO and siRNA delivered by liposomes were found in the brain (Fig. 6.5).

6.4 Discussion

The *in vivo* application of ASO and siRNA for targeting disease relevant genes has been limited by several technical obstacles such as stability of the oligonucleotides in body fluids, functional intracellular uptake, bioavailability and cell-type-specific targeting. Antisense oligonucleotides have been vigorously pursued as a therapeutic strategy for over 20 years. One ASO, fomivirisen has been approved for treatment of cytomegalovirus retinitis and is administered by intraocular injection [159]. Balanced against this success, systemically administered ASOs have failed to gain approval after

Phase 3 clinical trials. One of the most important lessons from antisense strategies is the need to understand oligonucleotide biodistribution and focus on diseases that affect organs and cell types in which synthetic nucleic acids may be most likely to have an impact after systemic administration. Most *in vivo* studies with naked siRNAs attempt to circumvent the problem of poor biodistribution by administering high doses directly to the target organ by injection [160-162]. However, the systemic administration is still the most clinically relevant route for indications such as cancer or metabolic diseases. It has been shown that systemically administered lipoplexed siRNAs have better pharmacokinetic properties than non-formulated siRNA molecules that are rapidly excreted through the kidney [154]. The application of cationic lipids to deliver nucleic acids *in vivo* has hitherto been limited by their low efficiency and high systemic toxicity after i.v. administration.

The charge of liposomes has been shown to affect tissue specific liposome uptake. Macrophages seem to preferentially take up negatively charged liposomes. Liposomal makeup also influences cellular toxicity, with oligonucleotide delivery using a liposome with a higher proportion of neutral lipids leading to less cellular toxicity. A complete understanding of the best liposomal makeup for delivery of therapeutic substances is still evolving. Literature evidence suggests that in case of cationic liposomes, lipoplex efficiency is partially attributed to a rapid and efficient escape from the acidic lysosomal compartment, or to delayed transfer to lysosomes. There is sufficient evidence that lipoplexes are able to destabilize endosomal/lysosomal membranes [163,164] and it was demonstrated that efficient cationic lipid formulations are able to perforate the endosomal

membrane, whereas less efficient lipid formulations are not [165]. This process is explained by electrostatic interaction between the oppositely charged cationic lipids of lipoplex and anionic phospholipids composing intracellular compartments leading to disturbances in the curvature of the vesicles and finally lead to leakage or bursting and release of endosomal contents to the cytoplasm [119]. The role of this phenomenon on transfection efficiency, as well as its correlation with lipoplex structure is not well understood. Landen et al. showed that siRNA delivery using a neutral lipid, such as DOPC, allows liposomal uptake and breakdown of the intracellular liposome with release of its contents into the cytoplasm [166]. Neutral liposomes have been used in our laboratory successfully to deliver ASO [12,13]. Here, we used cationic liposomes prepared using monocationic lipid DOTAP for the delivery of siRNA and neutral liposomes for the delivery of p-ethoxylated neutral ASO. Based on fluorescence intensity, it was found that the total accumulation of cationic liposomes was less as compared to neutral liposomes in all organs.

6.5 Conclusion

Liposomes and liposomal complexes of different sizes (100-1000 nm) used in this study were able to provide an efficient delivery of biologically active substances, antisense oligonucleotides and small interfering RNA in mice with accumulation in liver, kidneys and lungs.

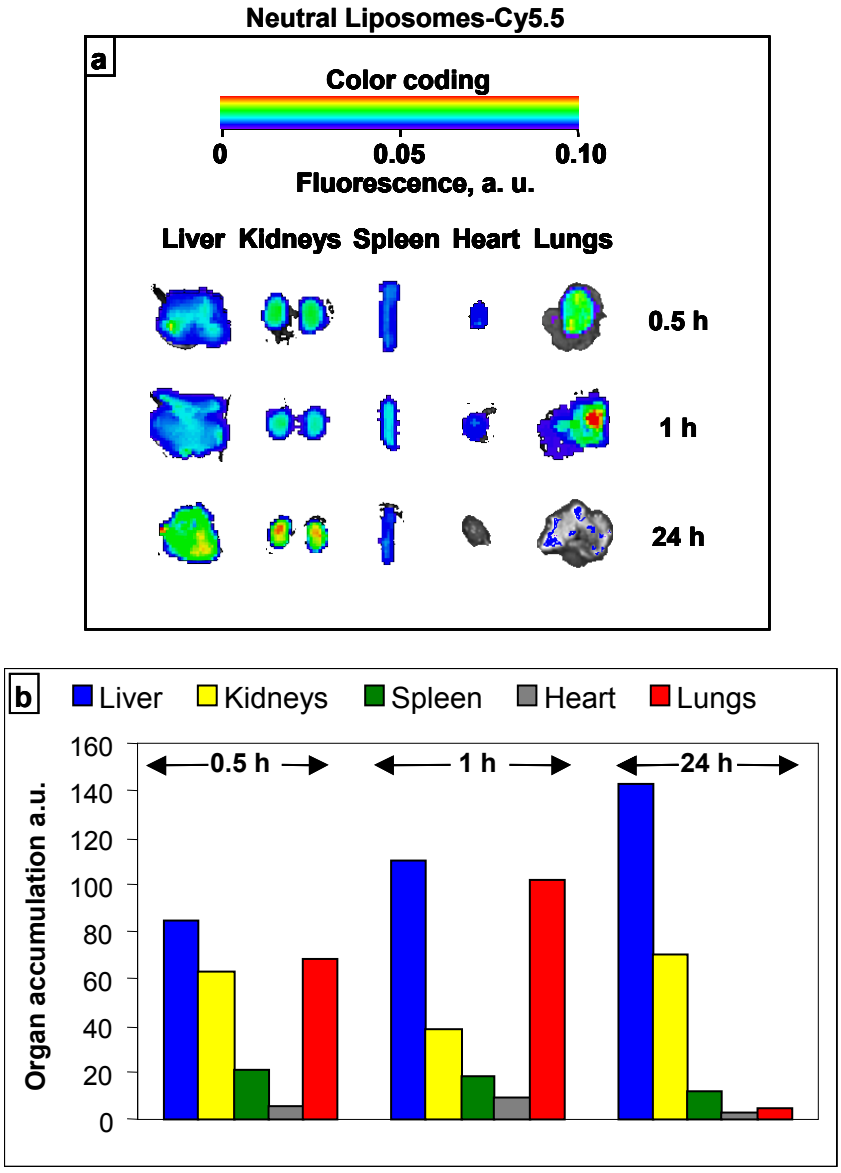

Figure 6.1. Body distribution of neutral liposomes. Liposomes were labeled with near infrared Cy5.5 dye and delivered intravenously. The distribution was measured using IVIS Xenogen imaging system. The upper panel (a) contains representative images of different organs excised 0.5, 1 and 24 hours after injection. The intensity of fluorescence is expressed by different colors with blue color reflecting the lowest intensity and red color, highest intensity. The bottom panel (b) demonstrates average organ accumulation of labeled liposomes. Means are shown.

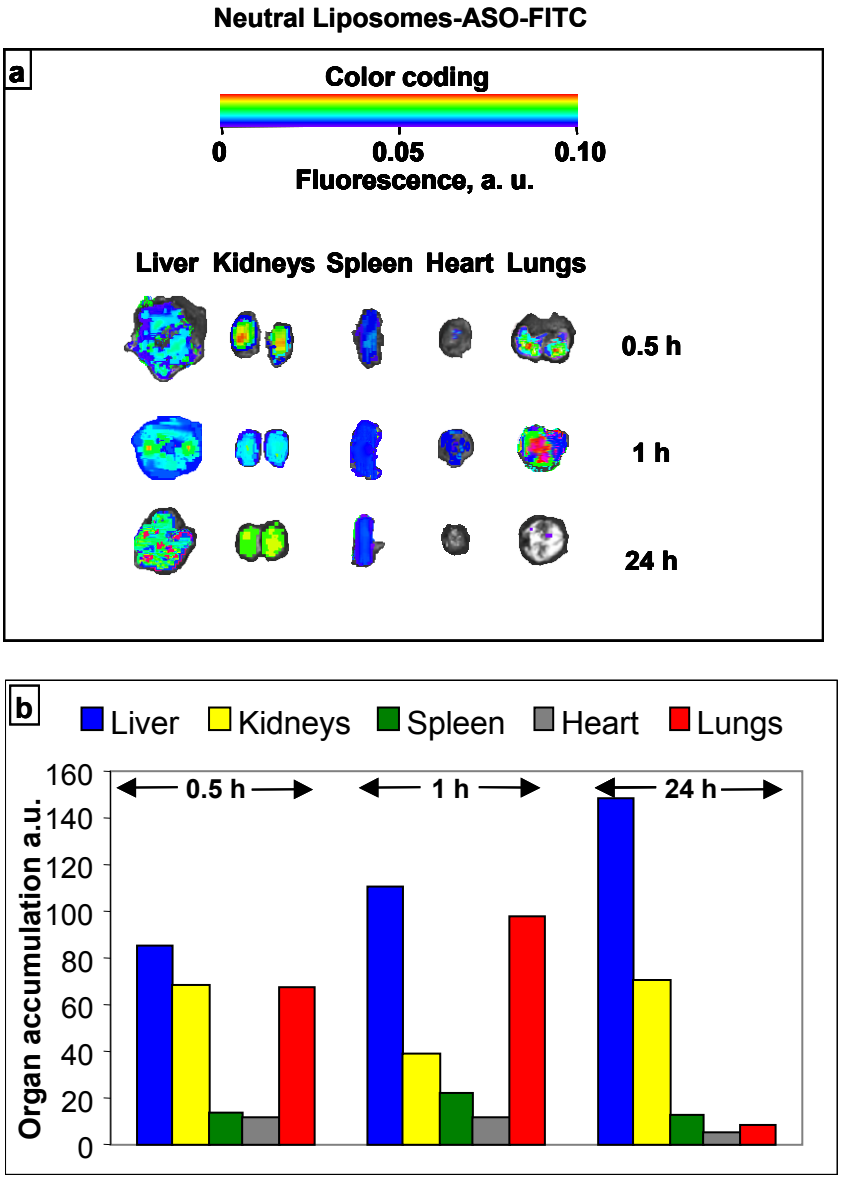

Figure 6.2. Body distribution of antisense oligonucleotides delivered by neutral liposomes. P-ethoxy neutral ASO were labeled with fluorescein isothiocyanate (FITC), encapsulated into neutral liposomes and delivered intravenously into mice. The distribution was measured using IVIS Xenogen imaging system. The upper panel (a) contains representative images of different organs excised 0.5, 1 and 24 hours after injection. The intensity of fluorescence is expressed by different colors with blue color reflecting the lowest intensity and red color reflecting the highest intensity. The bottom panel (b) demonstrates average organ accumulation of labeled ASO. Means are shown.

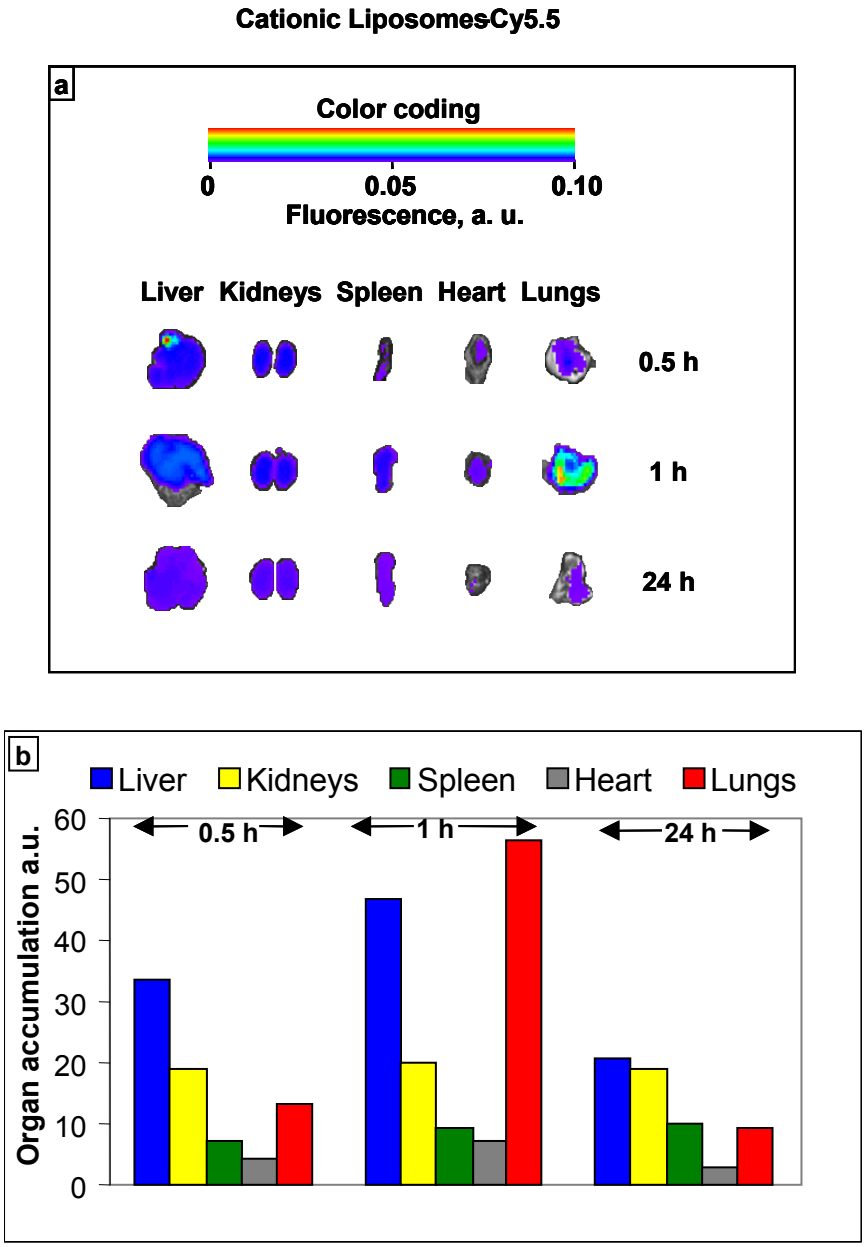

Figure 6.3. Body distribution of cationic liposomes. Liposomes were labeled with near infrared dye Cy5.5 and injected intravenously into mice. The distribution was measured using IVIS Xenogen imaging system. The upper panel (a) contains representative images of different organs excised 0.5, 1 and 24 hours after injection. The intensity of fluorescence is expressed by different colors with blue color reflecting the lowest intensity and red color, the highest intensity. The bottom panel (b) demonstrates average organ accumulation of labeled liposomes. Means are shown.

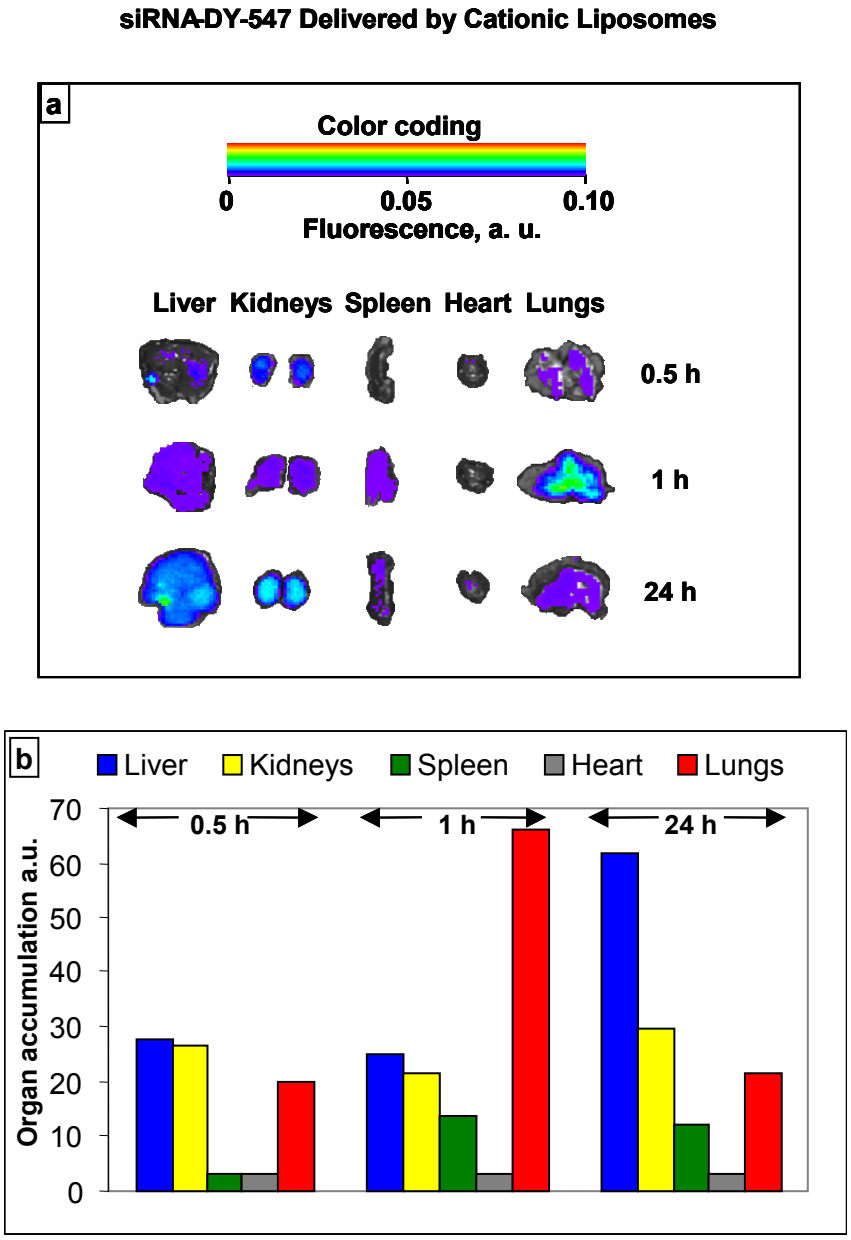

Figure 6.4. Body distribution of siRNA delivered by cationic liposomes. siRNA labeled with near infrared dye (siGLO red) was complexed with cationic liposomes and delivered intravenously into mice. The distribution was measured using IVIS Xenogen imaging system. The upper panel (a) contains representative images of different organs excised 0.5, 1 and 24 hours after injection. The intensity of fluorescence is expressed by different colors with blue color reflecting the lowest intensity and red color reflecting the highest intensity. The bottom panel (b) demonstrates average organ accumulation of labeled siRNA. Means are shown.

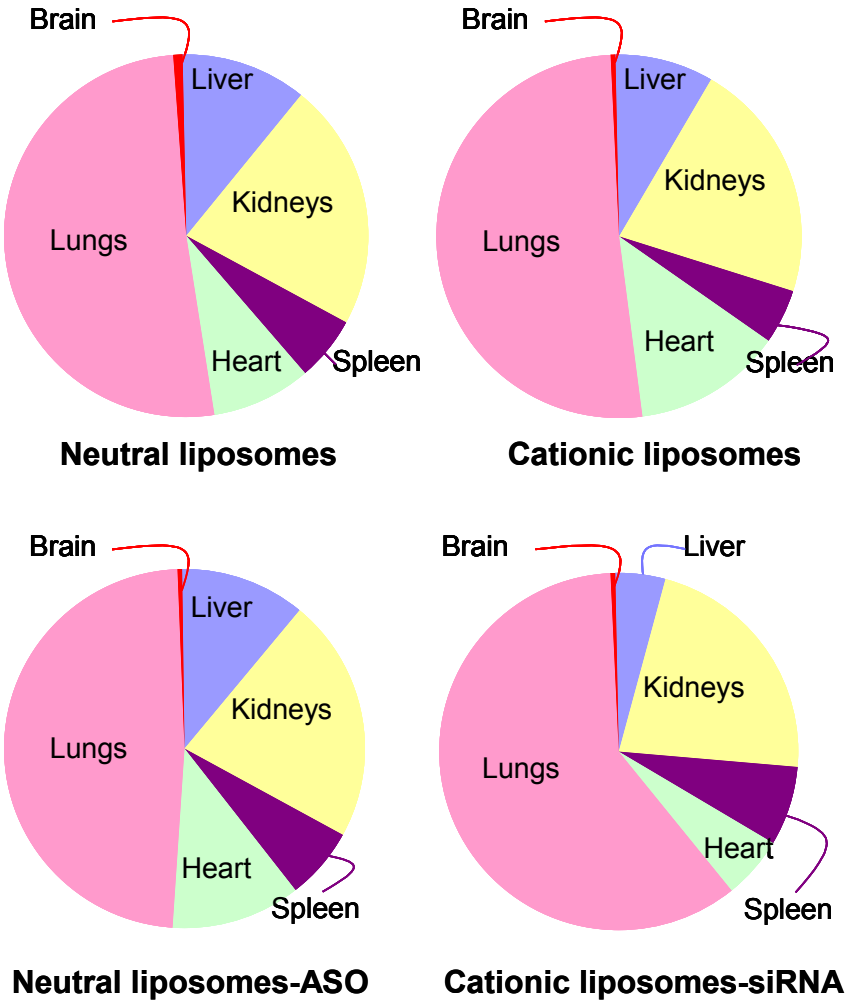

Figure 6.5. Relative tissue concentration of empty neutral and cationic liposomes, ASO and siRNA in different organs. ASO and siRNA were delivered by neutral and cationic liposomes, respectively. Liposomes, ASO and siRNA were labeled with fluorescent dyes and intravenously injected to hairless mice. Two hours after treatment, mice were euthanized, their organs were excised, fluorescence was registered by IVIS imaging system and normalized per gram of tissue weight in each organ.

7 TO DEVELOP AN EXPERIMENTAL *IN VIVO* MODEL OF HYPOXIA AND EXPLORE REMEDIATION OF HYPOXIC DAMAGE BY ANTISENSE OLIGONUCLEOTIDES AND siRNA TARGETED TO JNK1 MRNA.

7.1 Introduction

Alterations in oxygen tension (PO_2) elicit a variety of functional responses in different cell types, including gene expression, altered metabolic function, altered ion channel activation, and release of neurotransmitters. The ability to respond to hypoxia is an essential evolutionary adaptation in higher vertebrates. Hypoxia can be caused by a generalized reduction in oxygen delivery, such as in altitude and pulmonary diseases, or by disruption in the local blood supply, such as in ischemic disorders. In vivo, hypoxic conditions exist when oxygen demand exceeds supply. Hypoxia affects many organ systems including the lungs, brain, heart, kidney, and liver. Important in the adaptations to hypoxia is the activation of genes that respond to this oxygen deficit. Hypoxia inducible factor alpha (HIF1A) protein is a key initiator of cell death signal under hypoxic conditions [1]. We investigated the role of this protein as a possible target for the remediation of hypoxic cellular damage and found that HIF1A plays a bimodal role during hypoxia [2]. On the one hand, the activation of HIF1A during hypoxia initiates cell death signal inducing apoptosis (programmed cell death, or cellular suicide) and necrosis (pathological cell death). On the other hand, overexpression of HIF1A boosts the power of anti-hypoxic systems that increase cellular resistance to hypoxia.

It has been shown that another major player in the activation of apoptosis signaling pathways and hypoxic damage from the MAPK family of proteins, is Jun N-terminal kinase (JNK) – a stress-activated protein kinase that can be induced by inflammatory cytokines, bacterial endotoxin, osmotic shock, UV radiation, and hypoxia [5-7]. We recently investigated the role of this protein as a possible target for the remediation of hypoxic cellular damage. We demonstrated that inhibition of JNK1 by antisense oligonucleotides (ASO) or small interfering RNA (siRNA) targeted to JNK1 mRNA substantially suppressed JNK1 protein expression in vitro and effectively limited apoptosis induction and cellular death under severe hypoxic conditions [151]. Simulating hypoxia *in vitro* and *in vivo* in a controlled environment is a relatively complex exercise. In our *in vitro* studies, simulation of hypoxic condition was conducted using a gas mixture of 1% oxygen, 5% carbon dioxide and 94% nitrogen. Experimental *in vivo* models for tissue hypoxia and injury induced by hypoxia have been reported in literature [49]. In the present study, we have investigated remediation of hypoxic damage by ASO and siRNA targeted to JNK1 in an experimental mouse model of hypoxia.

Hypoxia has elicited a great deal of interest among the scientific community due to its role in life-threatening pathologies such as stroke, acute renal failure, myocardial infarction, lung edema, cancer etc. Oxygen deprivation associated with ischemia has recently become a subject of intense scrutiny. Hypoxia that accompanies ischemia has been investigated both *in vivo* and *in vitro* within the last decade [20,122]. Hypoxia can induce significant tissue damage. For instance, in lungs, hypoxia causes several destructive changes within the lung parenchyma, including the surfactant system-forming

structures, edematous changes, damage to the alveolar lining and accumulation of alveolar macrophages. Experimental models for lung tissue hypoxia and acute lung injury induced by hypoxia have been reported in literature [15,112]. We propose to study the effect of ASO and siRNA targeted to JNK1 in an experimental mouse model exposed to acute normobaric hypoxia (low concentration of oxygen in gas mixture under normal barometric pressure). Treatment of mice *in vivo* will be reproduced from the treatment used in the *in vitro* experiments where 1% oxygen was used.

The concentration of oxygen that cell cultures were exposed to in our previous study was 1% [151]. Using following equation:

Partial pressure of O_2 = Mole fraction of O_2 x Total pressure,

the partial pressure of O_2 required to achieve 1% concentration at a barometric pressure of 760 mm Hg is ~ 7.6 mm Hg.

Assuming that the respiratory quotient and $PACO_2$ are similar in rodents and humans [167] and using the alveolar gas equation shown below, the fraction O_2 that the mice are required be exposed to, was calculated. The calculated value is ~ 8% fraction of O_2.

$PAO_2 = FIO_2 (P_B\text{-}PH_2O) – PACO_2 [FIO_2 + (1\text{-}FIO_2)/R]$

Where,

PAO_2 = alveolar PO_2

P_B = barometric pressure

FIO_2 = fraction of inspired oxygen

PH_2O = water vapor pressure in airways

$PACO_2$ = alveolar PCO_2

PAO_2 is calculated using an assumed R value of 0.8

7.2 Material and Methods

7.2.1 Cell line

The human embryonic kidney 293 cells were obtained form American Type of Tissue Culture (Manassas, VA). Cells were cultured in Dulbecco's modified Eagle's medium (GIBCO Inc., Cincinnati, OH) supplemented with 10% fetal bovine serum (Fisher Chemicals, Fairlawn, NJ). Experiments were performed on cells in the exponential growth phase.

7.2.2 *In vivo* hypoxia model

Studies were conducted in 6-8 week old female SKH1 mice weighing 25-35 g (Charles River Laboratories, Wilmington, MA). The animals were housed at room temperature with a humidity of 40 ± 15 % and light-dark cycle on 12 h/day. Mice received food and water *ad libitum*. For each of normoxia and hypoxia, five groups of animals were used. Group 1 was untreated control, Group 2 was treated with empty neutral liposomes, Group 3 was treated with empty cationic liposomes, Group 4 was treated with ASO targeted to

JNK1 mRNA delivered by neutral liposomes and Group 5 was treated with siRNA targeted to JNK1 mRNA delivered by cationic liposomes. Mice in the normoxia group were kept at room temperature and humidity and breathed room air. Mice in the normobaric hypoxia group were placed in a 300 x 350 x 600 mm plexiglass chamber specifically designed for this project (Billups-Rothenberg Inc., Del Mar, CA). Hypoxia was induced by subjecting the chamber to a constant flow (15-20 L/min) of hypoxic gas mixture, either 8% oxygen-92% nitrogen or 6% oxygen-94% nitrogen. The oxygen concentration in the chamber was continuously monitored using an oxygen analyzer (Vascular Technology Inc, Nashua, NH). A heating pad was placed inside the plexiglass chamber to maintain the body temperature of mice. Mice from each experimental group were treated with 100 μL of different formulations by intraperitoneal injection. The dose of siRNA and ASO was 13 nmoles/mouse (173 and 80 ug siRNA and ASO, respectively). After treatment, mice were immediately exposed to either normoxia or normobaric hypoxia for a period of two hours after which they were sacrificed. The organs were excised and divided in four portions. Three portions were frozen for subsequent lactate, apoptosis, protein and RNA analyses, while the other portion was stored in 10% phosphate buffered formalin for further histological evaluation.

7.2.3 Liposomal delivery of ASO and siRNA targeted to JNK1 mRNA

The sequence of antisense oligonucleotides targeted to JNK1 mRNA was 5' – CTC TCT GTA GGC CCG CTT GG – 3' [116]. The DNA backbone of all bases in oligonucleotides was P-ethoxy modified to enhance nuclease resistance and increase incorporation

efficacy into liposomes. P-ethoxy modification of oligonucleotides neutralizes negative charge of their DNA backbone making the ASO neutral. Antisense oligonucleotides were synthesized by Oligos Etc. (Wilsonville, OR) according to our design. Neutral liposomes were used to deliver neutral antisense oligonucleotides to cells. Neutral liposomes were prepared using previously described lipid film rehydration method [2,13,112,151]. Briefly, lipids (Avanti Polar Lipids, Alabaster, AL) were dissolved in chloroform, evaporated to a thin film in a rotary evaporator, and rehydrated with citrate buffer. The lipid ratio was 7:3:10 (egg phosphatidylcholine: 1,2-dipalmitoyl-sn-glycero-3-phosphatidylcholine: cholesterol). Oligonucleotides were loaded into the liposomes by dissolving them in the rehydration buffer at concentrations of ~1.4 mM. The liposomes were extruded gradually using polycarbonate membranes 200 nm and 100 nm at room temperature using extruder device from Northern Lipids Inc (Vancouver, BC, Canada). The encapsulation efficacy ranged from 50 to 60% in different series of experiments. The mean liposome diameter was about 100-200 nm. The sequence of siRNA targeted to exon 1 JNK1 mRNA (sense sequence GGA GCU CAA GGA AUA GUA UTT) was selected based on the results of our preliminary experiments. siRNA was synthesized by Ambion (Austin, TX). siRNA possesses negative charge requiring positively charged (cationic) liposomes to form stable complexes. Cationic liposomes were prepared from positively charged dioleoyl-2-trimethylammonium propane - DOTAP (Avanti Polar Lipids, Alabaster, AL) in concentration 5 mg/mL using thin layer procedure described above and followed by extrusion through 100 nm polycarbonate membrane. The siRNA was dissolved in RNase free water at a concentration of 400 μM. To this solution, appropriate volume of DOTAP (5 mg/mL) was added, mixed by pipette and incubated for

30 minutes at room temperature. The molar ratio of siRNA: DOTAP was ~1:100. Resulting siRNA-cationic liposome complex was used in the studies.

7.2.4 Lactic acid and protein concentration

Approximately 30-40 mg of tissues (lung, heart, brain, liver, kidney and spleen) were weighed, lysed in Ripa buffer (Santa Cruz Biotechnologies, Inc., Santa Cruz, CA) and homogenized using Ultra Turrax T-25 basic homogenizer (IKA Works, Wilmington, NC). To confirm the existence of cellular hypoxia, the concentration of lactic acid in tissue homogenates was measured by an enzymatic assay kit (Sigma, St. Louis, MO) and was expressed per g of protein determined using the BCA protein assay kit (Pierce, Rockford, IL).

7.2.5 Gene expression

Quantitative RT-PCR was used for the analysis of genes encoding JNK1, caspase 9 and β-actin as previously described [2,112,113,149]. RNA was isolated using an RNeasy kit (Qiagen, Valencia, CA). Approximately 25-30 mg of tissue was homogenized in lysis buffer using Ultra Turrax T-25 basic homogenizer (IKA Works, Wilmington, NC). The following pair of primers were used: JNK1, 5' –TTGGAACACCATGTCCTGAA – 3' (sense) and 5' – ATG TAC GGG TGT TGG AGA GC – 3' (antisense); caspase 9, 5' – TGA CTG CCA AGA AAA TGG TG – 3' (sense) and 5' – CAG CTG GTC CCA TTG AAG AT – 3' (antisense); and β-actin, 5' –GAC AAC GGC TCC GGC ATG TGC A – 3'

(sense) and 5' –TGA GGA TGC CTC TCT TGC TCT G– 3' (antisense). PCR products were separated in 4% NuSieve 3:1 Reliant agarose gel (Lonza, Allendale, NJ) in 1X TBE buffer (0.089 M Tris/Borate, 0.002 M EDTA, pH 8.3; Research Organics Inc., Cleveland, OH) by gel electrophoresis. Gene expression was calculated as the ratio of analyzed RT-PCR product to the internal standard (β-actin).

7.2.6 Protein expression

To confirm RT-PCR data the expression of JNK1 protein and caspase 9 were measured by two methods: Western immunoblotting analysis and immunohistochemistry.

Western Immunoblotting

The identification of the above proteins was determined by Western immunoblotting analysis and processed using scanning densitometry to quantify the expressed protein. To this end, approximately 30-40 mg of each tissue was weighed, lysed in Ripa buffer (Santa Cruz Biotechnologies, Inc., Santa Cruz, CA) and homogenized using Ultra Turrax T-25 basic homogenizer (IKA Works, Wilmington, NC). Following incubation on ice for 45 minutes, the tissues were centrifuged at 10,000 g for 10 min. Protein content in the supernatant was determined using the BCA Protein Assay Kit (Pierce, Rockford, IL) and 40 µg of protein was run on a 15% sodium dodecyl sulphate (SDS) polyacrylamide gel immersed in Tris/Glycine/SDS buffer (BioRad, Hercules, CA) for 90 minutes at 70 V. Proteins were transferred to an Immobilon-P nitrocellulose membrane (Millipore,

Bedford, MA) in a Tris/Glycine buffer (BioRad, Hercules, CA) for 90 minutes at 100 V. The membrane was blocked in non-fat milk for 2 h at room temperature on a rotating shaker to prevent non-specific binding, washed and incubated overnight with anti-JNK1 mouse primary antibody (1:2,000 dilution, Cell Signaling Technology, Inc., Beverly, MA), anti-caspase 9 rabbit primary antibody (1:2,000 dilution, Stress Gen Biotechnologies, Victoria State, BC Canada) and anti-β-actin mice primary antibody (1:2,000 dilution, Oncogene Research, San Diego, CA) at 4ºC. Following further washing, the membrane was immersed in goat anti-rabbit and goat anti-mouse IgG biotinylated antibody (1:3000 and 1:1000 dilution, respectively, BioRad, Hercules, CA) at room temperature for 1.5 h on a rotating shaker. Bands were visualized using an alkaline phosphatase color development reagent (BioRad, Hercules, CA). The bands were digitally photographed and scanned using Gel Documentation System 920 (NucleoTech, San Mateo, CA). β-Actin was used as an internal standard to normalize protein expression. Protein expression was calculated as the ratio of mean band density of analyzed protein to that of the internal standard (β-actin).

Immunohistochemistry

The identification of the JNK1 protein was also made by immunohistochemical staining of paraffin embedded tissue sections. After deparaffinization and rehydration, the slides were stained using Vector® M.O.M. Immunodetection Kit (Vector Laboratories, Inc., Burlingame, CA). Mouse monoclonal antibody to JNK1 (Cell Signaling Technology, Inc., Beverly, MA, 1:40 dilution) was used as primary antibody for detection.

Biotinylated anti-mouse IgG Reagent (1:250 dilution, Vector Laboratories, Inc., Burlingame, CA) and HSP-Streptavidine Detection System (1:500 dilution, Vector Laboratories, Inc., Burlingame, CA) in combination with DAB substrate kit for peroxidase were used for visualization. After staining the slides were analyzed by light microscopy and photographed.

7.2.7 Apoptosis

Apoptosis was analyzed by measuring the enrichment of histone-associated DNA fragments (mono- and oligo-nucleosomes) in tissue homogenates using anti-histone and anti-DNA antibodies by a cell death detection ELISA Plus kit (Roche, Nutley, NJ) as previously described [2,13,107,108].

7.2.8 Statistical analysis

Data obtained were analyzed using descriptive statistics, single factor analysis of variance (ANOVA) and presented as mean value ± SD from 4 to 8 independent measurements. The difference between variants was considered significant if $P < 0.05$.

7.3 Veterinary care

Veterinary care followed the guidelines described in the guide for the care and use of laboratory animals (AAALAC) as well as the requirements established by the Rutgers

Institutional Animal Care and Use Committee (IACUC). Animal experiments were performed according to the Rutgers IAUC protocol # 04-007.

7.4 Results

7.4.1 Intracellular localization of liposomes, antisense oligonucleotides and siRNA

The use of ASO or siRNA to suppress the expression of a specific mRNA is limited by their low ability to penetrate the cellular plasma membrane and interfere with cell genetic material. Therefore, an appropriate delivery system is required to enhance the cell penetration of ASO and siRNA. As shown in Chapter 6 and previous work conducted in our laboratory, we have successfully used liposomes to deliver genetic material [12,13] [12,13,115]. To show that liposomes and incorporated ASO/siRNA can penetrate into the cellular cytoplasm and nuclei, liposomes were labeled with Cy5.5; ASO were labeled with fluorescein isothiocyanate (FITC) and siRNA were labeled with FAM (siGLO green). The labeled substances were incubated with human embryonic kidney 293 cells for 2 hours and visualized by confocal microscopy. Typical images obtained in these experiments are presented in Fig. 7.1. Confocal microscope images show that Cy5.5 labeled neutral and cationic liposomes (red fluorescence) penetrated and accumulated inside cells (Fig. 7.1 A, B). Further confocal microscopy analysis showed that antisense oligonucleotides and siRNA delivered by liposomes also were successfully internalized by cells and accumulated in the cytoplasm (Fig. 7.1 C, D). In addition, ASO delivered by liposomes demonstrated an efficient nuclear penetration (Fig. 7.1, C). Therefore, it was

shown that liposomes could penetrate human cells and deliver genetic material in the cytoplasm and cellular nuclei.

7.4.2 Development of hypoxia model *in vivo*

Based on the alveolar gas equation and concentration of oxygen used in *in vitro* studies, the value for oxygen concentration that was calculated for use in i*n vivo* studies was 8%. Studies were conducted by inducing hypoxia in mice using a gas mixture with 8% oxygen and balance nitrogen for two hours. At the end of the experiment, mice were sacrificed, their organs excised and analyzed for lactate levels, JNK1 gene and protein expression. In addition, a histological analysis of hypoxic damage of tissues was performed. Results of lactate levels for each tissue from these studies indicated that although hypoxia was achieved in mice with exposure to 8% oxygen, the degree of hypoxic damage was not severe. Lactate levels under hypoxia were found to be slightly higher than those under normoxia (data not shown). Results of gene and protein expression studies indicated mild overexpression of JNK1 gene and protein. Histological analysis showed that hypoxic changes in tissues were not significant. Based of these results, we increased the severity of hypoxic exposure by decreasing oxygen concentration in inhalation mixture down to 6%.

Hypothermia is known to have protective effects on hypoxia-induced lethality. Moderate hypothermia has shown to improve survival [168-171]. The exact mechanism for this protection is not known. Since hypothermia could potentially be activated in mice under

hypoxia, this mechanism was suppressed by increasing the body temperature of mice by utilizing a heating pad (37˚C) in the hypoxia chamber for the duration of the experiment.

7.4.3 Suppression of JNK1 decreases apoptosis under hypoxia

Hypoxia was induced in mice by inhalation of gas mixture containing 6% oxygen and balance nitrogen for two hours. Control mice (normoxia, 1) breathed room air in similar chamber as animals with hypoxia. As was mentioned above, tissue level of lactate was used as an indicator of tissue hypoxia. Significant lactate accumulation was observed in tissues indicating that hypoxia was achieved accompanied by activation of anaerobic glycolysis. Figure 7.2 shows the average relative increase in lactate levels represented by the ratio of lactate level in studied tissues under hypoxia to that under normoxia. The lactate levels showed the highest increase in brain, followed by heart, spleen and lungs. The severity of hypoxia was not influenced by suppression of JNK1 and did not change the concentration of lactic acid in normoxic and hypoxic conditions.

Hypoxia significantly ($P < 0.05$) increased the expression of JNK1 mRNA as shown in Figure 7.3a for lung, heart and brain (bar #2). Empty liposomes did not appear to have an influence on the expression of JNK1 gene under hypoxia. In contrast, liposomal ASO and siRNA targeted to JNK1 mRNA significantly ($P < 0.05$) decreased the expression of JNK1 gene and prevented its overexpression under hypoxia. The expression of JNK1 gene under hypoxia after treatment with liposomal ASO and siRNA was significantly ($P < 0.05$) lower when compared with untreated control. This suppression of JNK1 was

highly pronounced in heart, followed by lung. In brain, the suppression of JNK1 was also found, but to a lower extent, possibly due to inefficient penetration of liposomal delivery system through the blood-brain barrier (BBB). Immunohistochemical analysis of JNK1 protein confirms the gene expression data. It was found that hypoxia induced the expression of JNK1 protein in all studied organs. Liposomal ASO and siRNA targeted to JNK1 mRNA substantially downregulated JNK1. However, in the brain there was marginal decrease in the overexpression of JNK1 protein (Fig. 7.3 b).

The upregulation of JNK1 gene and protein under hypoxia led to the overexpression of procaspase 9 and active caspase 9 (Fig. 7.4). The activation of caspase-dependent signaling pathway of apoptosis led to significant ($P < 0.05$) apoptosis induction under hypoxia (Fig. 7.5). Empty liposomes did not influence pro- and active caspase 9 expression. Suppression of JNK1 gene and protein in mice treated with liposomal ASO and siRNA targeted to JNK1 mRNA led to significant decrease in the expression of pro- and active caspase 9 in lung and heart. Consequently, apoptotic cell death under hypoxia for those treatments significantly decreased as observed in Figure 7.5, bars 4 and 5. In brain, apoptosis could not be inhibited likely because liposomes used for the delivery of ASO and siRNA did not cross the BBB.

7.4.4 Morphology/Histological analysis

As an example of tissue histological changes, we used lung tissues of mice exposed to 6% oxygen for 2 hours. Hematoxylin-eosin stain in lung tissue under normoxia and

hypoxia showed that hypoxia led to serious lung injury. In addition to apoptosis, hypoxia leads to necrotic cell death. As shown in the bottom panel of Figure 7.6, lung tissue edema is observed under hypoxia (no treatment). In mice treated with liposomal ASO and siRNA targeted to JNK1 mRNA, necrotic damage and edema produced by hypoxia were significantly less pronounced.

7.5 Discussion

Tissue hypoxia is often a concomitant manifestation of the primary disorders caused by environmental impacts, stress and diseases of different etiology. This secondary tissue hypoxia and accompanying cellular metabolic disorders complicate the progress of the primary disease and/or the normal physiological adaptive responses to the damaging environmental impacts. Based on our previous research and literature data [16,112], we suggested that the most effective strategy which can lead to substantial limitation of tissue damage under the conditions of continuous severe secondary hypoxia is the increase in cellular resistance against hypoxia. Jun N-terminal kinase, attracted our attention as a key regulator of cellular damage under different stresses including hypoxia [5-7,151]. We have shown that antisense oligonucleotides and siRNA targeted to JNK1 mRNA delivered using a nanoscale liposomal delivery system in an *in vitro* cell model of hypoxia was effective in breaking the cell death signal induced by severe hypoxia. In the present research, we confirmed these results in an *in vivo* mouse model of hypoxia. We showed that suppression of JNK1 gene and protein led to significant decrease in apoptotic cell death by limitation of the caspase-dependent apoptotic signaling pathway.

Severe hypoxia induces significant damage in all studied tissues. The mechanisms of hypoxic damage are complicated and not well understood. We studied effect of hypoxia mainly in three organs, lung, heart and brain. In the case of lung, hypoxia has been shown to induce destructive-exudative changes within lung parenchyma including surfactant forming structures, edematous changes and damage to the alveolar lining. Activation of lipid peroxidation and limitation in cellular antioxidant defense during hypoxia also contribute to lung injury [112]. In the present study, however, the lipid peroxidation pathway was not investigated. A variety of experimental and clinical studies have demonstrated that chronic hypoxia, whether constant or intermittent, has major effects on heart structure and function [172]. Brain is an active tissue in terms of glucose metabolism and almost all the energy supplied to maintain its vital functions is derived from glucose oxidation. Hypoxia leads to restriction of glucose supply and metabolism, which leads to cerebral edema and infarct. Under hypoxic conditions, the anaerobic glycolytic pathway is activated which is known to induce cerebral edema formation as a consequence of depletion of ATP and accumulation of lactate in cerebral tissues. In our investigations, increased lactate levels were observed in all studied tissues under hypoxia when compared with normoxia.

In the lung and heart, we showed that suppression of JNK1 gene and protein using a liposomal delivery system led to significant decrease in apoptotic cell death by limitation of the caspase-dependent apoptotic signaling pathway. However in brain, this suppression

was marginal, likely due to poor penetration of the liposomes across the blood-brain barrier.

The present studies provide confirmation of the role of JNK1 gene in the modulation of cell death due to hypoxia. Our *in vitro* and *in vivo* studies demonstrate that remediation of cell damage resulting from hypoxia can be achieved by suppression of JNK1. Literature evidence indicates that JNK is also activated during reperfusion following ischemia in rat heart as well as during hypoxia/reoxygenation [116]. A strong correlation between JNK activation and apoptosis induction has been described previously in heart and kidney exposed to ischemia/reperfusion [173]. Injury resulting from ischemia/reperfusion has been identified as a major stimulus for organ dysfunction and cellular death in several disease states including angina and myocardial infarction. The future direction of the investigations in our laboratory may focus on ischemia/reperfusion injury in the context of activation of JNK1.

7.6 Conclusion

The selected ASO and siRNA delivered by neutral and cationic liposomes demonstrated showed high efficiency in suppressing JNK1 protein. Such suppression prevented activation of caspase-dependent apoptotic signaling pathway under hypoxia. It decreased hypoxic activation of apoptosis close to normal levels and consequently limited cellular mortality induced by severe cellular hypoxia. The *in vivo* results corroborate the data obtained *in vitro*. Therefore, JNK1 protein might be an attractive target for antihypoxic

therapy to increase resistance to many pathological conditions and diseases leading to oxygen deficit.

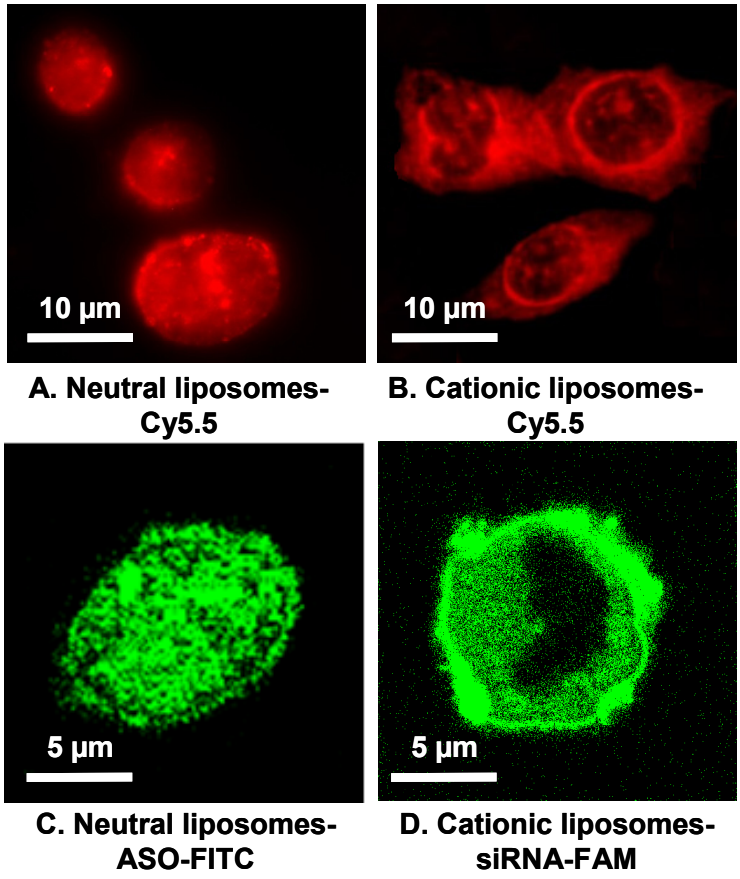

Figure 7.1. Intracellular localization of neutral and cationic liposomes, ASO and siRNA delivered by neutral and cationic liposomes, respectively. Typical images of 293 cells incubated 120 min with substanced indicated. Neutral and cationic liposomes were labeled with Cy5.5 (red fluorescence), ASO were labeled with FITC (green), siRNA were labeled with FAM (siGLO green).

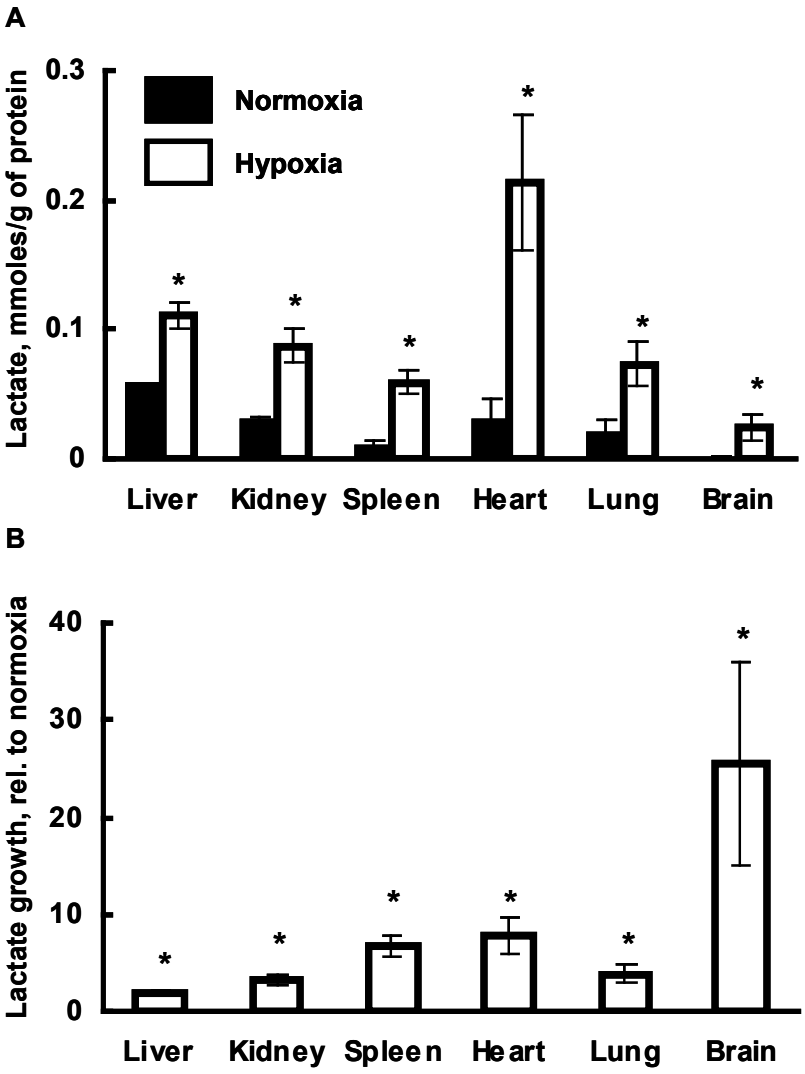

Figure 7.2. Accumulation of lactic acid in different organs under hypoxia. (A) Absolute values. (B) Lactate growth under hypoxia relative to normoxia values. Hypoxia was induced in mice by the inhalation of gas mixture containing 6% of O_2 for 2 hours. Means ± SD are shown. *$P < 0.05$ when compared with normoxia.

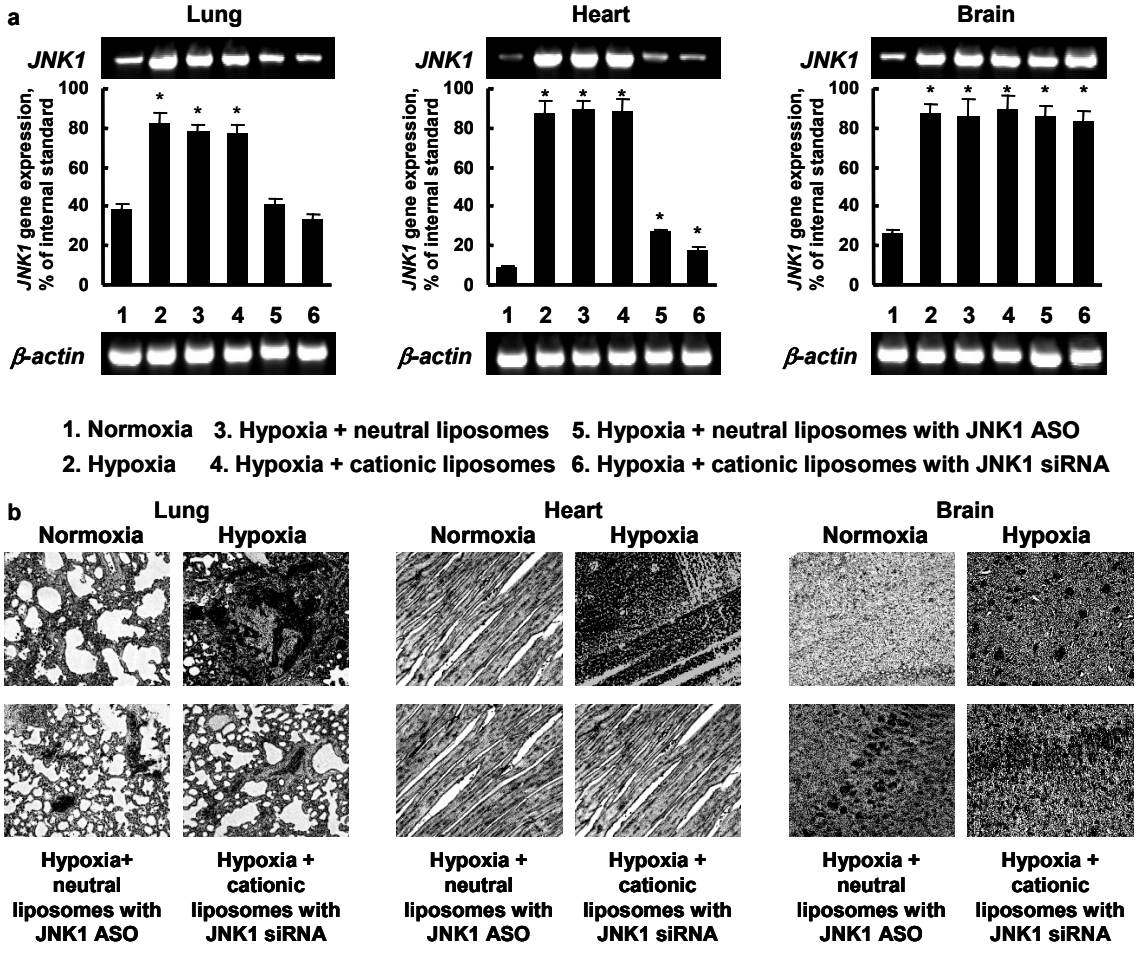

Figure 7.3. Expression of JNK1 gene and protein in mouse organs under normoxia and hypoxia. Hypoxia was induced in mice by the inhalation of gas mixture containing 6% O_2 for 2 hours. Control mice (normoxia, 1) breathed room air in the same chamber as animals with hypoxia. Mice were treated with saline (control, 1, 2) and indicated substances (3-6) immediately before hypoxic exposure. (a) Typical gel electrophoresis images of RT-PCR products and average expression of JNK1 gene. Gene expression was calculated as a ratio of band intensity of JNK1 gene to that of internal standard (b-actin). Means ± SD are shown. *$P < 0.05$ when compared with control. (b) Typical images of tissue section stained with antibody against JNK1 protein. Dark color indicates high protein expression.

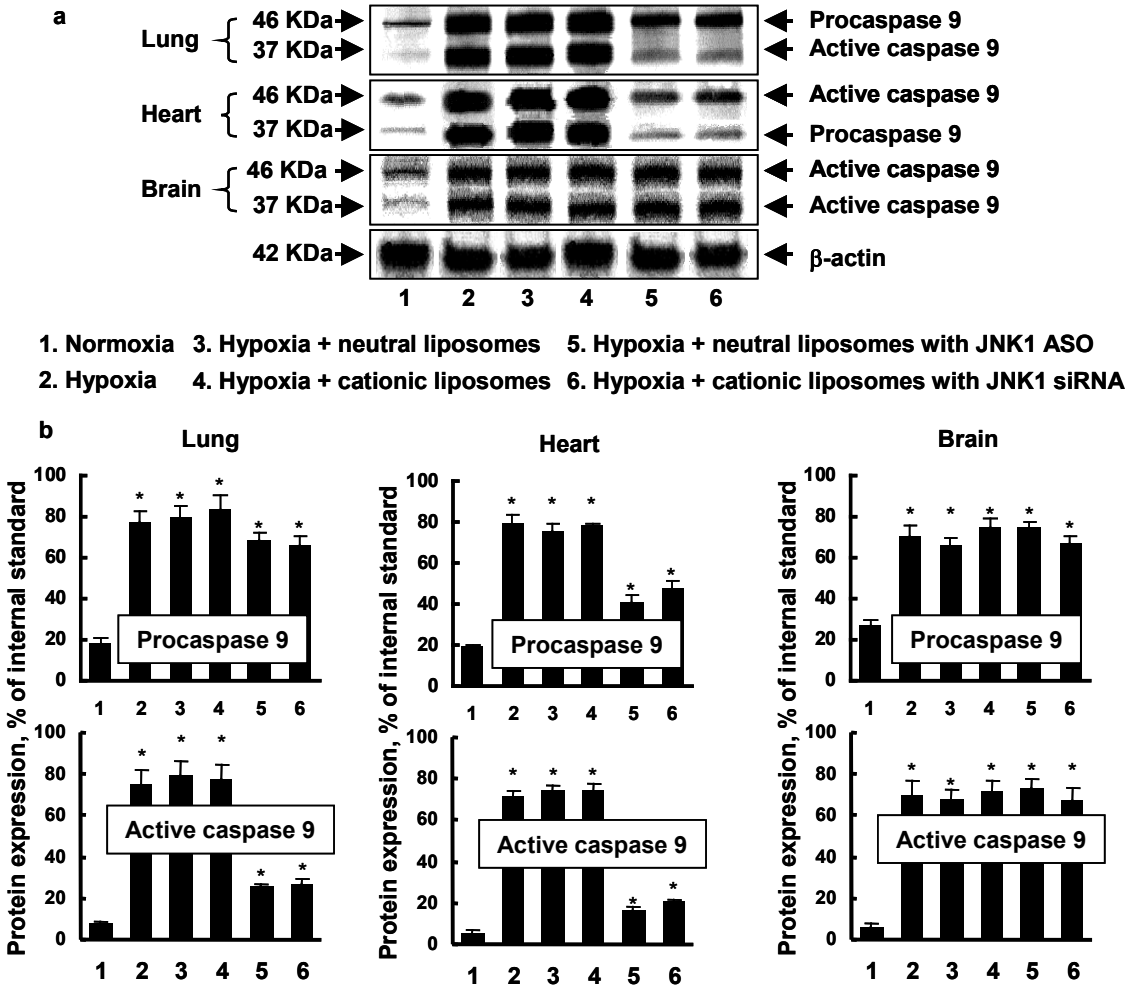

Figure 7.4. Expression of caspase 9 in mouse organs under normoxia and hypoxia. Hypoxia was induced in mice by the inhalation of gas mixture containing 6% O_2 for 2 hours. Control mice (normoxia, 1) breathed room air in the same chamber as animals with hypoxia. Mice were treated with saline (control, 1, 2) and indicated substances (3-6) immediately before hypoxic exposure. (a) Typical images of Western blotting membranes stained with antibodies against caspase 9. (b) Average expression of caspase 9 calculated as a ratio of band intensity of caspase 9 to that of internal standard (b-actin). Means ± SD are shown. *$P < 0.05$ when compared with control.

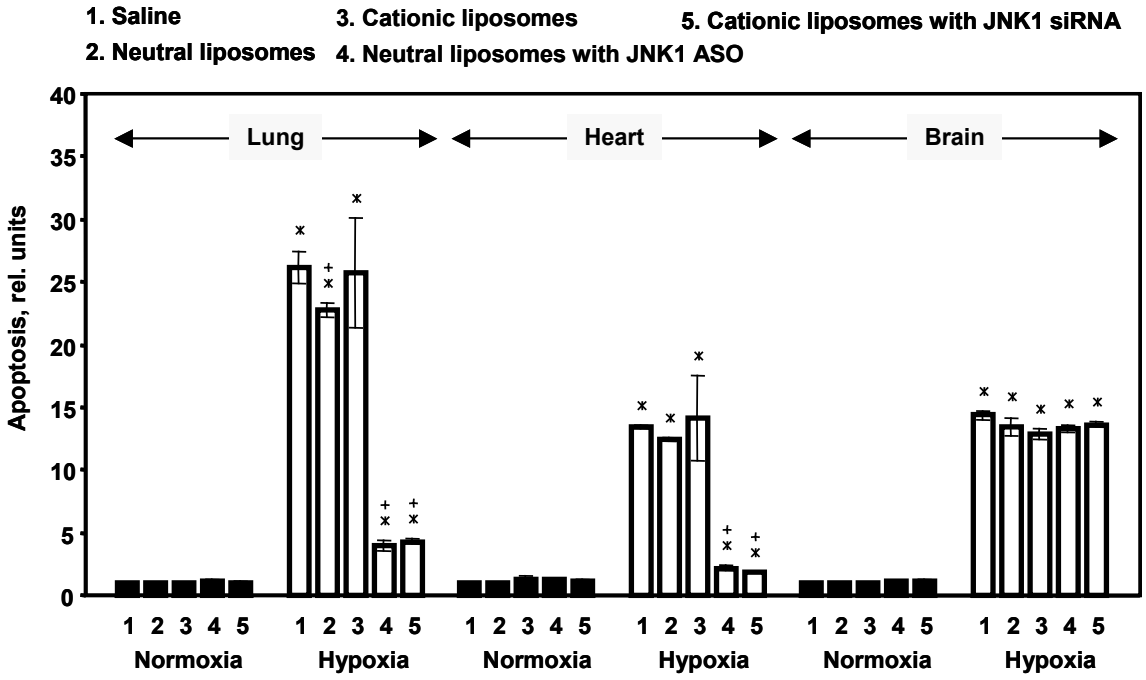

Figure 7.5. Apoptosis induction by hypoxia in different organs. Hypoxia was induced in mice by the inhalation of gas mixture containing 6% of O_2 for 2 hours. Mice were treated with saline (control, 1) and indicated substances (2-5) immediately before hypoxic exposure. Means ± SD are shown. *P < 0.05 when compared with normoxia. +P < 0.05 when compared with hypoxia treated with saline.

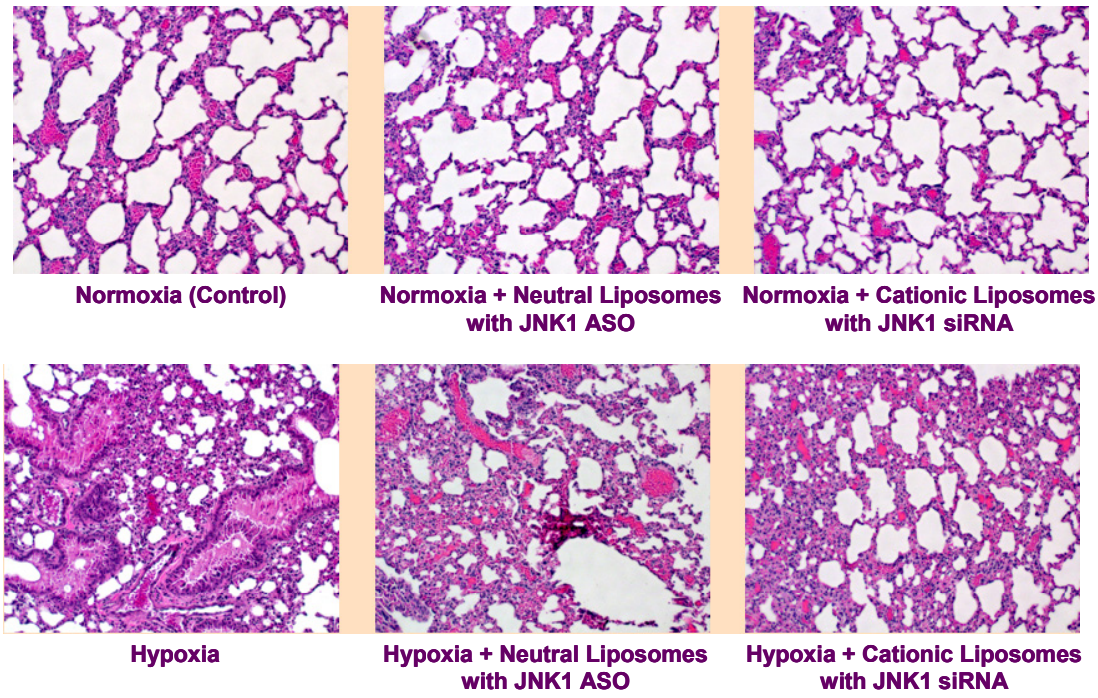

Figure 7.6. Lung tissue histology showing hematoxylin-eosin stain under normoxia and hypoxia (top and bottom panels, respectively). Hypoxia leads to apoptotic and necrotic cell death. Lung tissues in mice treated with ASO and siRNA targeted to JNK1 showed decrease in tissue necrosis and edema.

8 REFERENCES

1. Hellwig-Burgel, T., Stiehl, D. P., Wagner, A. E., Metzen, E., and Jelkmann, W. (2005). Review: hypoxia-inducible factor-1 (HIF-1): a novel transcription factor in immune reactions. *Journal of Interferon Cytokine Research, 25*(6), 297-310.

2. Wang, Y., Pakunlu, R. I., Tsao, W., Pozharov, V., and Minko, T. (2004). Bimodal effect of hypoxia in cancer: Role of hypoxia inducible factor in apoptosis. *Molecular Pharmaceutics, 1*(2), 156-165.

3. Johnson, G. L., Dohlman, H. G., and Graves, L. M. (2005). MAPK kinase kinases (MKKKs) as a target class for small-molecule inhibition to modulate signaling networks and gene expression. *Current Opinion in Chemical Biology, 9*(3), 325-331.

4. Haddad, J. (2004). Hypoxia and the regulation of mitogen-activated protein kinases: gene transcription and the assessment of potential pharmacologic therapeutic interventions. *International Immunopharmacology, 4*(10-11), 1249-1285.

5. Zhou, G., Golden, T., Aragon, I. V., and Honkanen, R. E. (2004). Ser/Thr protein phosphatase 5 inactivates hypoxia-induced activation of an apoptosis signal-regulating kinase 1/MKK-4/JNK signaling cascade. *Journal of Biological Chemistry, 279*(45), 46595-46605.

6. Chihab, R., Ferry, C., Koziel, V., Monin, P., and Daval, J. L. (1998). Sequential activation of activator protein-1-related transcription factors and JNK protein kinases may contribute to apoptotic death induced by transient hypoxia in developing brain neurons. *Brain Res Mol Brain Res, 63*(1), 105-120.

7. Bennett, B. L., Sasaki, D. T., Murray, B. W., O'Leary, E. C., Sakata, S. T., Xu, W., et al. (2001). SP600125, an anthrapyrazolone inhibitor of Jun N-terminal kinase. *Proc Natl Acad Sci U S A, 98*(24), 13681-13686.

8. Ahmad, A., Evans, H. M., Ewert, K., George, C. X., Samuel, C. E., and Safinya, C. R. (2005). New multivalent cationic lipids reveal bell curve for transfection efficiency versus membrane charge density: lipid-DNA complexes for gene delivery. *The Journal of Gene Medicine, 7*(6), 739-748.

9. Chabaud, P., Camplo, M., Payet, D., Serin, G., Moreau, L., Barthelemy, P., et al. (2006). Cationic nucleoside lipids for gene delivery. *Bioconjugate Chemistry, 17*(2), 466-472.

10. Lindner, L. H., Brock, R., Arndt-Jovin, D., and Eibl, H. (2006). Structural variation of cationic lipids: minimum requirement for improved oligonucleotide delivery into cells. *Journal of Controlled Release, 110*(2), 444-456.

11. Sen, J., and Chaudhuri, A. (2005). Design, syntheses, and transfection biology of novel non-cholesterol-based guanidinylated cationic lipids. *Journal of Medicinal Chemistry, 48*(3), 812-820.

12. Wang, Y., and Minko, T. (2004). A novel cancer therapy: Combined liposomal hypoxia inducible factor 1 alpha antisense oligonucleotides and an anticancer drug. *Biochemical Pharmacology, 68*(10), 2031-2042.

13. Pakunlu, R. I., Wang, Y., Tsao, W., Pozharo, V., Cook, T. J., and Minko, T. (2004). Enhancement of the efficacy of chemotherapy for lung cancer by simultaneous suppression of multidrug resistance and antiapoptotic cellular defense: novel multicomponent delivery system. *Cancer Research, 64*(17), 6214-6224.

14. Zhu, H., Jackson, T., and Bunn, F. (2002). Detecting and responding to hypoxia. *Nephrology Dialysis Transplantation, 17*(Supplement 1), 3-7.

15. Agorreta, J., Zulueta, J. J., Montuenga, L. M., and Garayoa, M. (2005). Adrenomedullin expression in a rat model of acute lung injury induced by hypoxia and LPS. *American Journal of Physiology - Lung Cellular & Molecular Physiology, 288*(3), L536-545.

16. Minko, T., Wang, Y., and Pozharo, V. (2005). Remediation of Cellular hypoxic damage by pharmacological agents. *Current Pharmaceutical Design, 11*(24), 3185-3199.

17. Nangaku, M. (2004). Hypoxia and Tubulointerstitial Injury:A Final Common Pathway to End-Stage Renal Failure. *Nephron Experimental Nephrology, 98*, e8-e12.

18. Russ, A. L., Haberstroh, K. M., and Rundell, A. E. (2007). Experimental strategies to improve in vitro models of renal ischemia. *Experimental and Molecular Pathology, 83*, 143-159.

19. Seta, K. A., Spicer, Z., Yuan, Y., Lu, G., and D.E.Millhorn. (2002). Responding to Hypoxia: Lessons from a model cell line. *Science Signaling* (146), 1-16.

20. Pitts, K. R., and Toombs, C. F. (2004). Coverslip hypoxia: a novel method for studying cardiac myocyte hypoxia and ischemia in vitro. *American Journal of Physiology: Heart and Circulatory Physiology, 287*, H1801-H1812.

21. Mitsuyoshi, A., Nakagami, M., Mashima, S., Terasaki, M., Morimoto, T., and Yamaoka, Y. (1994). A new experimental model of specific liver hypoxia using membrane oxygenator. *Research in Experimental Medicine, 194*(6), 367-374.

22. Berant, M., Alon, U., Antebi, D., Diamond, E., Koerner, H., and Mordechovitz, D. (1986). Effects of nonischemic hypoxia on jejunal mucosal structure and function: Study of an experimental model in dogs. *Pediatric Research, 20*(11), 1143-1146.

23. Poizat, C., Keriel, C., Garnier, A., Dubois, F., Cand, F., and Cuchet, P. (1993). An experimental model of hypoxia on isolated rat heart in recirculating system: study of fatty acid metabolism with an iodinated fatty acid. *Archives Internationales de Physiologie, de Biochimie et de Biophysique, 101*(6), 347-356.

24. Welt, K., Schaffranietz, L., Lukas, H., Wassilev, G., and Fitzl, G. (1998). N2O-induced hypoxia as a model of hypoxic stress of rat myocardium. An ultrastructural-morphometric study. *Experimental and Toxicologic Pathology, 50*(3), 229-237.

25. Adamus, W. S., Jansen, U., Schlling, C., and Lohmann, H. F. (1988). Bronchospasm induced by methacholine inhalation as a model for testing of bronchospasmolytics in healthy volunteers. *Methods & Findings in Experimental & Clinical Pharmacology, 10*(2), 135-139.

26. Konduri, G. G., Solimano, A., Sokol, G. M., Singer, J., Ehrenkranz, R. A., and Singhal, N. (2004). Neonatal inhaled nitric oxide study group. A randomized trial of early versus standard inhaled nitric oxide therapy in term and near-term newborn infants with hypoxic respiratory failure. *Pediatrics, 113*, 559-564.

27. Sin, D. D., McAlister, F. A., Man, S. F., and Anthonisen, N. R. (2003). Contemporary management of chronic obstructive pulmonary disease: scientific review. *JAMA, 290*, 2301-2312.

28. Jie, Z., Cai, Y., Yang, W., Jin, M., Zhu, W., and Zhu, C. (2003). Protective effects of endotoxin. *Chinese Medical Journal, 116*, 1678-1682.

29. Toller, J. K. (2003). Key current clinical issues in alpha-1 antitrypsin deficiency. *Respiratory Care, 48*, 1216-1221.

30. Berg, J. T., Ramanathan, S., and Swenson, E. R. (2004). Inhibitors of hypoxic pulmonary vasoconstriction prevent high-altitude pulmonary edema in rats. *Wilderness Environ Med, 15*, 32-37.

31. Booker, R. (2004). Pharmacology of bronchodilators. *Nursing Times, 100*, 54-57.

32. Kuklin, V. N., Kirov, M. Y., Evgenov, O. V., Sovershaev, M. A., Sjoberg, J., and Kirova, S. S. (2004). Novel endothelin receptor antagonist attenuates endotoxin-induced lung injury in sheep. *Critical Care in Medicine, 32*, 766-773.

33. Nilsson, G., Gustafsson, M., Vandenbussche, G., Veldhuizen, E., Griffiths, W. J., Sjovali, J., et al. (1998). Synthetic peptide containing surfactants evaluation of transmembrane versus amphipathic helices and surfactant protein C poly-valyl to poly-leucyl substitution. *European Journal of Biochemistry, 255*, 116-124.

34. Robertson, B., and Halliday, H. L. (1998). Principles of surfactant replacement. *Biochimica et Biophysica Acta, 1408*, 116-124.

35. Robertson, B., Johansson, J., and Curstedt, T. (2000). Synthetic surfactants to treat neonatal lung disease. *Molecular Medicine Today, 6*, 119-124.

36. Daugherty, W. P., Levasseur, J. E., D, D. S., Spiess, B. D., and Bullock, M. R. (2004). Perfluorocarbon emulsion improves cerebral oxygenation and mitochondrial function after fluid percussion brain injury in rats. *Neurosurgery, 54*, 1223-1230.

37. Duong, T. Q., Ladecola, C., and Kim, S. G. (2001). Effect of hyperoxia, hypercapnia, and hypoxia on cerebral interstitial oxygen tension and cerebral blood flow. *Magnetic Resonance Medicine, 45*, 61-70.

38. Dolgikh, V. T., Rusakov, V. V., Korpacheva, O. V., and Sudakova, A. N. (1992). Pathogenesis and pharmacorrection of early postresuscitation cardiac arrhythmia. *Resuscitation, 23*(179-91).

39. Kaverina, N. V., Turilova, A. I., Rozonov, Y. B., Azvolinskaya, T. N., and Kryzhanovsky, S. A. (1983). On the mechanism of action of the antianginal drug, nonachlazine on ischemic myocardium. *Advances in Myocardiology, 4*, 575-587.

40. Piatak, O. A., Yanovskii, G. V., and Lizogub, V. G. (1991). The influence of adrenoreactive preparations on clinical and hemodynamic parameters in patients with ischaemic heart disease. *Cor Vasa, 33*, 19-25.

41. Bickler, P. E., Warner, D. S., Startmann, G., and Schuyler, J. A. (2003). Gamma aminobutyric acid-A receptors contribute to isoflurane neuroprotection in organotypic hippocampal cultures. *Anesthesia and Analgesia, 97*, 564-571.

42. CahillJr, G. F., and Veech, R. L. (2003). Ketoacids? Good Medicine? *Trans Am Clin Climatol Assoc, 114*, 149-161.

43. Sasaki, T., Sakuma, J., Ichikawa, T., Matsumoto, M., Tiwari, P., Young, W., et al. (2002). Effects of methylprednisolone on axonal depression induced by hypoxia, gamma amino butyric acid, and (+/-)-8-hydroxy-dipropylaminotetralin hydrobromide. *Neurosurgery, 51*, 1477-1483.

44. Shuaib, A. (2003). The role of taurine in cerebral ischemia: studies in transient forebrain ischemia and embolic focal ischemia in rodents. *Advances in Experimental Medicine and Biology, 526*, 421-431.

45. Waters, S. L., Miller, G. W., Aleo, M. D., and Schnellmann, R. G. (1997). Neurosteroid inhibition of cell death. *American Journal of Physiology, 273*, F869-876.

46. El-Beshlawy, A., Ragab, L., Fattah, A. A., Ibrahim, I. Y., Hamdy, M., Makhlouf, A., et al. (2004). Improvement of cardiac function in thalassemia major treated with L-carnitine. *Acta Haematologica, 111*(3), 143-148.

47. Huber, R., Spiegel, T., Buchner, M., and Riepe, M. W. (2004). Graded reoxygenation with chemical inhibition of oxidative phophorylation improves posthypoxic recovery in murine hippocampal slices. *Journal of NeuroScience Research, 75*, 441-449.

48. Janssens, D., Delaive, E., Houbion, A., Eliaers, F., Remacle, J., and Michiels, C. (2000). Effect of venotropic drugs on the respiratory activity of isolated mitochondria and in endothelial cells. *British Journal of Pharmacology, 130*, 1513-1524.

49. Suzuki, M., Suzuki, M., Saato, K., Dohi, S., Sato, T., Matsuura, A., et al. (2001). Effect of beta-hydroxybutyrate, a cerebral function improving agent, on cerebral hypoxia, anoxia and ischemia in mice and rats. *Japanese Journal of Pharmacology, 87*, 143-150.

50. Wei, Z. Z., and Xia, S. S. (2004). Gamma-hydroxybutyrate protects the liver from warm ischemia-reperfusion injury in rat. *Hepatobiliary Pancreat. Dis. Int., 3*, 245-249.

51. Yosunkaya, A., Ak, A., Bariskaner, H., Ustun, M. E., Tuncer, S., and Gurbilek, M. (2004). Effect of gamma-hydroxybutyric acid on lipid peroxidation and tissue lactate level in experimental head trauma. *Journal of Trauma, 56*, 585-590.

52. Abdel-aleem, S., Louis, J. S., Hendrickson, S. C., El-Shewy, H. M., Dawy, K. e., Taylor, D. A., et al. (1998). Regulation of carbohydrate and fatty acid utilization by L-carnitine during cardiac development and hypoxia. *Molecular and Cellular Biochemistry, 180*, 95-103.

53. Anderson, C. M., Woodside, K. J., Spencer, T. A., and Hunter, G. C. (2004). Methemoglobinemia: an unusual cause of postoperative cyanosis. *Journal of Vascular Surgery, 39*, 686-690.

54. Benzi, G. (1998). Pharmacological features of an almitrine-raubasine combination: Activity of cerebral levels. *European Neurology, 39*, 31-38.

55. Berger, R., Middelanis, J., Vaihinger, H. M., Mies, G., Wilken, B., and Jensen, A. (2004). Creatin protects the immature brain from hypoxic-ischemic injury. *Journal of the Society for Gynecologic Investigation, 11*, 9-15.

56. Borle, A. B., and Stanko, R. T. (1996). Pyruvate reduces anoxic injury and free radical formation in perfused rat hepatocytes. *American Journal of Physiology, 270*, G535-540.

57. Bradberry, S. M. (2003). Occupational Methaemoglobinaemia. Mechanisms of production, features, diagnosis and management including the use of methylene blue. *Toxicological Reviews, 22*, 13-27.

58. Cater, H. L., Chandratheva, A., Benham, C. D., Morrison, B., and Sundstrom, L. E. (2003). Lactate and glucose as energy substrates during and after oxygen deprivation in rat hippocamal acute and cultured slices. *Journal of Neurochemistry, 87*, 1381-1390.

59. Haas, S., Schmitt, C. P., Arbeiter, K., Bonzel, K. E., Fischbach, M., John, U., et al. (2003). Improved acidosis correction and recovery of mesothelial cell mass with neutral pH bicarobonate dialysis solution among children undergoing automated peritoneal dialysis. *Journal of American Society of Nephrology, 14*, 2632-2638.

60. Kallet, R. H., Liu, K., and Tang, J. (2003). Management of acidosis during lung protective ventilation in acute respiratory distress syndrome. *Respiratory Care Clinics of North America, 9*, 437-456.

61. Luft, F. C. (2001). Lactic acidosis update for critical care clinicians. *Journal of American Society of Nephrology, 12*, S15-19.

62. Bordoni, A., Hrelia, S., Angeloni, C., Giordano, E., Guarnieri, C., Caldarera, C., et al. (2002). Green tea protection for hypoxia / reoxygenation injury in cultured cardiac cells. *Journal of Nutritional Biochemistry, 13*, 103-111.

63. Chen, H., Li, D., Saldeen, T., Romeo, F., and Mehta, J. L. (2002). Mixed tocopherol preparation is superior to alpha-tocopherol alone against hypoxia-reoxygenation injury. *Biochemical and Biophysical Research Communications, 291*, 349-353.

64. Gonchar, O., Klyuchko, E., Seredenko, M., and Oliynik, S. (2003). Corrections of proxidant-antioxidant homeostasis of organism under hypoxia of different genesis by yackton, a new pharmacological preparation. *Acta Physiol. Pharmacol. Bulg., 27*, 53-58.

65. Ilavazhagan, G., Bansal, A., Prasad, D., Thomas, P., Sharma, S. K., Kain, A. K., et al. (2001). Effect of vitamin E supplementation on hypoxia-induced oxidative

damage in male albino rats. *Aviation, Space and Environmental Medicine, 72*, 899-903.

66. Wu, J., Parungo, C., Wu, G., Kang, P. M., Laham, R. J., Sellke, F. W., et al. (2004). PR39 inhibits apoptosis in hypoxic endothelial cells: role of inhibitor apoptosis protein-2. *Circulation, 109*, 1660-1667.

67. Tabakman, R., Jiang, H., Levine, R. A., Kohen, R., and Lazarovici, P. J. (2004). Apoptotic characteristics of cell death and the neuroprotective effect of homocarnosine on pheochromocytoma PC12 cells exposed to ischemia. *Journal of Neuroscience Research, 75*(4), 499-507.

68. Jacobson, M. D., Weil, M., and Raff, M. C. (1997). Programmed cell death in animal development. *Cell, 88*, 347-354.

69. Kerr, J. F., Wyllie, A. H., and Currie, A. R. (1972). Apoptosis: a basic biological phenomenon with wide-ranging implications in tissue kinetics. *British Journal of Cancer, 26*, 239-257.

70. Rinkenberger, J. L., and Korsmeyer, S. J. (1997). Errors of homeostasis and deregulated apoptosis. *Current opinion in genetics and development., 7*, 589-596.

71. Thompson, C. B. (1995). Apoptosis in the pathogenesis and treatment of disease. *Science, 267*, 1456-1462.

72. Ashkenazi, A., and Dixit, V. M. (1998). Death receptors: signaling and modulation. *Science, 281*, 1305-1308.

73. Cohen, G. M. (1997). Caspases: the executioners of apoptosis. *Biochemical Journal, 326*, 1-16.

74. Green, D. R., and Reed, J. C. (1998). Mitochondria and apoptosis. *Science, 281*, 1312-1316.

75. Thornberry, N. A., and Lazebnik, Y. (1998). Caspases: enemies within. *Science, 281*, 1312-1316.

76. Chang, L., and Karin, M. (2001). Mammalian MAP kinase signalling cascades. *Nature, 410*, 37-40.

77. Davis, R. J. (2000). Signal transduction by the JNK group of MAP kinases. *Cell, 103*, 239-252.

78. Lin, A. (2003). Activation of the JNK signaling pathway: Breaking the brake on apoptosis. *Bioessays, 25*(1), 17-24.

79. Shaulian, E., and Karin, M. (2002). MAP-1 as a regulator of cell life and death. *Nature Cell Biology, 4*, E131-136.

80. Hibi, M., Lin, A., Smeal, T., Minden, A., and Karin, M. (1993). Identification of an oncoprotein- and UV-responsive protein kinase that binds and potentiates the c-Jun activation domain. *Genes and Development, 7*, 2135-2148.

81. Liu, J., and Lin, A. (2005). Role of JNK activation in apoptosis: A double-edged sword. *Cell Research, 15*(1), 36-42.

82. Johnson, G., and Lapadat, R. (2002). Mitogen-activated protein kinase pathways mediated by ERK, JNK and p38 protein kinases. *Science, 298*, 1911-1912.

83. Karin, M. (1995). The regulation of AP-1 activity by mitogen-activated protein kinases. *Journal of Biological Chemistry, 270*, 16483-16486.

84. Ham, J., Babij, C., Whitfield, J., Pfarr, C. M., Lallemand, D., Yaniv, M., et al. (1995). A c-Jun dominant negative mutant protects sympathetic neurons against programmed cell death. *Neuron, 14*, 927-939.

85. Le-Niculescu, H., Bonfoco, E., Kasuya, Y., Claret, F. X., Green, D. R., and Karin, M. (1999). Withdrawal of survival factors results in activation of the JNK pathway in neuronal cells leading to Fas ligand induction and cell death. *Molecular and Cellular Biology, 19*, 751-763.

86. Xia, Z., Dickens, M., Raingeaud, J., Davis, R. J., and Greenberg, M. E. (1995). Opposing effects of ERK and JNK-p38 MAP kinases on apoptosis. *Science, 270*, 1326-1331.

87. Tournier, C., Hess, P., Yang, D. D., Xu, J., Turner, T. K., Nimnual, A., et al. (2000). Requirement of JNK for Stress- Induced Activation of the Cytochrome c Mediated Death Pathway. *Science, 288*(5467), 870-873.

88. Fire, A., Xu, S., Montgomery, M. K., and al, e. (1998). Potent and specific genetic interference by double stranded RNA in Caenorhabditis elegans. *Nature, 391*, 806-811.

89. Tuschl, T., Zamore, P. D., Lehmann, R., and al., e. (1999). Targeted mRNA degradation by double stranded RNA in vitro. *Genes and Development, 13*, 3191-3197.

90. Dykxhoorn, D. M., and Lieberman, J. (2005). The Silent Revolution: RNA interference as basic biology, research tool and therapeutic. *Annual Review of Medicine, 56*, 401-423.

91. Hannon, G. (2002). RNA Interference. *Nature, 418*, 244-251.

92. Song, E., Zhu, P., Lee, S.-K., Chowdhury, D., Kussman, S., Dykxhoorn, D. M., et al. (2005). Antibody mediated in vivo delivery of small interfering RNAs via cell-surface receptors. *Nature Biotechnology, 23*, 709-717.

93. Simeoni, F., Morris, M. C., Heitz, F., and al, e. (2003). Insight into the mechanism of the peptide-based gene delivery of siRNA into mammalian cells. *Nucleic Acids Research, 31*, 2717-2724.

94. Soutschek, J., Akinc, A., Bramlage, B., Charisse, K., Constien, R., Donoghue, M., et al. (2004). Therapeutic silencing of an endogenous gene by systemic administration of modified siRNAs. *Nature, 432*(7014), 173-178.

95. Park, T. G., Jeong, J. H., and Kim, S. W. (2006). Current status of polymeric gene delivery systems. *Advanced Drug Delivery Reviews, 58*, 467-486.

96. Gary, D. J., Puri, N., and Won, Y. Y. (2007). Polymer-based siRNA delivery: perspectives on the fundamental and phenomenological distinctions from polymer-based DNA delivery. *Journal of Controlled Release, 121*, 64-73.

97. McCaffrey AP, Nakai H, Pandey K, Huang Z, Salazar FH, Xu H, et al. (2003). Inhibition of hepatitis B virus in mice by RNA interference. *Nature Biotechnology, 21*(6), 629-630.

98. Sorensen, D. R., Leirdal, M., and Sioud, M. (2003). Gene silencing by systemic delivery of synthetic siRNAs in adult mice. *Journal of Molecular Biology, 327*, 761-766.

99. Sioud, M., and Sorensen, D. R. (2003). Cationic liposome-mediated delivery of siRNAs in adult mice. *Biochemical and Biophysical Research Communications, 312*, 1220-1225.

100. Zhang, Y., Zhang, Y. F., Bryant, J., and al, e. (2004). Intravenous RNA interference gene therapy targeting the human epidermal growth factor receptor prolongs survival in intracranial brain cancer. *Clinical Cancer Research, 10*, 3667-3677.

101. Behlke, M. A. (2006). Progress towards in vivo use of siRNAs. *Molecular Therapy*, 644-670.

102. Hu-Lieskovan, S., Heidel, J. D., Bartlett, D. W., Davis, M. E., and Triche, T. J. (2005). Sequence-specific knockdown of EWS-FLI1 by targeted, nonviral delivery of small interfering RNA inhibits tumor growth in a murine model of metastatic Ewing's sarcoma. *Cancer Research, 65*, 8984-8992.

103. McNamara, J. O., Andrechek, E. R., Wang, Y., Viles, K. D., Rempel, R. E., Gilboa, E., et al. (2006). Cell type-specific delivery of siRNAs with aptamer-siRNA chimeras. *Nature Biotechnology, 24*, 1005-1015.

104. Patil, S., Rhodes, D., and Burgess, D. (2005). DNA-based Therapeutics and DNA Delivery Systems: A Comprehensive Review. *The AAPS Journal, 7*(1), E61-E77.

105. Lebedeva, I., Benimetskaya, L., Stein, C. A., and Vilenchik, M. (2000). Cellular delivery of antisense oligonucleotides. *European Journal of Pharmaceutics & Biopharmaceutics, 50*(1), 101-119.

106. Mahato, R. I., Ye, Z., and Ramareddy V, G. (2005). Antisense and Antigene Oligonucleotides: Structure, Stability and Delivery. In R. I. Mahato (Ed.), *Biomaterials for Delivery and targeting of proteins and nucleic acids* (pp. 432-569). Boca Raton: CRC Press, Boca Raton, FL.

107. Bangham, A. D. (1981). Introduction. In C. G. Knight (Ed.), *Liposomes: physical structure to therapeutic applications* (pp. 1-14). North Holland, Amsterdam: Elsevier.

108. Mann, M. J., Morishita, R., Gibbons, G. H., Leyen, H. E. v. d., and Dzau, V. J. (1997). DNA transfer into vascular smooth muscle using fusigenic Sendai virus (HVJ)-liposomes. *Molecular and Cellular Biochemistry, 172*, 3-12.

109. Fasbender, A., Zabner, J., Chillon, M., Moninger, T. O., Puga, A. P., Davidson, B. L., et al. (1997). Complexes of adenovirus with polycationic polymers and cationic lipids increase the efficiency of gene transfer in vitro and in vivo. *Journal of Biological Chemistry, 272*, 6479-6489.

110. Simberg, D., Weisman, S., Talman, Y., and Barenholz, Y. (2004). DOTAP (and other Cationic Lipids): Chemistry, Biophysics, and Transfection. *Critical Reviews in Therapeutic Drug Carrier Systems, 21* (4), 257-317.

111. Aagaard, L., and Rossi, J. J. (2007). RNAi therapeutics: Principles, prospects and challenges. *Advanced Drug Delivery Reviews, 59*, 75-86.

112. Minko, T., Stefanov, A., and Pozharov, V. (2002). Selected contribution: Lung hypoxia: antioxidant and antiapoptotic effects of liposomal alphatocopherol. *Journal of Applied Physiology, 93*(4), 1550-1560.

113. Pakunlu, R. I., Cook, T. J., and Minko, T. (2003). Simultaneous modulation of multidrug resistance and antiapoptotic cellular defense by MDR1 and BCL-2 targeted antisense oligonucleotides enhances the anticancer efficacy of doxorubicin. *Pharmaceutical Research, 20*(3), 351-359.

114. Akhtar, S., Hughes, M. D., Khan, A., Bibby, M., Hussain, M., Nawaz, Q., et al. (2000). The delivery of antisense therapeutics. *Advanced Drug Delivery Reviews, 44*, 3-21.

115. Hreniuk, D., Garay, M., Gaarde, W., Monia, B. P., McKay, R. A., and Cioffi, C. L. (2001). Inhibition of c-Jun N-terminal kinase 1, but not c-Jun N-terminal kinase 2, suppresses apoptosis induced by ischemia/reoxygenation in rat cardiac myocytes. *Molecular Pharmacology, 59*(4), 867-874.

116. Garay, M., Gaarde, W., Monia, B. P., Nero, P., and Cioffi, C. L. (2000). Inhibition of hypoxia/reoxygenation-induced apoptosis by an antisense oligonucleotide targeted to JNK1 in human kidney cells. *Biochemical Pharmacology, 59*(9), 1033-1043.

117. Crenesse, D., Laurens, M., Heurteaux, C., Cursio, R., Saint-Paul, M. C., Schmid-Alliana, A., et al. (2003). Rat liver ischemia-reperfusion-induced apoptosis and necrosis are decreased by FK506 pretreatment. *European Journal of Pharmacology, 473*(2-3), 177-184.

118. Paroo, Z., and Corey, D. R. (2004). Challenges for RNAi *in vivo*. *Trends in Biotechnology, 22*, 390-394.

119. Eliyahu, H., Barenholz, Y., and Domb, A. J. (2005). Polymers for DNA delivery. *Molecules, 10*, 34-64.

120. Geary, R. S., Watanabe, T. A., Truong, L., Freier, S., Lesnik, E. A., Sioufi, N. B., et al. (2001). Pharmacokinetic properties of 2'-O-(2-methoxyethyl)-modified oligonucleotide analogs in rats. *The Journal of Pharmacology and Experimental Therapeutics, 296*(3), 890-897.

121. Waterhouse, D. N., Dragowska, W. H., Gelmon, K. A., Mayer, L. D., and Bally, M. B. (2004). Pharmacodynamic behavior of liposomal antisense oligonucleotides targeting Her-2/neu and vascular endothelial growth factor in an ascitic MDA435/LCC6 human breast cancer model. *Cancer Biology and Therapy, 3*(2), 197-204.

122. Potter, C., and Harris, A. L. (2004). Hypoxia inducible carbonic anhydrase IX, marker of tumour hypoxia, survival pathway and therapy target. *Cell Cycle, 3*, 164-167.

123. Alarcon-Vargas, D., and Ronai, Z. (2004). c-Jun-NH2 Kinase (JNK) contributes to the regulation of c-Myc protein stability. *The Journal of Biological Chemistry, 279*(6), 5008-5016.

124. Li, G., Xiang, Y., Sabapathy, K., and Silverman, R. H. (2004). An apoptotic signaling pathway in the interferon antiviral response mediated by RNase L and c-

Jun NH2 terminal kinase. *The Journal of Biological Chemistry, 279*(2), 1123-1131.

125. Santibanez, J. F. (2006). JNK mediates TGF-B1-induced epithelial mesenchymal transdifferentiation of mouse transformed keratinocytes. *FEBS Letters, 580*, 5385-5391.

126. Wickstrom, E. (1986). Oligodeoxynucleotide Stability In Subcellular Extracts and Culture Media. *Journal of Biochemical and Biophysical Methods, 13*(2), 97-102.

127. Akhtar, S., Kole, R., and Juliano, R. L. (1991). Stability Of Antisense DNA Oligodeoxynucleotide Analogs In Cellular Extracts and Sera. *Life Sciences, 49*(24), 1793-1801.

128. Hudson, A. J., Normand, N., Ackroyd, J., and Akhtar, S. (1999). Cellular delivery of hammerhead ribozymes conjugated to a transferrin receptor antibody. *International Journal of Pharmaceutics, 182*(1), 49-58.

129. Ion, G. (1988). Oligonucleotide Analogs as potential chemotherapeutic - Agents. *Pharmaceutical Research, 5*(9), 539-549.

130. Kashihara, N., Maeshima, Y., and Makino, H. (1998). Anisense Oligonucleotides. *Experimental Nephrology, 6*(1), 84-88.

131. Konopleva, M., Tari, A. M., Estrov, Z., Harris, D., Xie, Z., Zhao, S., et al. (2000). Liposomal BCl-2 antisense oligonucleotides enhance proliferation, sensitize acute myeloid leukemia to cytosine-arabinoside and induce apoptosis independent of other antiapoptotic proteins. *Blood, 95*(12), 3929-3938.

132. Zhang, S., Zhao, B., Jiang, H., Wang, B., and Ma, B. (2007). Cationic lipids and polymers mediated vectors for delivery of siRNA. *Journal of Controlled Release* (123), 1-10.

133. Akhtar, S., and Benter, I. (2007). Non-viral delivery of synthetic siRNAs in vivo. *Journal of Clinical Investigation, 117*(12), 3623-3632.

134. Bouxsein, N. F., McAllister, C. S., Ewert, K. K., Samuel, C. E., and Safinya, C. R. (2007). Structure and gene silencing activities of monovalent and pentavalent cationic lipid vectors complexed with siRNA. *Biochemistry, 46*(16), 4785-4792.

135. Bozzola, J. J., and Russell, L. D. (1992). *Electron Microscopy: Principles and Techniques for Biologists*: Jones and Bartlett, Boston, MA.

136. Hayat, M. A. (1981). Fixation for Electron Microscopy.

137. Raghuraman, H., Shrivastava, S., and Chattopadhyay, A. (2007). Monitoring of acyl chain labeled NBD lipids in membranes as a function of membrane phase state. *Biochimica et Biophysica Acta, 1768*(5), 1258-1267.

138. Chandna, P., Saad, M., Wang, Y., Ber, E., Khandare, J., Vetcher, A. A., et al. (2007). Targeted proapoptotic anticancer drug delivery system. *Molecular Pharmaceutics, 4*, 668-678.

139. Wang, Y., Saad, M., Pakunlu, R. I., Khandare, J., Garbuzenko, O. B., Vetcher, A. A., et al. (2008). Non-viral nanoscale-based delivery of antisense oligonucleotides targeted to HIF1 alpha enhances the efficacy of chemotherapy in drug resistant tumor. *Clinical Cancer Research, 14*, 3607-3616.

140. Tsukioka, Y., Matsumura, Y., Hamaguchi, T., Koike, H., Moriyasu, F., and Kakizoe, T. (2002). Pharmaceutical and biomedical differences between micellar doxorubicin (NK911) and liposomal doxorubicin (Doxil). *Japanese Journal of Cancer Research, 93*, 1145-1153.

141. Minko, T., Pakunlu, R. I., Wang, Y., Khandare, J., and Saad, M. (2006). New generation of liposomal drugs for cancer. *Anticancer Agents Medicinal Chemistry, 6*, 537-552.

142. Pakunlu, R. I., Wang, Y., Saad, M., Khandare, J., Starovoytov, V., and Minko, T. (2006). In vitro and in vivo intracellular liposomal delivery of antisense oligonucleotides and anticancer drug. *Journal of Controlled Release, 114*, 153-162.

143. Fahr, A., Hoogevest, P. v., May, S., Bergstrand, N., and Leigh, M. L. S. (2005). Transfer of lipophilic drugs between liposomal membranes and biological interfaces: Consequences for drug delivery. *European Journal of Pharmaceutical Sciences, 26*, 251-265.

144. Torchilin, V. P. (2005). Recent advances with liposomes as pharmaceutical carriers. *Nature Reviews in Drug Discovery, 4*, 145-160.

145. Torchilin, V. P. (2006). Recent approaches to intracellular delivery of drugs and DNA and organelle targeting. *Annual Review of Biomedical Engineering, 8*, 343-375.

146. Karin, M. (1995). The regulation of AP-1 activity by mitogen-activated protein kinases. *Journal of Biological Chemistry, 270*(28), 16483-16486.

147. Derijard, B., Hibi, M., Wu, I. H., Barrett, T., Su, B., Deng, T., et al. (1994). JNK1: a protein kinase stimulated by UV light and Ha-Ras that binds and phosphorylates the c-Jun activation domain. *Cell, 76*(6), 1025-1037.

148. Rapisarda, A., Uranchimeg, B., Scudiero, D. A., Selby, M., Sausville, E. A., Shoemaker, R. H., et al. (2002). Identification of small molecule inhibitors of hypoxia-inducible factor 1 transcriptional activation pathway. *Cancer Research, 62*(15), 4316-4324.

149. Dharap, S. S., Wang, Y., Chandna, P., Khandare, J. J., Qiu, B., Gunaseelan, S., et al. (2005). Tumor-specific targeting of an anticancer drug delivery system by LHRH peptide. *Proc Natl Acad Sci U S A, 102*(36), 12962-12967.

150. Minko, T., Kopeckova, P., Pozharov, V., and Kopecek, J. (1998). HPMA copolymer bound adriamycin overcomes MDR1 gene encoded resistance in a human ovarian carcinoma cell line. *Journal of Controlled Release, 54*(2), 223-233.

151. Betigeri, S., Pakunlu, R. L., Wang, Y., Khandare, J., and Minko, T. (2006). JNK1 as a molecular target to limit cellular mortality under hypoxia. *Molecular Pharmaceutics, 3*(4), 424-430.

152. Fenske, D. B., Chonn, A., and Cullis, P. R. (2008). Liposomal Nanomedicines: An emerging field. *Toxicologic Pathology, 36*(1), 21-29.

153. Juliano, R., Alam, M. R., Dixit, V., and Kang, H. (2008). Mechanisms and strategies for effective delivery of antisense and siRNA oligonucleotides. *Nucleic Acids Research, 36*(12), 4158-4171.

154. Santel, A., Aleku, M., Keil, O., Endruschat, J., Esche, V., Fisch, G., et al. (2006). A novel siRNA-lipoplex technology for RNA interference in the mouse vascular endothelium. *Gene Therapy, 13*, 1222-1234.

155. Phillips, J. A., Craig, S. J., Bayley, D., Christian, R. A., Geary, R. S., and Nicklin, P. L. (1997). Pharmacokinetics, metabolism and elimination of a 20-mer phosphorothioate oligodeoxynucleotide (CGP 69846A) after intravenous and subcutaneous administration. *Biochemical Pharmacology, 54*, 657-668.

156. Geary, R. S., Leeds, J. M., Henry, S. P., Monteith, D. K., and Levin, A. A. (1997). Antisense oligonucleotide inhibitors for the treatment of cancer: 1. Pharmacokinetic properties of phosphorothioate oligodeoxynucleotides. *Anticancer Drug Design, 12*(5), 383-393.

157. Levin, A. A., Geary, R. S., Leeds, J. M., Monteith, D. K., Yu, R. Z., Templin, M. V., et al. (1998). *The pharmacokinetics and toxicity of phosphorothioate oligonucleotides*. Philadelphia, PA: Taylor and Francis.

158. Braasch, D. A., Paroo, A., Constantinescu, A., Ren, G., Oz, O. K., Mason, R. P., et al. (2004). Biodistribution of phosphodiester and phosphorothioate siRNA. *Bioorganic & Medicinal Chemistry Letters, 14*, 1139-1143.

159. Corey, D. R. (2007). RNA learns from antisense. *Nature Chemical Biology, 3*(1), 8-11.

160. Reich, S. J., Fosnot, J., Kuroki, A., Tang, W., Yang, X., and Maguire, A. M. (2003). Small interfering RNA (siRNA) targeting VEGF effectively inhibits ocular neovascularization in a mouse model. *Molecular Vision, 9*, 210-216.

161. Zhang, W., Yang, H., Kong, X., Mohapatra, S., San Juan-Vergara, H., and G., H. (2005). Inhibition of respiratory syncytial virus infection with intranasal siRNA nanoparticles targeting the viral NS1 gene. *Nature Medicine, 11*, 56-62.

162. Zhang, X., Shan, P., Jiang, D., Noble, P. W., Abraham, N. G., and Kappas, A. (2004). Small interfering RNA targeting heme oxygenase-1 enhances ischemia-repurfusion induced lung apoptosis. *Journal of Biological Chemistry, 279*, 10677-10684.

163. Friend, D. S., Papahadjopoulos, D., and Debs, R. J. (1996). Endocytosis and intracellular processing accompanying transfection mediated by cationic liposomes. *Biochimica et Biophysica Acta, 1278*, 41-50.

164. Hafez, I. M., Maurer, N., and Cullis, P. R. (2001). On the mechanism whereby cationic lipids promote intracellular delivery of polynucleic acids. *Gene Therapy, 8*, 1188-1196.

165. El Ouahabi, L., Thiry, M., Pector, V., Fuks, R., Ruysschaert, J. M., and Vandenbranden, M. (1997). The role of endosome destabilizing activity in the gene transfer process mediated by cationic lipids. *FEBS Letters, 414*, 187-192.

166. Landen, C. N., Chavez-Reyes, A., Bucana, C., Schmandt, R., Deavers, M. T., Lopez-Berestein, G., et al. (2005). Therapeutic EphA2 gene targeting in vivo using neutral liposomal small interfering RNA delivery. *Cancer Research, 65*(15), 6910-6918.

167. Krinke, G. J. (2000). *The laboratory rat*. San Diego, CA: Academic Press.

168. Artru, A. A., and Michenfelder, J. D. (1981). Influence of hypothermia or hyperthermia alone or in combination with pentobarbital or phenytoin on survival time in hypoxic mice. *Anesthesia and Analgesia, 60*(12), 867-870.

169. King, G. A. (1987). Protection against hypoxia-induced lethality in mice: A comparison of the effects of hypothermia and drugs. *Archives Internationales de Pharmacodynamie et de therapie, 286*, 282-298.

170. King, G. A. (1987). Protective effects of vinpocetine and structurally related drugs on the lethal consequences of hypoxia in mice. *Archives Internationales de Pharmacodynamie et de therapie, 286*, 299-307.

171. Steen, P. A., and Michenfelder, J. D. (1979). Barbiturate protection in tolerant and non-tolerant hypoxic mice: comparison to hypothermic protection. *Anesthesiology, 50*, 404-408.

172. Fan, C., Lacobas, D. A., Zhou, D., Chen, Q., Lai, J. K., Gavrialov, O., et al. (2005). Gene expression and phenotypic characterization of mouse heart after chronic constant or intermittent hypoxia. *Physiological Genomics, 22*, 292-307.

173. Yin, T., Sandhu, G., Wolfgang, C. D., Burrier, A., Webb, R. L., Rigel, D. F., et al. (1997). Tissue-specific pattern of stress kinase activation in ischemic/reperfused heart and kidney. *Journal of Biological Chemistry, 272*, 19943-19950.

CURRICULUM VITA

SEEMA S. BETIGERI

EDUCATION

June 1997:	Bachelor of Pharmacy, University of Pune, India
December 1999:	M.S. Pharmaceutical Science, University of Missouri-Kansas City
January 2009:	Ph.D. Pharmaceutical Science, Rutgers, The State University of New Jersey

PROFESSIONAL EXPERIENCE

1996	Summer Internship at Nucron Pharmaceuticals, Pune, India
1997-1999	Research Assistant, School of Pharmacy, University of Missouri-Kansas City
2000-present	Research Scientist, Exploratory Biopharmaceutics and Stability, Bristol-Myers Squibb Company, New Brunswick, NJ

PUBLICATIONS:

1. **Betigeri S. S.** and Neau S. H. Immobilization of lipase using hydrophilic polymers in the form of beads. *Biomaterials*, 23 (17), 3627-36, 2002.

2. Alsarra I. A., **Betigeri S. S.** and Neau S. H. Molecular weight and degree of deacetylation effects on lipase-loaded chitosan bead characteristics., *Biomaterials,* 23 (17), 3637-44, 2002.

3. **Betigeri S**., Thakur A. and Raghavan K. Use of 2,2'-azobis(2-amidinopropane) dihydrochloride as a reagent tool for evaluation of oxidative stability of drugs. *Pharmaceutical Research,* 22(2), 310-7, 2005.

4. **Betigeri S**., Pakunlu R. I., Wang Y., Khandare J. J. and Minko T. JNK1 as a molecular target to limit cellular mortality under hypoxia. *Molecular Pharmaceutics*, 3(4), 424-430, 2006.

5. **Betigeri S.**, Thakur A. B., Shukla R., Raghavan K.. Effect of Polymer Additives on the Transformation of BMS-566394 Anhydrate to the Dihydrate Form. *Pharmaceutical Research,* 25(5), 1043-51, 2008.

6. Patil M. L., Zhang M., **Betigeri S.**, Taratula O., He H., and Minko T. Surface Modified and Internally Cationic Polyamidoamine Dendrimers for Efficient siRNA Delivery. Bioconjugate Chemistry, 19, 1396-1403, 2008.

7. Garbuzenko O. B., Saad M, **Betigeri S.**, Zhang M., Vetcher A. A., Soldatenkov V. A., Reimer D. C., Minko T. Intratracheal versus intravenous liposomal delivery of siRNA, antisense oligonucleotides and anticancer drug. *Pharmaceutical Research*, Oct 29, 2008 [Epub ahead of print].

8. **Betigeri, S.,** Garbuzenko O., Minko, T. Remediation of cellular hypoxic damage by the suppression of Jun N-terminal kinase 1, in preparation.